

NOTE TO USERS

This reproduction is the best copy available.

UMI[®]

**Modeling of dissolved oxygen levels in the bottom
waters of the Lower St. Lawrence Estuary: coupling of
benthic and pelagic processes**

by

Philippe Benoit

Earth and Planetary Sciences

McGill University

Montréal, Canada

November, 2004

A thesis submitted to

McGill University

in partial fulfillment of the requirements for the degree of

Master of Science

© Philippe Benoit, 2004



Library and
Archives Canada

Bibliothèque et
Archives Canada

Published Heritage
Branch

Direction du
Patrimoine de l'édition

395 Wellington Street
Ottawa ON K1A 0N4
Canada

395, rue Wellington
Ottawa ON K1A 0N4
Canada

Your file *Votre référence*

ISBN: 0-494-12401-6

Our file *Notre référence*

ISBN: 0-494-12401-6

NOTICE:

The author has granted a non-exclusive license allowing Library and Archives Canada to reproduce, publish, archive, preserve, conserve, communicate to the public by telecommunication or on the Internet, loan, distribute and sell theses worldwide, for commercial or non-commercial purposes, in microform, paper, electronic and/or any other formats.

The author retains copyright ownership and moral rights in this thesis. Neither the thesis nor substantial extracts from it may be printed or otherwise reproduced without the author's permission.

AVIS:

L'auteur a accordé une licence non exclusive permettant à la Bibliothèque et Archives Canada de reproduire, publier, archiver, sauvegarder, conserver, transmettre au public par télécommunication ou par l'Internet, prêter, distribuer et vendre des thèses partout dans le monde, à des fins commerciales ou autres, sur support microforme, papier, électronique et/ou autres formats.

L'auteur conserve la propriété du droit d'auteur et des droits moraux qui protègent cette thèse. Ni la thèse ni des extraits substantiels de celle-ci ne doivent être imprimés ou autrement reproduits sans son autorisation.

In compliance with the Canadian Privacy Act some supporting forms may have been removed from this thesis.

Conformément à la loi canadienne sur la protection de la vie privée, quelques formulaires secondaires ont été enlevés de cette thèse.

While these forms may be included in the document page count, their removal does not represent any loss of content from the thesis.

Bien que ces formulaires aient inclus dans la pagination, il n'y aura aucun contenu manquant.


Canada

<i>List of Figures</i>	4
<i>List of Tables</i>	6
<i>Abstract</i>	7
<i>Résumé</i>	8
<i>Acknowledgements</i>	9
<i>Contribution of Authors</i>	10
CHAPTER 1	11
1 General Introduction	11
1.1 Hypoxia and eutrophication	11
1.2 Hypoxia in the St. Lawrence Estuary	12
1.3 Impact of hypoxia on the biota	13
1.4 Conditions leading to hypoxia	15
1.5 Autochthonous sources of organic matter	15
1.6 Allochthonous sources of organic matter	16
1.7 Physics of the St. Lawrence	17
1.8 Enhanced horizontal diffusivity	19
1.9 Stratification of the water column and development of hypoxic bottom waters	20
1.10 Organic carbon fluxes and the sediment record in the Laurentian Channel	22
1.11 Thesis Objectives	24
1.12 Figures	27
1.13 References	35
CHAPTER 2	40
2 Modeling of dissolved oxygen levels in the bottom waters of the Lower St. Lawrence Estuary: coupling of benthic and pelagic processes.	40
2.1 Abstract	40
2.2 Introduction	41
2.3 Water column parameterization	44
2.3.1 Advection-diffusion	45
2.3.2 Parameter sensitivity	47
2.4 Early diagenesis model	48
2.4.1 Biochemical reactions	50
2.4.2 Transport equations	52
2.4.3 Model Implementation	54
2.4.4 Parameter calibration	55

2.4.4.1	Carbon fluxes to the sediment and dissolved oxygen fluxes across the sediment-water interface along the Laurentian Trough	55
2.4.4.2	Molecular diffusion	58
2.4.4.3	Bioturbation	58
2.4.4.4	Rates of bacterial organic matter degradation	59
2.4.5	Validation of the diagenetic model	59
2.5	Simulation scenarios	60
2.5.1	High flux scenario	61
2.5.2	Low flux scenario	61
2.6	Discussion	62
2.6.1	Parameter variations	63
2.6.2	Sediment oxygen demand	64
2.7	Conclusions	67
2.8	Tables	69
2.9	Figures	72
2.10	Acknowledgements	81
2.11	References	82
CHAPTER 3		89
3	General Conclusions	89
3.1	Summary and review of objectives	89
3.2	Conclusions	94
3.3	Recommendations for future work	96
3.4	References	99

List of Figures

Fig. 1. 1 The Estuary and Gulf of St. Lawrence system, showing the location of important topographic features such as the upper and lower estuaries, the Laurentian Channel and Cabot Strait. Modified from Koutitonsky and Bugden (1991).	27
Fig. 1. 2 Map of the LSLE-GSL showing some of the stations sampled during the R/V Coriolis II, July 2003 cruise.	28
Fig. 1. 3 Dissolved oxygen (in $\mu\text{mol L}^{-1}$) in the lower 150 m of the Laurentian Channel between stations 25 and 16. Samples were taken and analyzed in July, 2003. The lowest measured value ($51.3 \pm 0.2 \mu\text{mol L}^{-1}$) is highlighted in black.	29
Fig. 1. 4 Historical record of dissolved oxygen concentrations measured between 300 m and 355 m depth in the LSLE. The error bars show the 95% confidence intervals for the means when three or more measurements were made in a given year. The pale grey dot is the average of measurements carried out in 2003. Modified from Gilbert et al. (2004).	30
Fig. 1. 5 Temperature-salinity (T-S) diagram of the two parent water masses, Labrador Current Water (LCW) and North Atlantic Central Water (NACW). On each water mass T-S curve are superimposed the inter-annual standard deviations of temperature and salinity at intervals of 0.25 kg m^{-3} . The dashed lines represent a T-S mixing line joining LCW and NACW source water types. Modified from Gilbert et al. (2004).	31
Fig. 1. 6 Water column profiles of dissolved oxygen (solid line), temperature (dash-dotted line), salinity (dotted line) and density (dashed line) taken at STN 23 in July 2003.	32
Fig. 1. 7 Vertical cross-section of the Laurentian Channel showing the location and flow direction of the different water masses. Modified from Dickie and Trites (1983).	33
Fig. 1. 8 (A) Percentage of organic carbon content, (B) organic carbon/nitrogen molar ratio and (C) carbon-13 isotopic signature (‰) as a function of sediment depth in composite sediment core of box core AH00-2220 and piston core MD2220, taken near STN 23 (see Fig. 1.2). The dashed line show the approximate depths for the 1940, 1970 and 1700 annum dates. Modified from St-Onge et al. (2003).	34
Fig. 2. 1 The Estuary and Gulf of St. Lawrence system in Eastern Canada, showing some of the stations sampled during the R/V Coriolis II, July 2003 cruise.	72
Fig. 2. 2 Dissolved oxygen concentrations (in $\mu\text{mol L}^{-1}$) in the lower 150 m of the Laurentian Channel measured in July 2003.	73
Fig. 2. 3 Historical record of dissolved oxygen concentrations measured between 300 m and 355 m depth in the LSLE. The error bars show the 95% confidence intervals for the means when three or more measurements were made in a given year. The pale grey dot is the average of measurements carried out in 2003. Modified from Gilbert et al. (2004).	74
Fig. 2. 4 Schematic diagram of the advection-diffusion system conceptualized in this study.	75
Fig. 2. 5 Sensitivity of modeled DO concentrations at STN 25 to horizontal advection and horizontal + vertical diffusivity (A) DO vs. u for lines of constant K_z ($\text{cm}^2 \text{ s}^{-1}$) = 1: 9.80 2: 3.47 3: 1.91 4: 0.96 5: 0.64 6: 0.32 7: 0.20 8: 0.10, (B) DO vs. K_z for lines of constant u (cm s^{-1}), the results are too cluttered for proper discernment of specific curves, (C) DO vs. u for lines of constant K_h ($10^6 \text{ cm}^2 \text{ s}^{-1}$) = 1: 7.94 2: 6.35 3: 4.77 4: 3.18 5: 2.80, (D) DO vs. K_h for lines of constant K_z ($\text{cm}^2 \text{ s}^{-1}$) = 1: 9.80 2: 3.47 3: 1.91 4: 0.96 5: 0.64 6: 0.32 7: 0.20 8: 0.10. (Note the different vertical DO scales.)	76
Fig. 2. 6 Comparison between modeled (full lines) and measured (dashed lines) O_2 sediment fluxes for stations 25 (A-B) and 19 (C-D). The input carbon fluxes and output oxygen fluxes are noted on each subplot, the parameter values are: (A-B) sedimentation rate $w = 0.8 \text{ cm/yr}$, bioturbation coefficient $D_B = 13.4 \text{ cm}^2/\text{yr}$, terrigenous organic matter degradation rate constant $k_T = 0.35 \text{ yr}^{-1}$ (C-D) sedimentation rate $w = 0.08 \text{ cm/yr}$, bioturbation coefficient $D_B = 2.68 \text{ cm}^2/\text{yr}$, terrigenous organic matter degradation rate constant $k_T = 0.088 \text{ yr}^{-1}$.	77

Fig. 2. 7 Organic carbon flux scenarios along the Laurentian Channel. (A) High flux scenario based on data acquired from 150 m depth sediment traps. (B) Low flux scenario that reproduces the oxygen fluxes calculated from oxygen gradients measured with voltammetric micro-electrodes across the sediment-water interface on cores recovered along the Laurentian Channel. _____ 78

Fig. 2. 8 Modeled DO values at the bottom of STN 25. (A) Low carbon flux scenario. (B) High carbon flux scenario. The dashed, vertical line represents an average flow velocity of 1 cm s^{-1} . _____ 79

Fig. 2. 9 Water column DO (in $\mu\text{mol L}^{-1}$) concentration isolines and sediment oxygen demand along the Laurentian Channel for (A, C) the low carbon flux scenario and (B,D) the high carbon flux scenario. ___ 80

List of Tables

<i>Table 2. 1 Characteristics of the sampled stations in the Laurentian Channel.....</i>	<i>69</i>
<i>Table 2. 2 Physical parameters used in the hydrodynamic model.</i>	<i>70</i>
<i>Table 2. 3 Compilation of sediment data along the Laurentian Trough.</i>	<i>71</i>

Abstract

Recent measurements of dissolved oxygen (DO) along the Laurentian Trough revealed the presence of hypoxic waters in the bottom 50 meters of the water column of the Lower St. Lawrence Estuary (LSLE). In addition to the change in the oceanic regime on the continental shelf at the mouth of the Gulf of St. Lawrence proposed by others, a large sediment oxygen demand along the LSOLE though to contribute to this DO depletion. To verify the latter hypothesis, I developed a laterally integrated, two-dimensional model of the DO distribution for the bottom waters of the Laurentian Trough. The fluid transport is parameterized in a simple advection-diffusion finite-element grid where the sedimentation of organic matter feeds the mineralization processes that lead to O₂ depletion in the deep waters. Using realistic parameters obtained from field data, the diagenetic model reproduces the measured sediment oxygen demands (SODs) along the Gulf of St. Lawrence portion of the trough but overestimates them in the lower estuary. Since our modeled estuary DO levels are comparable to the measured DO values when a large SOD is applied, we suggest that the oxygen fluxes, calculated from the DO gradients measured with micro-electrodes across the sediment-water interface of cores recovered in the LSOLE, are underestimated.

Résumé

De récentes données d'oxygène dissous présent à la tête du Chenal Laurentien ont révélées la présence d'une masse d'eau hypoxique dans les 50 derniers mètres de la colonne d'eau de l'Estuaire Maritime du Saint-Laurent (EMSL). En plus des changements de régime océanique sur le plateau continental à l'embouchure du Golfe proposés par d'autres chercheurs, une forte demande en oxygène dissous des sédiments le long de l'EMSL est potentiellement responsable de cette diminution en oxygène dissous. Afin de vérifier cette hypothèse, j'ai développé un modèle numérique bi-dimensionnel, intégré latéralement, de la distribution d'oxygène dissous dans les eaux profondes du Saint-Laurent. La paramétrisation du transport des eaux est réduite à une simple équation d'advection-diffusion, alors que la sédimentation de la matière organique mène à la dégradation du carbone organique et ainsi à la diminution d'oxygène dans la colonne d'eau. En utilisant des paramètres réalistes issus de données de terrain, le modèle diagenétique reproduit les flux d'oxygène sédimentaire aux stations du chenal situées dans le Golfe du Saint-Laurent, mais il surestime les flux pour l'estuaire maritime. Puisque nos résultats de la modélisation des niveaux d'oxygène à la tête de l'Estuaire Maritime du Saint-Laurent génère une hypoxie qu'en présence d'une grande demande sédimentaire en oxygène dissous, nous suggérons que les flux d'oxygène calculés à partir des gradients mesurés à l'aide de micro-électrode à l'interface eau-sédiment sur des carottes prélevées dans l'EMSL sont sous-estimés.

Acknowledgements

Finally, a section where I can remain ambiguous.... ahem! Well, firstly I am ever grateful to my supervisor Prof. Alfonso Mucci for rescuing me on the brink of melancholy and giving me the opportunity to work on this project. This has been the best decision of my life. His dedication to his work, great insight, tireless commitment to his students and all-around good humor are what makes him a role model to any future scientist. I am also greatly indebted to my co-supervisor Prof. Yves Gratton for his guidance and criticism throughout this study, his critical attitude towards research and for his encouragements that gave me confidence when solutions were elusive. A student could hardly ask for a better cadre of support than from these gentlemen.

This study would not have been possible without the National Sciences and Engineering Research Council of Canada, which financed my 2 years as a graduate student with a PGS-M fellowship. I also extend my deepest gratitude to Prof. Richard H. Tomlinson and his established McGill graduate fellowships, for which I was an awardee for the past 2 years. I am truly honored to have been a recipient of these scholarships and hope that this thesis makes me somewhat worthy of them. I am also grateful to Dr. Denis Gilbert for doing a thorough review of this work and for providing figures 1.4, 1.5 and 2.3 and the data for figures 1.2 and 2.1.

These two years would not have been as interesting without the support and friendships here in the EPS department, namely my fellow lab mates Cédric, Geneviève, Sandy, Lisa, Sang-Tae, Adrian, Pascale, Constance, Gwen, Shaily, and from all others in the department, particularly Anne, Carol and Crystal. Special thanks to Prof. Bjorn Sundby and Prof. Andrew Hynes for their constructive criticisms and discussions towards my work.

Well, last but not least, special thanks to my parents Serge and Lynn for their love and support, my brother Dave and all my other family and friends (and various dogs) for encouraging me on this endeavor.

Contribution of Authors

This is a manuscript-based thesis. Chapter 1 is a general introduction which provides an overview of the literature concerning the topics presented in this work. Chapter 3 presents the major conclusions resulting from the work and recommendations for future undertakings. Chapter 2 was written in manuscript format and will be submitted to the scientific journal *Marine Chemistry* as authored by Philippe Benoit, Yves Gratton and Alfonso Mucci. I (Philippe Benoit) was responsible for all the scientific work described in the manuscript, as well as the primary author of all texts, tables and figures. Yves Gratton and Alfonso Mucci, both co-supervisor of this M.Sc. project, contributed heavily towards the conception of the models involved, the edition of the manuscript and financed my participation in multiple conferences.

Figure 1.1 is essentially a copied version of figure 2 in:

Koutitonsky, V.G. and Bugden, G.L., 1991. The physical oceanography of the Gulf of St. Lawrence: a review with emphasis on the synoptic variability of the motion. In: J.-C. Therriault (Editor), *The Gulf of St. Lawrence: small ocean or big estuary?* Can. Spec. Publ. Fish. Aquat. Sci., 113 : 57-90.

Professor Koutitonsky has kindly provided the copyright waiver to allow the reproduction of his figure, and it was included with each initial submission of this thesis.

CHAPTER 1

1 General Introduction

1.1 Hypoxia and eutrophication

The rapid expansion of coastal human populations over the last century has placed tremendous pressure on the adjacent marine environments (GESAMP, 2001; US COP, 2004). In this respect, one of the most important impacts of this pressure on water quality has been the proliferation of hypoxic zones along inhabited coastlines (Gray et al., 2002). The major cause of this phenomenon is an increase in the discharge of nitrogen, phosphorus and dissolved organic matter (OM) to coastal waters. In turn, the availability of excess nutrients favors the proliferation of algae beyond their natural levels and to a greater sedimentation rate of particulate organic matter of algal and planktonic origin (Cloern, 2001). This phenomenon is defined as eutrophication by Nixon (1995).

Under pristine conditions, the amount of OM in the water column can be assumed to reflect a steady state between production, grazing, export and degradation processes (Gray et al., 2002). Eutrophication results in an accumulation of OM beyond what can effectively be removed by grazing organisms and exported by physical processes (i.e., lateral advection and sedimentation). Much of the material that settles through the water column and reaches the sediment-water interface is mineralized in a reaction that consumes oxygen from the water column (e.g., Froelich et al., 1979; Berner, 1980; Bender and Heggie, 1984). If the bottom water circulation in the system is restricted and dissolved oxygen (DO) is not replenished fast enough, the oxygen concentrations may decrease to hypoxic (i.e., below $2\text{ ml O}_2\text{ L}^{-1}$ or $62.5\ \mu\text{mol L}^{-1}$, according to Rabalais and Turner (2001)) or even anoxic levels (i.e., no measurable DO) with dramatic consequences on the marine biota. By the end of the 20th century, it became apparent that

the effect of eutrophication and oxygen depletion were becoming widespread in open coastal environments (Nixon, 1990; 1995; Diaz and Rosenberg, 1995; Cloern, 2001; Wu, 2002 GESAMP, 2001; USCOP, 2004).

Hypoxic water masses occur naturally in many parts of the world. Some areas such as the western boundary upwelling systems of the coast of Peru, Walvis Bay in SW Africa and the Horn of Africa (Gray et al., 2002) receive high nutrient inputs from natural sources and have correspondingly low oxygen concentrations in sections the water column. Other aquatic systems such as fjords and deep basins have bathymetric features (e.g., high sills) that inhibit water circulation and renewal, thus they periodically generate and trap low oxygen bottom waters (Nordberg et al., 2001). Whereas hypoxic and anoxic events are documented throughout geological times (e.g. Hoffman and Schrag, 2001), their occurrence in shallow open coastal and estuarine environments as recently been on the increase (Diaz and Rosenberg, 1995). Where the water column is shallow or seasonally stratified, such areas are not hypoxic throughout the year; they are ventilated seasonally through fall and winter mixing events (e.g., shelf region of the northern Gulf of Mexico, Rabalais and Turner (2001)). Likewise, many hypoxic fjords (e.g., Saanich Inlet; Anderson and Devol, 1973) and inland seas (e.g., Baltic Sea; Wulff et al., 1990) are not permanently hypoxic since they can be ventilated by episodic deep water renewal events. In this thesis, I will investigate a possible increase in sediment oxygen mineralization which may have lead to the recent emergence of persistent hypoxia in the Lower St. Lawrence Estuary (Fig. 1.1), a large estuarine system that receives the second largest freshwater discharge ($11900 \text{ m}^3 \text{ s}^{-1}$) in North America (El-Sabh and Silverberg, 1990) and an important entry point for container ships to the mid-West of the U.S.A..

1.2 Hypoxia in the St. Lawrence Estuary

A recent study (Gilbert et al., 2004) has documented the presence of hypoxic waters in the Lower St. Lawrence Estuary (LSLE; between Tadoussac and Pointe-des-Monts, Fig. 1.1) and more specifically in the bottom waters of the Laurentian Channel (LC). The latter is a submarine valley with an average 300 m depth that extends 1240 km

from the NW Atlantic Canadian continental shelf, through the Gulf of St. Lawrence and ends at the mouth of the Saguenay Fjord near a town called Tadoussac, 100 km east of Quebec City (Fig. 1.1). There is no detailed, published record of the LSLE ever harboring hypoxic waters, yet recent measurements of DO in the LSLE have shown that approximately 1300 km² of the seafloor is presently bathed in hypoxic waters (Gilbert et al., 2004). Winkler titrations of deep (i.e., 200-300 m) waters sampled in September 2002 and July 2003 revealed that DO concentrations were less than 65 $\mu\text{mol L}^{-1}$ between Tadoussac and Pointe-des-Monts (i.e., from stations 25 to 21; see Fig. 1.2). The lowest ever recorded DO concentration was measured in July 2003, $51.2 \pm 0.2 \mu\text{mol L}^{-1}$ at 250 m depth on the southern edge of the LC near Rimouski (Fig. 1.3). A recent compilation of archival data revealed that bottom water oxygen concentrations have been steadily decreasing in the LSLE, from levels of about 115-135 $\mu\text{mol L}^{-1}$ in the 1930's to 95-120 $\mu\text{mol L}^{-1}$ in the early 1970's and down to 55-85 $\mu\text{mol L}^{-1}$ in the 1990's (Gilbert et al., 2004; see Fig. 1.4).

1.3 Impact of hypoxia on the biota

Oxygen is one of the basic fuels required by both complex land and marine organisms. Diaz and Rosenberg (1995) define hypoxic waters as having DO concentrations under 2.8 mg O₂ L⁻¹ (91.4 $\mu\text{mol L}^{-1}$) whereas near null DO concentrations characterize anoxic waters. Various definitions of hypoxia can be found in the literature, they are most often related to the effect of oxygen depletion upon the marine biota. For example, waters with DO levels below 2.0 mg O₂ L⁻¹ (62.5 μM) are considered hypoxic in the northern Gulf of Mexico because, at this DO concentration, trawlers rarely capture any fish or other seafood in their nets (Rabalais and Turner, 2001). The 2.0 mg O₂ L⁻¹ (62.5 $\mu\text{mol L}^{-1}$) threshold is the one most commonly used in the literature to define severe hypoxia and the one I refer to from now on in this work. Nevertheless, Breitburg (2002) states that even DO concentrations as high as 50% saturation (i.e., $\sim 160 \mu\text{mol L}^{-1}$ at 5°C and S = 35) can be considered hypoxic because signs of physiological stress appear in some aquatic organisms at this DO level. Generally, fish are more sensitive to reduced oxygen concentrations, followed by annelids and crustaceans, whereas benthic fauna such

as bivalves are the most tolerant (Rosenberg et al., 1991). Aquatic organisms exposed to hypoxic conditions respond by going through multiple phases of adaptation (Wu, 2002). The first stage usually consists of compensation for the decrease in oxygen delivery by increasing gill efficiency and/or hemoglobin content. The second stage sees the organisms restrict their energy output by metabolic depression and a reduction of locomotive alacrity. Lastly, energy can be derived from anaerobic resources as an ultimate option. Consequences of these adaptations usually include a reduction in growth rate, largely due to changes in feeding habits. Mobile marine organisms can detect and subsequently avoid hypoxia by migrating to more oxygenated areas (Breitburg, 2002). On the other hand, more sluggish organisms, such as most of the benthic fauna, will leave their residences deep in the sediment column to reach a more oxygenated region in the water column. Organisms that cannot escape the hypoxic zone will die and be replaced by other, more adapted species, suspension feeders will substitute for deposit feeders, macrobenthos will be supplanted by meiobenthos whereas metazoans, macroflagellates and nanoplanktons will dominate the phytoplankton community (Diaz & Rosenberg, 1995; Cloern, 2001; Wu, 2002). Regardless, the diversity of the fauna is greatly reduced and can take decades to recover if oxygen is replenished (Gray et al., 2002).

More relevant to the LC, numerous studies have been carried out on the tolerance of the Atlantic Cod, *Gadus morhua*, to hypoxia. Once at the foundation of a viable commercial fishery, it is now in danger due to overfishing (Dutil et al., 1999). Studies show a 60% reduction in *G. morhua* locomotive activity and 45% reduction in growth when exposed to waters with less than 45% oxygen saturation (Schurmann and Steffensen, 1994; Chabot and Dutil, 1999). A 90-hour continuous exposure of cod at a DO saturation of 28 % resulted in a 5% mortality of the group, whereas DO levels at 21% saturation resulted in a 50% mortality rate (Plante et al., 1998). Since cod migrate when oxygen levels fall below 40-25% saturation (Wu, 2002), we would expect the bottom waters of the LSLE to be devoid of this animal, thus revealing a grim outcome for its survival in the St. Lawrence region.

1.4 Conditions leading to hypoxia

Conditions leading to the development and persistence of hypoxia are varied but usually fall into a broad range of both chemical and physical processes. Rabalais and Turner (2001) define two major factors in a given coastal environment that will lead to the formation and persistence of a hypoxic region. The first condition requires adequate stratification in the water column so that bottom waters are isolated from normoxic surface waters. Since the most important oxygen producing processes occur in the surface waters (i.e., air/sea exchange and photosynthesis in the euphotic zone), hypoxia will most likely occur when a steep density gradient (pycnocline) partitions the water column (Richardson & Jørgensen, 1998). Areas with persistent anoxic regions, such as the central Baltic (Wulff et al., 1990) and Black seas (Zaitsez, 1992) as well as numerous Swedish and Finnish fjords (Rosenberg et al., 1990; Diaz and Rosenberg, 1995) are characterized by deep basins with limited water exchange, so that replenishment of oxygen is either episodic or simply restricted to molecular diffusion, a very slow process. Furthermore, most of these areas are also subject to anthropogenic inputs of nutrients (Gray et al., 2002). The second factor responsible for the development of hypoxia is the supply of excess reactive OM that serves as a sink for oxygen in the water column through catabolic processes.

1.5 Autochthonous sources of organic matter

The production of excess autochthonous OM can result from loading of nutrients in aquatic systems (Cloern, 2001). The abundance of nutrients favors the growth of phytoplankton which, in turn, leads to an increased export of particulate OM from the surface to the bottom waters and the sediment-water interface. The more reactive OM will drive a sequence of microbially-mediated degradation reactions that oxidize it to CO₂, starting in the water column where the magnitude of this process depends on the residence time of the particulate matter (Timothy, 2004). In shallow marine environments, most of the reactive OM exported from the surface waters is remineralized after it reaches the sediment-water interface, whereas more refractory material may

survive and become permanently buried. The sequential use of terminal electron acceptors is determined by the energy gained through the mineralization process. Oxygen is the most powerful oxidant in aquatic environments and, thus, is used first, followed by nitrate, nitrite, manganese oxides, iron oxides and sulphate (Froelich et al., 1979). Oxidic degradation in organic-rich sediment will deplete oxygen, generate a concentration gradient across the sediment-water interface and induce a direct flux of DO from the water column to the sediment, hereby depleting the water column. As stated earlier, although some aquatic environments naturally receive high nutrient inputs and are characterized by low DO waters (e.g. see Gray et al., 2002), most of the increase in N and P loadings have been recorded in modern times and are due to anthropogenic forcing caused by dramatic population growth along coastal zones (Cloern, 2001; Wu, 2002). Documented areas where an increase in nutrient loading is found with concomitant low oxygen zones include the inner Oslofjord, Norway (Paasche and Erga 1988), the Kattegat (Richardson and Jørgensen, 1996), the Baltic Sea (Wulff et al., 1990), the Dutch and German coastal waters (Reise et al., 1989), the Black Sea (Zaitsev, 1992), Chesapeake Bay (Bratton et al., 2003) and the Gulf of New Mexico (Rabalais and Turner, 2001). In many of these regions, particularly in open coastal environments, hypoxia is a seasonal phenomenon driven by hydrographic and meteorological forcing (Gray et al., 2002).

1.6 Allochthonous sources of organic matter

According to Nixon (1990, 1995), the major sources of allochthonous OM in marine coastal systems are from domestic sewage, industrial effluents (e.g., pulp and paper mills) and soil erosion due to deforestation and expansion of agricultural territories. The bulk composition and reactivity of the total organic carbon in the sedimenting OM is differentiated according to its marine (autochthonous) or terrestrial (allochthonous) origin. Whereas autochthonous particulate organic carbon (POC), such as planktonic cells, faecal pellets, is rich in lipid and proteaceous material (Colombo et al., 1996), allochthonous POC is characterized by its abundance of complex aromatic and cellulosic material, such as humics, lignin and vascular plant debris. This difference in composition translates into a much greater resilience of the terrigenous OM to bacterial degradation and, thus,

increases its likelihood of being buried/preserved within the sediment column (Westrich and Berner, 1994). The lower reactivity of allochthonous material also means that, under similar conditions (i.e., amount of organic carbon and availability of electron-acceptors), this material will generate a lower oxygen demand in the water and sediment column than autochthonous material. Nevertheless, an increase input of terrestrial material to coastal, marine environments will generally contribute to eutrophication through the eventual leaching of nutrients and dissolved OC. It can also significantly alter the nutrient ratios (i.e., Si:N:P) within the aquatic system and have profound ecological effects in coastal waters (e.g., changes in phytoplankton community structure and increases in the frequency of algal blooms) (e.g. Cloern, 2001 and references therein).

Since both physical and biochemical processes can be responsible for the formation of hypoxic waters, each of these must be examined in detail for the LSLE in order to understand how hypoxia developed.

1.7 Physics of the St. Lawrence

The Estuary and Gulf of St. Lawrence (GSL) form part of one of the largest freshwater systems in the world, ranking second in North America behind the Mississippi river basin (El-Sabh and Silverberg, 1990). The Gulf of St. Lawrence is a highly stratified semi-enclosed sea that connects to the Atlantic through Cabot Strait and the Strait of Belle Isle (see Fig. 1.1). As mentioned previously, the major topographic feature of the Estuary is the LC (a.k.a. the Laurentian Trough), the major entry point of deep Atlantic waters to the St. Lawrence system. Koutitonsky and Bugden (1991) define 4 major types of forcing that affect the St. Lawrence system: buoyancy, meteorological, tidal and oceanic. The buoyancy forcing is induced by the continuous supply of freshwater to the surface waters that ultimately drive the estuarine circulation along the LC. Two major regions have been singled out as the sources of freshwater runoff into the GSL system: the St. Lawrence River (referred to as RIVSUM by Koutitonsky and Bugden (1991)) and the lower northern shore rivers. Together, they account for an average freshwater discharge of more than $18900 \text{ m}^3 \text{ s}^{-1}$. The seaward flow of these low

salinity surface waters is balanced by the landward advection of deep, salty oceanic waters, the major input being from the bottom waters of the LC. The meteorological forcing refers to wind stresses from the predominantly easterly winds with a northeast orographic steering due to the Appalachian and Gaspé Peninsula mountains. The combination of buoyancy and meteorological forces generate the main water circulation pattern observed in the GSL, including a broadly cyclonic surface water flow in the central Gulf, outflow into the ocean on the western side of Cabot Strait and inflow on the eastern side, a strong anticyclonic cell in the north-western Gulf near Anticosti Island and a cyclonic cell west of Pointe-des-Monts in the LSLE. The large freshwater runoff at the head of the LC comes into contact with deep Atlantic water upwelled in this region due to the abrupt topographic shoaling. Mixing of the two water masses drives a baroclinic coastal jet along the south shore of the LSLE which, reinforced by the Anticosti gyre, becomes the feature known as the Gaspé Current with a peak velocity of 100 cm s^{-1} around the Gaspé peninsula (Koutitonsky and Bugden, 1991). The tidal characteristics of the GSL and LSLE are mostly generated by non-local tidal forcing in the Atlantic Ocean. The main constituent is the semidiurnal M2 component which propagates cyclonically around the GSL, with its amphidromic point located near the Magdalen Islands. Mean tidal amplitudes vary between 0.2 and 0.5 m in the Gulf, whereas they are roughly 2.5 meters at the mouth of the LSLE and reach 5.5 meters near Québec City. The oceanic forcing parameter refers to the composition of water masses entering the deeper waters of the GSL. Bugden (1991) established that the waters entering the LC at the continental shelf are composed of a mixture, in varying proportions, of Labrador Sea and northwest Atlantic waters (Fig. 1.5) and, thus, the mixture determines the physico-chemical properties of the bottom waters of the GSL.

The LC plays an important role in the physical oceanography of the St. Lawrence because it is the only deep access point for oceanic waters in the GSL system. Fig. 1.6 shows a typical vertical profile of temperature-salinity-density of the water column during the summer season, taken near the city of Rimouski in July 2003. The profile reveals a strongly stratified water column with three distinct layers, schematically represented in Fig. 1.7. The surface layer of roughly 50 m depth is mostly composed of

low salinity waters flowing downriver towards the Atlantic Ocean. The properties of the water in this layer are subject to large temporal variability due to diurnal changes in surface heating, meteorological processes and freshwater discharges. A cold intermediate layer (CIL) extends from 50 m to 150 m depth, its manifestation is seasonal. It forms in the fall and winter and is pushed down when the melting of sea ice, runoff, and subsequent warmer temperatures generate a new, fresher and warmer surface layer. The temperature contrast is greatest in August when the temperature differential between 60 m and the surface can be on the order of 18 degrees (Gilbert and Pettigrew, 1997). The CIL displays yearly variations in thickness and in temperature due to its dependence on climate forcing. Below 150 m depth lies a warmer but saltier layer extending to the bottom that displays only annual to secular variability in its properties due to its separation from the surface by a steep pycnocline (Bugden, 1991). The bottom waters that extend below 200 m show very limited temporal or spatial variability in temperature or salinity (Bugden, 1991; Gilbert et al, 2004) over the length of the Channel. Analysis of the mean deep current measurements (Bugden, 1991) in the LC revealed the dominance of along-channel flows, with a general downriver flow close to the western side of the Channel and an upriver flow on the Eastern side. The mean averaged flow of the bottom waters is landward and was estimated at 0.5 cm s^{-1} in the GSL and LSLE by Bugden (1991). Gilbert (pers. comm.) recently re-estimated the landward flow at 1 cm s^{-1} based on a statistical analysis of 30 years of data on temperature-salinity readings in the Channel, a value supported by the numerical model of Saucier et al. (2003).

1.8 Enhanced horizontal diffusivity

In the previous section, the bottom waters of the LC are described as a laterally-bounded water mass subject to strong cross-channel shear currents that result in a laterally well-mixed water column. Since predicting a tracer distribution in a strongly turbulent channel is nearly impossible, Fischer et al. (1979) used an approach derived by Taylor (1953) to parameterize the flow into a simple advection-diffusion equation. This theory states that once a tracer is added to a fluid undergoing homogeneous turbulent motion and after an initial period of increased spreading, the cloud of tracer dispersion

will grow linearly with time. Under this scenario, derivation of the subsequent tracer dispersion is greatly simplified by allowing the along-channel dispersion to be represented by a Fickian diffusion coefficient. Fischer et al. (1979) applied this concept to mixing in rivers and estuaries and showed that the dispersion can readily be represented by simple advection-diffusion mass-transfer equations if the distance between the initial tracer concentration and the application of Taylor's parameterization is greater than the distance crossed by a flow particle during its Lagrangian time scale. Bugden (1991) extended this reasoning to the LC's deep layer, stating that the strong cross-channel shear from the deep currents allow the parameterization of the bottom Trough waters as the advection-diffusion of the laterally-averaged concentration of a given tracer along the Channel, subject to a weak vertical diffusion due to the strong overlying pycnocline.

1.9 Stratification of the water column and development of hypoxic bottom waters

The hydrological conditions along the LC are conducive to the development of hypoxic bottom waters since these are isolated from the surface waters and the atmosphere by a strong pycnocline and, thus, cannot be readily replenished in oxygen. Consequently, a water parcel being slowly advected along the Trough up to the head will gradually lose its oxygen due to the degradation of OM at or near the sediment-water interface. There is some debate about whether or not significant amounts of respiration occur as OM settles through the deep water column of the LC. Silverberg et al. (2000) assume that only a negligible amount of mineralization occurs between 150 and 300 m depths along the Laurentian Trough, whereas Savenkoff et al. (1996) estimate that up to 40% of the OM exported below the pycnocline is degraded in the water column. The latter results agree with findings by Timothy et al. (2004) who estimated that, on average, 35% of the OC settling through a deep fjord in British Columbia is remineralized in the water column between 150 and 300 m. The impact of this water-born mineralization is mainly dependant on the composition and residence time of the sinking OM particles. In the LC, terrigenous POC sinking rates are estimated at about 10 m day^{-1} (Krone, 1978),

and can reach velocities up to 30-100 m day⁻¹ if they aggregate to biogenic particles during phytoplankton blooms (Syvitski et al., 1985). Marine POC sinks even more rapidly towards the sea floor, with settling rates estimated at 60 to 160 m day⁻¹ (Alldredge and Gotschalk, 1989). In other words, the organic carbon entering the deep layer from above sinks rapidly to the sediment, thus limiting its degradation in the water column. Whereas consideration of this DO sink could allow us to better reproduce the fine-scale structure of the DO profiles in the water column, it should not have any discernable impact in resolving the mass budget in the bottom layer. Following these assumptions, only three major factors are thought to influence the DO concentration of bottom waters in the LSLE: the chemical properties of the oceanic waters entering at the mouth of the LC, the rate at which they are replenished (i.e., landward flow and weak overlying diffusion), and the amount of oxic mineralization taking place at or near the sediment-water interface. If we assume that the age of a parcel of water is defined as the time elapsed since that parcel was last found at the ocean surface and in equilibrium with the atmosphere (i.e., 100% saturated with oxygen), a parcel of water at 250 m depth would be 3 to 5 years old when it reaches the LSLE from the continental shelf (Gilbert et al., 2004). This is a minimum estimate since the age of the same parcel of water at the mouth of the LC must be added to this value. There is, however, no evidence from field data (D. Gilbert, pers. comm.) or hydrodynamic modeling studies (Saucier et al., 2003) that the landward advection velocity of bottom waters has decreased significantly since the 1930s. This observation lead Gilbert et al. (2004) to suggest that the major factor accounting for the decrease of DO concentrations in the LSLE bottom waters was a change in the properties of the water entering the GSL. Their compilation of historical data revealed that, over the past 70 years, a 2.5 degree centigrade warming of the incoming waters was accompanied by a salinity increase of 0.27 and a decrease in DO concentrations of 65 $\mu\text{mol L}^{-1}$. On the basis of these data and consideration of the oceanic regime on the continental shelf at the mouth of the Estuary, they proposed that, over the last 70 years, a greater proportion of warmer, saltier and oxygen-depleted northwest Atlantic ocean waters is being mixed with the colder, fresher and oxygen-rich Labrador current waters that enter the LC, accounting for nearly two thirds of the 65 $\mu\text{mol L}^{-1}$ decrease in DO concentrations observed in the LSLE since the early 1930's

(Gilbert et al., 2004; see Fig. 1.5). Whereas the change in oceanic regime at the mouth of the Estuary accounts for most of the decrease until the early 1980's, there have been only minimal changes in the properties of the waters since then. This is in contrast to the DO gradient between Cabot Strait and the LSLE which has increased by $20.5 \pm 11.9 \mu\text{mol L}^{-1}$ during that period of time. It is important that we seek to explain the remaining DO decline, as without this, the bottom waters of the LSLE would presently have DO levels around $75\text{-}90 \mu\text{mol L}^{-1}$, above the threshold that defines hypoxic waters. The answer may reside in the sediment record.

1.10 Organic carbon fluxes and the sediment record in the Laurentian Channel

The amount of oxic mineralization taking place at or near the sediment-water interface (i.e., the strength of the DO sink in the bottom waters) is mostly determined by the amount and reactivity of the OM delivered to the bottom waters. In turn, the latter are determined by the productivity of the overlying waters, including the availability of nutrients, and the delivery of continental OM. Other important factors influencing the oxygen flux include the DO concentration in the overlying waters, the sediment porosity and temperature. Although no multi-decadal time series of nutrient loading for the St. Lawrence system has been carried out to date, there remains the fact that changes in organic carbon fluxes and nutrient dynamics (i.e., eutrophication) in coastal environments can be recorded in the sediments (e.g., Cloern, 2001). Fig. 1.8 presents profiles from a composite sediment core recovered at a station situated across from Rimouski in the LSLE (STN 23, Fig. 1.2), depicting the depth distribution of organic carbon content (Corg in Fig. 1.8A), organic carbon to nitrogen ratio (C/N in Fig. 1.8B) and the carbon-13 ($\delta^{13}\text{C}$ in Fig. 1.8C) isotopic signature of the Corg since before European settlement. Fig. 1.8A reveals a significant increase in the amount of Corg preserved in the sediment since the 17th century. Fig. 1.8B shows a concomitant increase in the C/N ratio of the OM, indicative of a higher contribution of terrigenous OM to the sediment (Lancelot and Billen, 1985). This increase can be accounted for by the massive deforestation and accompanying soil erosion that followed the arrival of Europeans some 400 years ago.

More recent sources of terrigenous OM include municipal sewage and pulp and paper mill wastewaters, particularly since the 1940's. The isotopic signature of the Corg can further distinguish between its continental (^{13}C -depleted $\sim -27\text{‰}$) and marine (^{13}C -enriched $\sim -20\text{‰}$) origin (Meyers, 1994). The $\delta^{13}\text{C}$ profile (Fig. 1.8C) confirms that up until 1970, the increase in OM flux in the LSLE was mostly from terrestrial sources as its value decreased progressively. After this date and above a depth of ~ 10 cm in the composite core, the isotopic signature of the preserved Corg increases from -24.7‰ to -24.3‰ , suggesting that a greater proportion of marine autochthonous carbon is being delivered to the sediment (St-Onge et al., 2003). The increase may be related to a decrease in municipal sewage and pulp and paper mill discharges to the St. Lawrence River following the implementation of strict government regulations in the early 1970's. Alternatively, the sediment record could reflect a greater flux of allochthonous OM (i.e., primary productivity in the surface waters) resulting from increased nutrient loading in the water column (i.e., eutrophication). The shift in isotopic composition within the sediments around STN 23 was linked to a significant increase in the abundance of dinocysts and organic linings of benthic foraminifera by Thibodeau et al., 2004. Whereas the former could be interpreted as a proxy of increased primary production in the surface waters, the latter may reflect a concomitant increase of benthic production (Thibodeau et al., 2004). The preliminary results from St-Onge et al. (2003) and Thibodeau et al. (2004) are mutually consistent and suggest that within the LSLE, an increase in primary production may have occurred over the last two to three decades. To verify whether or not this trend is due to the eutrophication of the water column will require additional evidence from the sediment record in future research endeavors.

The most recent estimates of OC fluxes and sedimentation rates along the LC are reviewed in the following manuscript chapter. Briefly, there is ample evidence for a direct relationship between the low DO levels observed in the LSLE and the large OC fluxes measured in sediment traps. With respect to the composition of the OM reaching the seafloor, the terrigenous carbon flux dominates over the autochthonous flux at the head of LSLE but decreases exponentially until only negligible amounts reach the seafloor in the Gulf. Conversely, the marine autochthonous flux remains relatively large

throughout the Gulf portion, and is twice as large in the LSLE. These results are a further indication that over-fertilization of the water column possibly occurs within the boundaries of the LSLE, which is potentially correlated with the persistent hypoxic zone.

1.11 Thesis Objectives

In summary, a historical data set (Gilbert et al., 2004) revealed a progressive depletion of DO concentrations in the deep waters of the LSLE within the last 70 years. Concentrations reached as low as $51.2 \pm 0.2 \mu\text{mol L}^{-1}$ in July 2003, well below the threshold value of $62.5 \mu\text{mol L}^{-1}$ that commonly defines severe hypoxia (Rabalais and Turner, 2001). Under these conditions, many fish species, such as cod and flounder, cannot reproduce or even survive for extended periods of time (Plante et al., 1998). Hypoxia in open coastal and estuarine environments is thought to be on the rise due to anthropogenic input of nutrients (nitrates and phosphates) in marine ecosystems. This enrichment favors the growth of phytoplankton and algal-derived OM which eventually sinks through the bottom waters, accumulates at or near the sediment-water interface, and is remineralized through processes that consume oxygen (Cloern, 2001). This phenomenon is known as eutrophication and has been recorded in numerous marine coastal environments around the world, notably in Chesapeake Bay (Bratton et al., 2003), the Kattegat (Richardson and Jørgensen, 1996) and in the shelf region of the northern Gulf of New Mexico (Rabalais and Turner, 2001).

The question then, is: ‘Have the bottom waters of the LSLE become hypoxic as a result of eutrophication?’

In a preliminary effort to answer this question, I elaborated a numerical model that couples water transport within the deep LC with an early diagenetic model of oxic OM mineralization in the sediment. Attempts to model eutrophication and, hence, DO depletion have been numerous using both analytical (e.g. Visser and Kamp-Nielsen, 1996; Kauppila et al., 2003) and numerical solutions (e.g. Park et al., 1996). The common link between all these models is their strict dependence on the specific

characteristics of the study area, i.e. the parameters and processes used in the coupling between the water and sediment columns may not apply to other regions of interests. Since no such model, to our knowledge, has ever been elaborated for the St. Lawrence Estuary, our first objective was to model the most obvious consequence of eutrophication which, according to Gray et al. (2002), is the hypoxia resulting from the degradation of sedimenting particulate OM. This required the parameterization of the fluid transport processes along the Laurentian Through in an advection-diffusion finite-element grid. The flow system is 2-D in which sedimentation of OM feeds the processes that lead to O₂ depletion in the deep waters. Two major types of OM are considered in this study: a fast-reacting marine component which mostly comes from the dead algal and planktonic material in the water column and a more refractory terrestrial component originating mostly from continental river discharges. To counter balance the OM oxygen sink, two sources are considered: weak diffusion from the overlying water and the deep, landward mean circulation that continuously brings O₂-rich waters from the Atlantic. The model was designed to represent a good initial attempt in balancing the inherent complexities of the physico-chemical processes involved and the need to minimize computational expenses (for a more detailed discussion of this subject the reader is referred to Soetaert et al., 2000).

In the formulation of this model and ultimately by its results, I aimed to answer the following objectives, best described in point form:

- Test the sensitivity of the water column with respect to DO levels to the following physical parameters: advection (horizontal) and diffusion (horizontal and vertical).
- Determine the organic carbon flux required to reproduce, to a first approximation, the DO profiles measured across the sediment-water interface from sediment cores recovered along the Laurentian Trough.
- Develop realistic scenarios of organic carbon fluxes to the sediment along the Laurentian Channel based on other proxies (i.e., OC burial rates, sediment trap measurements, primary productivity of the overlying waters) and distinguish between terrestrial and marine components.

- Ascertain whether or not the sediment oxygen demand resulting from the above-mentioned OC flux scenarios can reproduce the recently observed hypoxic DO levels in the LSLE.

Details of the model and its implementations are described in the next chapter which will be submitted to the journal *Marine Chemistry*. Finally, the third chapter contains a more general conclusion in which I explain how each of the objectives were met and offer ideas on how to refine the model and make it more realistic.

1.12 Figures

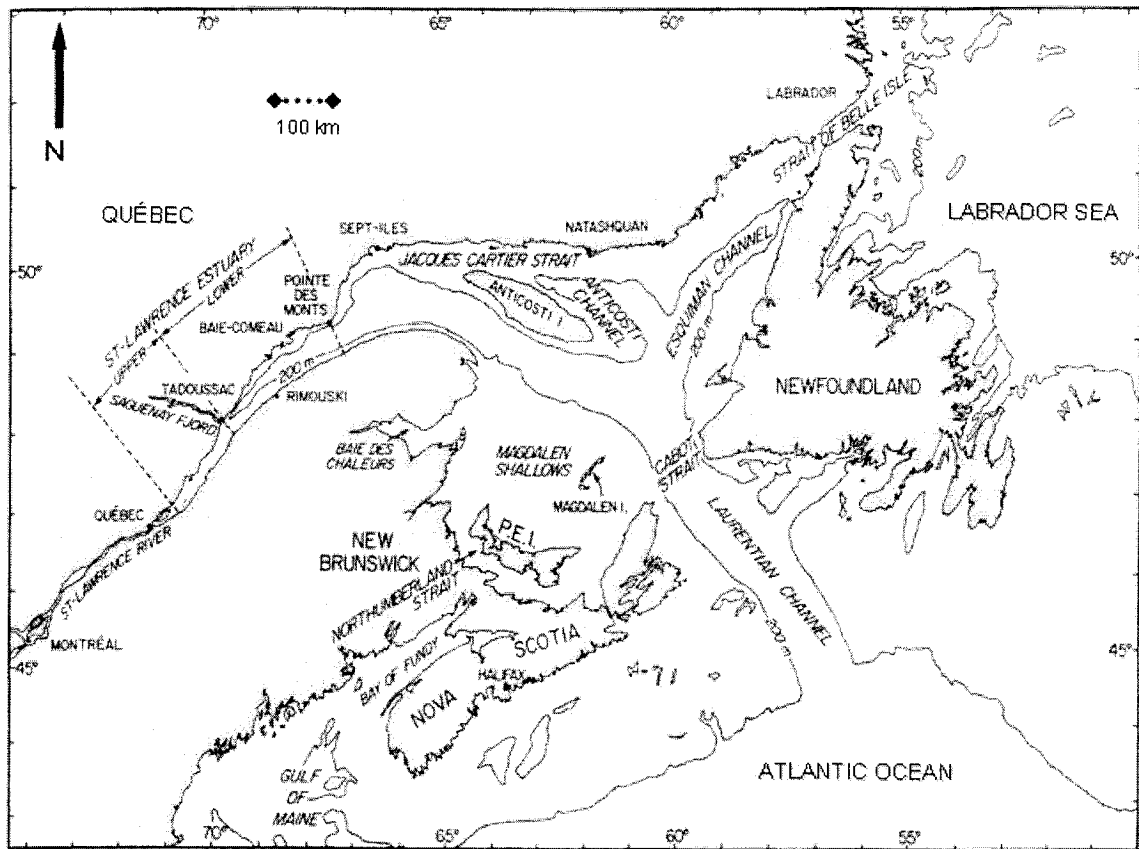


Fig. 1.1 The Estuary and Gulf of St. Lawrence system, showing the location of important topographic features such as the upper and lower estuaries, the Laurentian Channel and Cabot Strait. Modified from Koutitonsky and Bugden (1991).

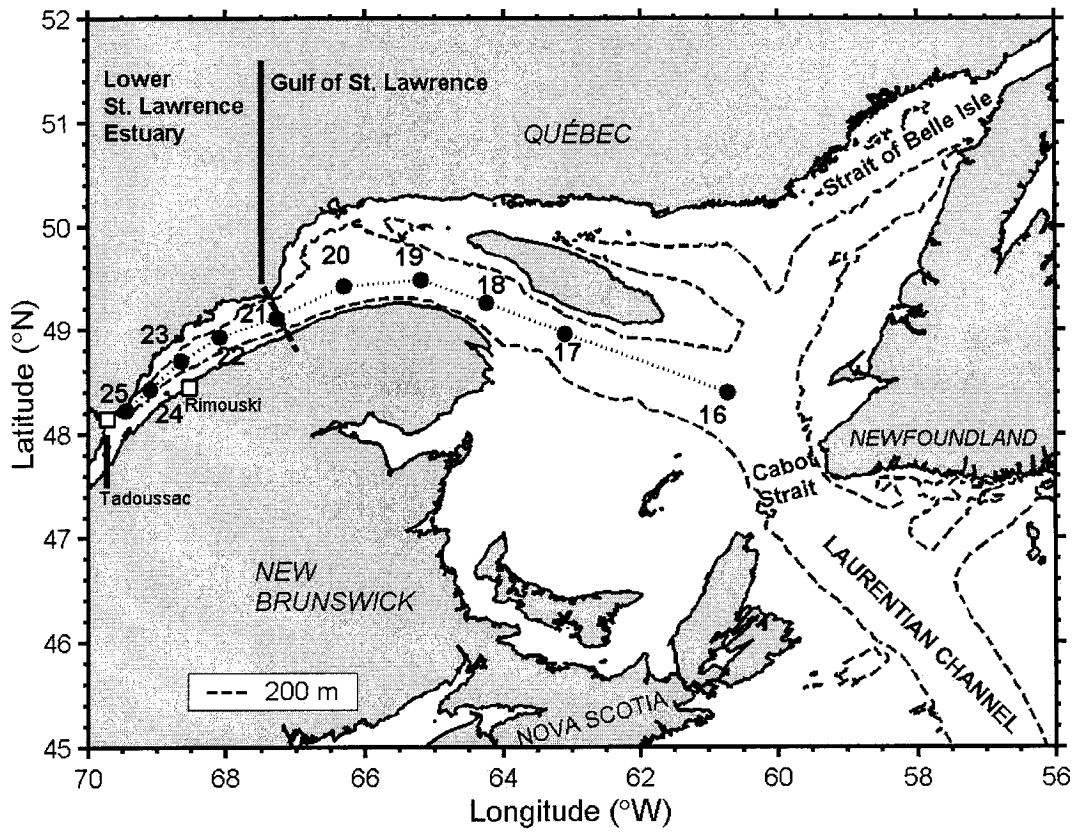


Fig. 1. 2 Map of the LSLE-GSL showing some of the stations sampled during the R/V Coriolis II, July 2003 cruise.

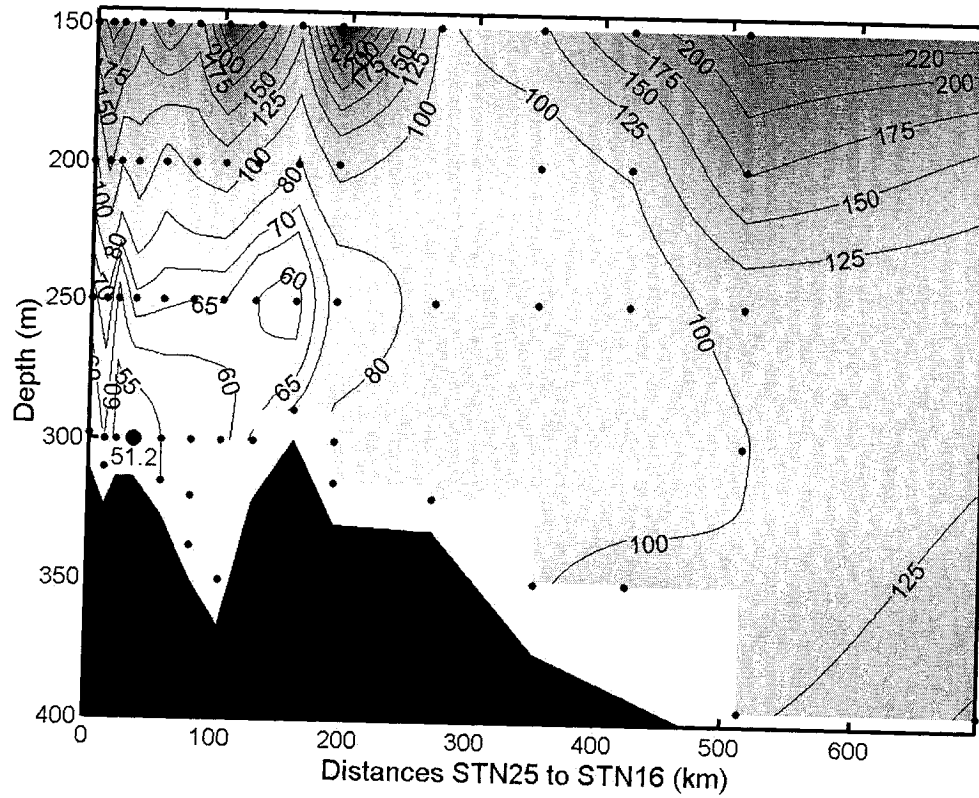


Fig. 1. 3. Dissolved oxygen (in $\mu\text{mol L}^{-1}$) in the lower 150 m of the Laurentian Channel between stations 25 and 16. Samples were taken and analyzed in July, 2003. The lowest measured value ($51.3 \pm 0.2 \mu\text{mol L}^{-1}$) is highlighted in black.

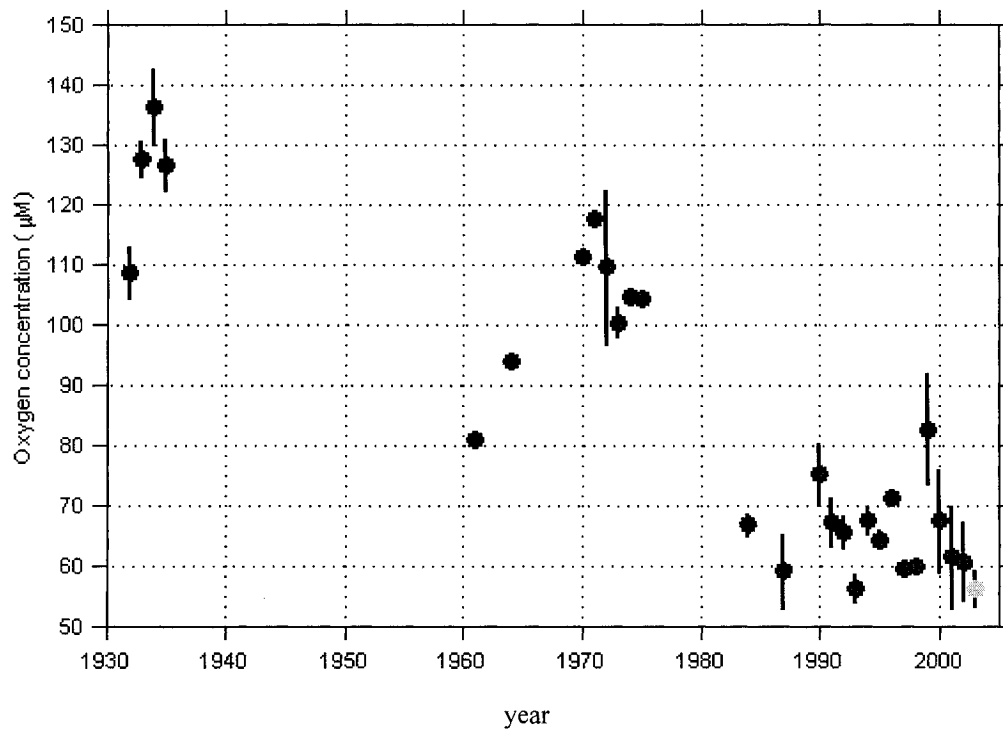


Fig. 1. 4 Historical record of dissolved oxygen concentrations measured between 300 m and 355 m depth in the LSLE. The error bars show the 95% confidence intervals for the means when three or more measurements were made in a given year. The pale grey dot is the average of measurements carried out in 2003. Modified from Gilbert et al. (2004).

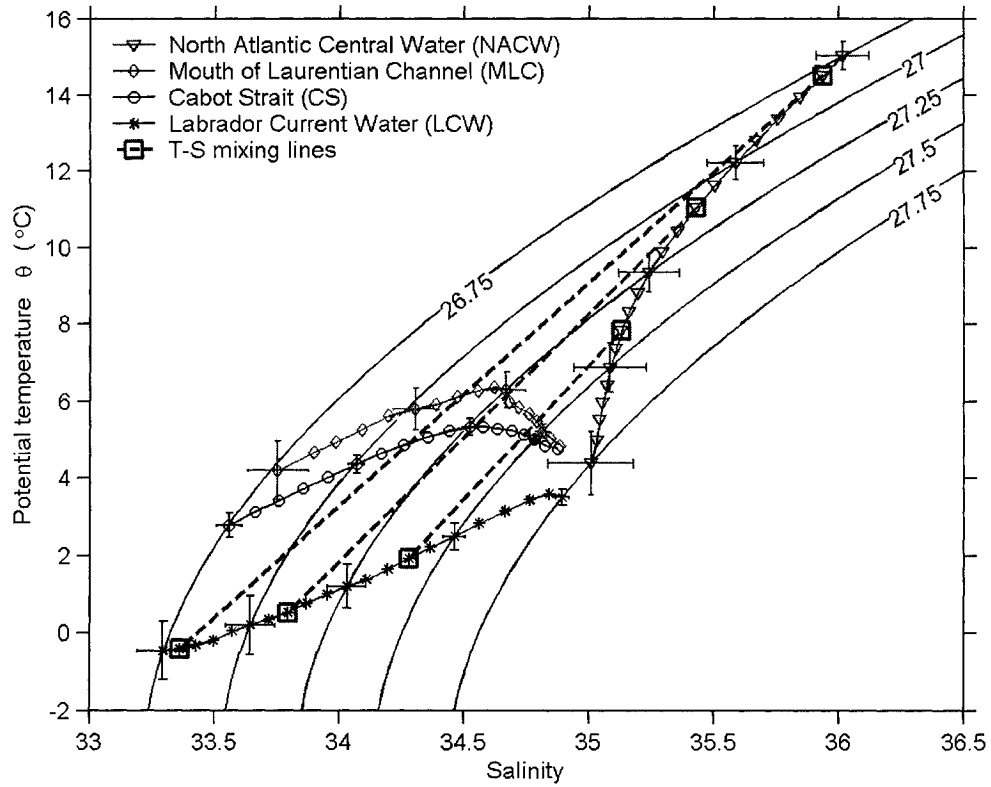


Fig. 1. 5 Temperature-salinity (T-S) diagram of the two parent water masses, Labrador Current Water (LCW) and North Atlantic Central Water (NACW). On each water mass T-S curve are superimposed the inter-annual standard deviations of temperature and salinity at intervals of 0.25 kg m⁻³. The dashed lines represent a T-S mixing line joining LCW and NACW source water types. Modified from Gilbert et al. (2004).

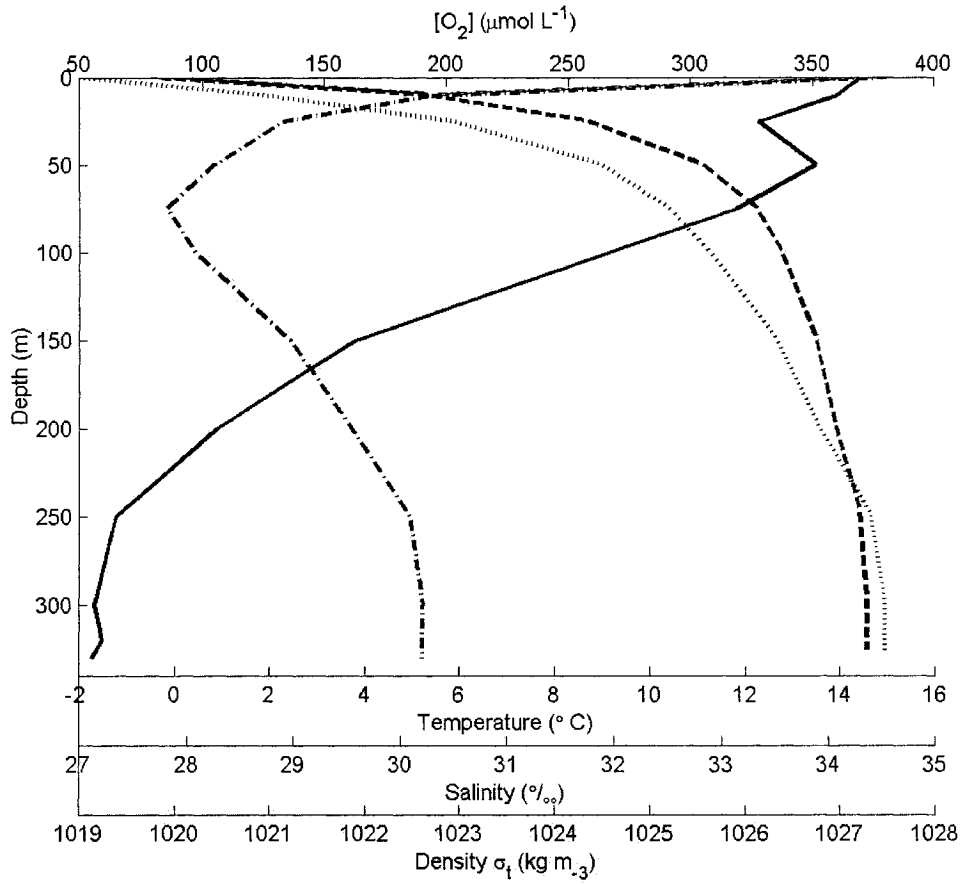


Fig. 1. 6 Water column profiles of dissolved oxygen (solid line), temperature (dash-dotted line), salinity (dotted line) and density (dashed line) taken at STN 23 in July 2003.

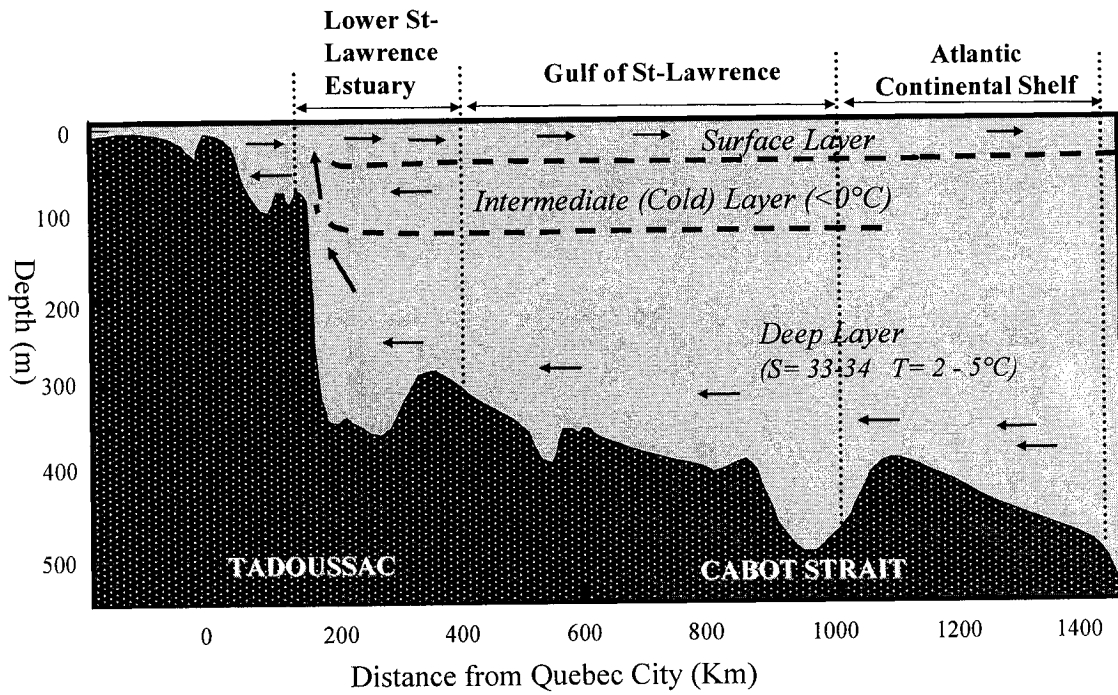


Fig. 1. 7 Vertical cross-section of the Laurentian Channel showing the location and flow direction of the different water masses. Modified from Dickie and Trites (1983).

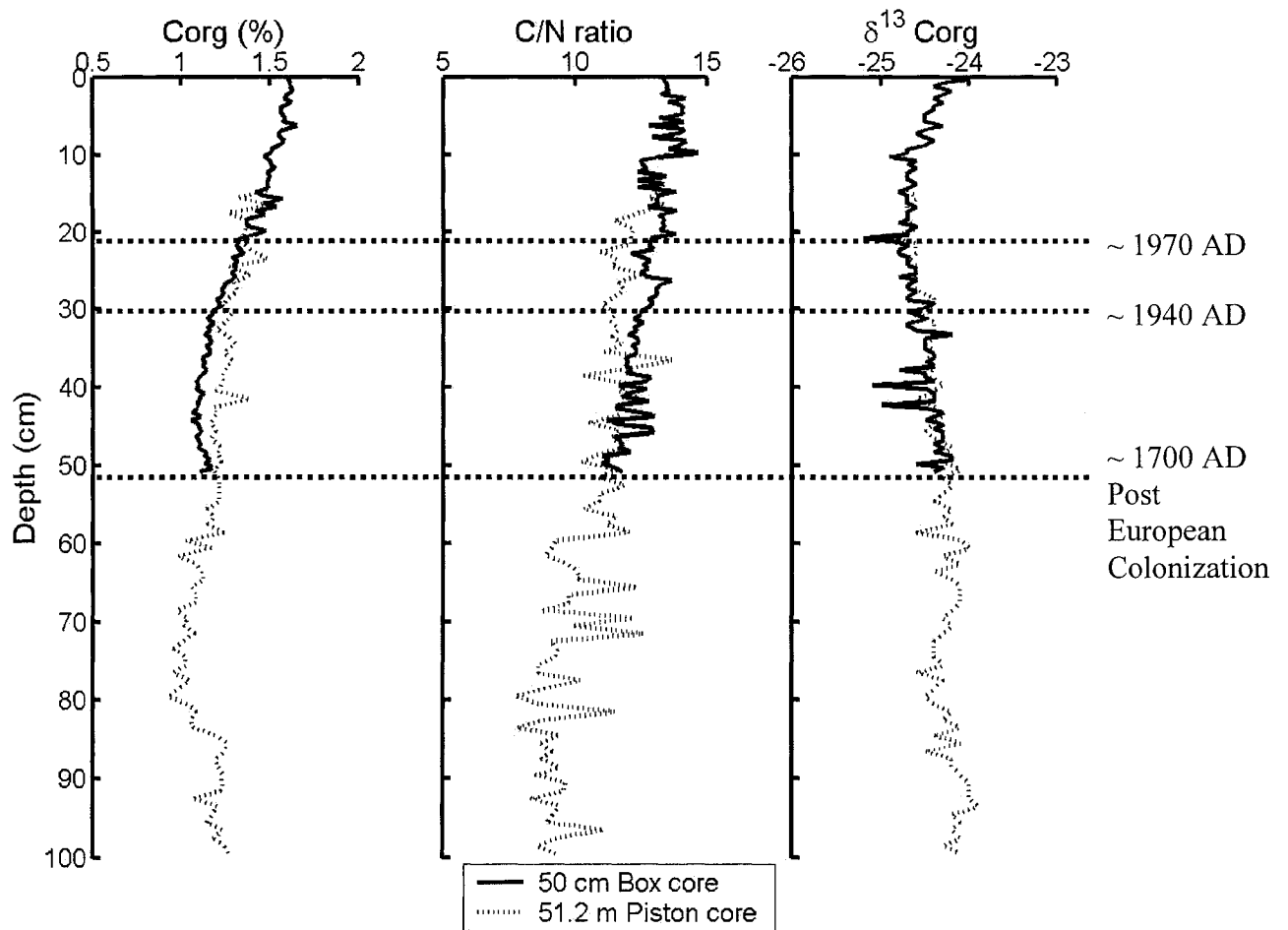


Fig. 1. 8 (A) Percentage of organic carbon content, (B) organic carbon/nitrogen molar ratio and (C) carbon-13 isotopic signature (‰) as a function of sediment depth in composite sediment core of box core AH00-2220 and piston core MD2220, taken near STN 23 (see Fig. 1.2). The dashed line show the approximate depths for the 1940, 1970 and 1700 annum dates. Modified from St-Onge et al. (2003).

1.13 References

- Allredge, A.L. and Gotschalk, C.C., 1989. Direct observations of the mass flocculation of diatoms blooms: characteristics, settling velocities and formation of diatom aggregates. *Deep-Sea Research I*, 36: 159-171.
- Anderson, J.J. and Devol, A.H., 1973. Deep water renewal in Saanich Inlet, an intermittently anoxic basin. *Estuarine and Coastal Marine Science*, 1: 1-10.
- Bender, M.L. and Heggie, D.T., 1984. Fate of organic carbon reaching the deep sea floor: a status report. *Geochimica et Cosmochimica Acta*, 48: 977-986.
- Berner, R.A., 1980. *Early diagenesis: A theoretical approach*. Princeton University Press, Princeton, NJ.
- Bratton, J.F., Colman, S.M. and Seal, R.R., 2003. Eutrophication and carbon sources in Chesapeake Bay over the last 2700 yr: Human impact in context. *Geochimica et Cosmochimica Acta*, 67: 3385-3402.
- Breitburg, D., 2002. Effects of hypoxia, and the balance between hypoxia and enrichment, on coastal fishes and fisheries. *Estuaries*, 25: 767-781.
- Bugden, G.L., 1991. Changes in the temperature-salinity characteristics of the deeper waters of the Gulf of St. Lawrence over the past several decades. In: J.-C. Therriault (Editor), *The Gulf of St. Lawrence: small ocean or big estuary?* Can. Spec. Publ. Fish. Aquat. Sci., 113 : 139-147.
- Chabot, D. and Dutil, J.-D., 1999. Reduced growth of Atlantic cod in non-lethal hypoxic conditions. *Journal of Fish Biology*, 55: 472-491.
- Cloern, J.E., 2001. Our evolving conceptual model of the coastal eutrophication problem. *Marine Ecology Progress Series*, 210: 223-253.
- Colombo, J.C., Silverberg, N. and Gearing, J.N., 1996. Biogeochemistry of organic matter in the Laurentian Trough, I. Composition and vertical fluxes of rapidly settling particles. *Marine Chemistry*, 51: 277-293.
- Diaz, J.R. and Rosenberg, R., 1995. Marine benthic hypoxia: a review, its ecological effects and the behavioural responses of benthic macrofauna. *Oceanography and Marine Biology Annual Review*, 33: 245-303.
- Dickie, L. and Trites, R.W., 1983. The Gulf of St. Lawrence. In: B.H. Ketchum (Editor), *Estuaries and semi-enclosed seas*. Elsevier Scientific Publication, Amsterdam, pp. 403-425.

- Dutil, J.-D., Castonguay, M., Gilbert, D. and Gascon, D., 1999. Growth, condition and environmental relationships in Atlantic cod (*Gadus morhua*) in the northern Gulf of St. Lawrence and implications for management strategies in the northwest Atlantic. *Canadian Journal of Fisheries and Aquatic Science*, 56: 1818-1831.
- Fisher, H.B., List, E.J., Koh, R.C.Y. and J., I., 1979. *Mixing in inland and coastal waters*. Academic Press, New York, NY.
- Froelich, P.N., Klinkhammer, G.P., Bender, M.L., Luedtke, N.A., Heath, G.R., Cullen, D., Dauphin, P., Hammond, D., Hartman, B. and V., M., 1979. Early oxidation of organic matter in pelagic sediments of the eastern equatorial Atlantic: suboxic diagenesis. *Geochimica et Cosmochimica Acta*, 43: 1075-1090.
- GESAMP, 2001. *A sea of troubles*. GESAMP Rep Stud 70, 1-35.
- Gilbert, D. and Pettigrew, B., 1997. Interannual variability (1948-1994) of the CIL core temperature in the Gulf of St. Lawrence. *Canadian Journal of Fisheries and Aquatic Science*, 54: 57-67.
- Gilbert, D., Sundby, B., Gobeil, C., Mucci, A. and Tremblay, G.H., 2004. A seventy-year record of diminishing deep-water oxygen levels in the St. Lawrence estuary - the northwest Atlantic connection. *Limnology and Oceanography*, (*in press, accepted with minor revisions Nov, 2004*).
- Gray, J.S., Wu, R.S.-S. and Or, Y.Y., 2002. Effects of hypoxia and organic enrichment on the coastal marine environment. *Marine Ecology Progress Series*, 238: 249-279.
- Hoffman, P.F. and Schrag, D.P., 2002. The snowball Earth hypothesis: testing the limits of global change. *Terra Nova*, 14: 129-155.
- Kaupila, P., Meeuwig, J.J. and Pitkänen, H., 2003. Predicting oxygen in small estuaries of the Baltic Sea: a comparative approach. *Estuarine, Coastal and Shelf Science*, 57: 1115-1126.
- Koutitonsky, V.G. and Bugden, G.L., 1991. The physical oceanography of the Gulf of St. Lawrence: a review with emphasis on the synoptic variability of the motion. In: J.-C. Therriault (Editor), *The Gulf of St. Lawrence: small ocean or big estuary?* Can. Spec. Publ. Fish. Aquat. Sci., 113 : 57-90.
- Krone, R.B., 1978. Aggregation of suspended particules in estuaries. In: B. Kjerfve (Editor), *Estuarine transport processes*. University of South Carolina Press, pp. 177-190.

- Lancelot, C. and Billen, G., 1985. Carbon-nitrogen relationships in nutrient metabolism of coastal marine ecosystems. *Advances in Aquatic Microbiology*, 3: 263-321.
- Meyers, P.A., 1994. Preservation of elemental and isotopic source identification of sedimentary organic matter. *Chemical Geology*, 114: 289-302.
- Nixon, S.W., 1990. Marine eutrophication: a growing international problem. *Ambio*, 19: 101.
- Nixon, S.W., 1995. Coastal marine eutrophication: a definition, social causes, and future concerns. *Ophelia*, 41: 199-220.
- Nordberg, K., Filipsson, H.L., Gustafsson, M., Harland, R. and Roos, P., 2001. Climate, hydrographic variations and marine benthic hypoxia in Koljoe Fjord, Sweden. *Journal of Sea Research*, 46: 187-200.
- Paasche, E. and Erga, S.R., 1988. Phosphorous and nitrogen limitations of phytoplankton in the inner Oslofjord (Norway). *Sarsia*, 73: 229-243.
- Park, K., Kuo, A.Y. and Neilson, B.J., 1996. A numerical model study of hypoxia in the tidal Rappahannock river of Chesapeake Bay. *Estuarine, Coastal and Shelf Science*, 42: 563-581.
- Plante, S., Chabot, D. and Dutil, J.-D., 1998. Hypoxia tolerance in Atlantic cod. *Journal of Fish Biology*, 53: 1342-1356.
- Rabalais, N.N. and Turner, R.E., 2001. Hypoxia in the Northern Gulf of Mexico: Description, Causes and Change. In: N.N. Rabalais and R.E. Turner (Editors), *Coastal Hypoxia: consequences for living resources and ecosystems*. American Geophysical Union, Washington, D.C., pp. 1-37.
- Reise, K., E., H. and Sturm, M., 1989. Historical changes in the benthos of the Wadden Sea around the island of Sylt in the North Sea. *Helgol Wiss Meeresunters*, 43: 417-433.
- Richardson, K. and Jørgensen, B.B., 1996. Eutrophication: Definition, History and Effects. In: K. Richardson and B.B. Jørgensen (Editors), *Eutrophication in Coastal Marine Ecosystems*. American Geophysical Union, Washington, D.C., pp. 1-21.
- Rosenberg, R., Elmgren, R., Fleischer, S., Jonsson, P., Persson, G. and Dahlin, H., 1990. Introduction - marine eutrophication in Sweden. *Ambio*, 19: 102-108.
- Rosenberg, R., Hellman, B. and Johansson, B., 1991. Hypoxic tolerance of marine benthic fauna. *Marine Ecology Progress Series*, 79: 127-131.

- Saucier, F.J., Roy, F., Gilbert, D., Pellerin, P. and Ritchie, H., 2003. Modeling the formation and circulation processes of water masses and sea ice in the Gulf of St. Lawrence, Canada. *Journal of Geophysical Research*, 108: 3269-3289.
- Savenkoff, C., Vézina, A.F., Packard, T.T., Silverberg, N., Therriault, J.-C., Chen, W., Bérubé, C., Mucci, A., Klein, B., Mesplé, F., Tremblay, J.-E., Legendre, L., Wesson, J. and Ingram, R.G., 1996. Distributions of oxygen, carbon, and respiratory activity in the deep layer of the Gulf of St. Lawrence and their implications for the carbon cycle. *Canadian Journal of Fisheries and Aquatic Science*, 53: 2451-2465.
- Schurmann, H. and Steffensen, J.F., 1994. Spontaneous swimming activity of Atlantic cod *Gadus morhua* exposed to graded hypoxia at three temperatures. *Journal of Experimental Biology*, 197: 129-142.
- Silverberg, N., Sundby, B., Mucci, A., Zhong, S., Arakaki, T., Hall, P., Landén, A. and Tengberg, A., 2000. Remineralization of organic carbon in eastern Canadian continental margin sediments. *Deep-Sea Research II*, 47: 699-731.
- Soetaert, K., Middelburg, J.J., Herman, P.M.J. and Buis, K., 2000. On the coupling of benthic and pelagic biogeochemical models. *Earth-Science Reviews*, 51: 173-201.
- St-Onge, G., Stoner, J.S. and Hillaire-Marcel, C., 2003. Holocene paleomagnetic records from the St. Lawrence Estuary, eastern Canada: centennial to millennial-scale geomagnetic modulation of cosmogenic isotopes. *Earth and Planetary Sciences Letters*, 209: 113-130.
- Syvitski, J.P.M., 1989. Quaternary sedimentation in the St. Lawrence Estuary and adjoining areas, eastern Canada: an overview based on high resolution seismography. *Géographie Physique et Quaternaire*, 43: 291-310.
- Taylor, G.I., 1953. Dispersion of soluble matter in solvent flowing slowly through a tube. *Proceedings of the Royal Society of London. Series A.*, 219: 186-203.
- Thibodeau, B., de Vernal, A. and Mucci, A., 2004. Development of micropaleontological and geochemical indicators of eutrophication in the St. Lawrence Estuary. Abstract, Spring AGU meeting, May 17-21, Montreal, QC, Canada,
- Timothy, D.A., 2004. Organic matter remineralisation and biogenic silica dissolution in a deep fjord in British Columbia, Canada: a regression analysis of upper ocean sediment-trap fluxes. *Deep-Sea Research I*, 51: 439-456.
- Visser, A.W. and Kamp-Nielsen, L., 1996. The Use of Models in Eutrophication Studies. In: K. Richardson and B.B. Jørgensen (Editors), *Eutrophication in Coastal Marine Ecosystems*. American Geophysical Union, Washington, D.C., pp. 221-243.

- Westrich, J.T. and Berner, R.A., 1984. The role of sedimentary organic matter in bacterial sulfate reduction: The G model tested. *Limnol. Oceanogr.*, 29: 236-249.
- Wu, R.S.-S., 2002. Hypoxia: from molecular responses to ecosystem responses. *Marine Pollution Bulletin*, 45: 35-45.
- Wulff, F., Stigebrandt, A. and Rahm, L., 1990. Nutrient dynamics of the Baltic Sea. *Ambio*, 19: 126-133.
- Zaitsev, Y.P., 1992. Recent changes in the trophic structure of the Black Sea. *Fisheries Oceanography*, 1: 180-189.

CHAPTER 2

2 Modeling of dissolved oxygen levels in the bottom waters of the Lower St. Lawrence Estuary: coupling of benthic and pelagic processes.

Philippe Benoit ^{a*}, Yves Gratton ^b and Alfonso Mucci ^a

^a *Department of Earth and Planetary Sciences, McGill University, 3450 Université,
Montréal, QC, Canada H3A 2A7*

^b *INRS-ETE, Université du Québec, 490 de la Couronne, Québec, QC, Canada G1K 9A9*

2.1 Abstract

Recent measurements of dissolved oxygen (DO) along the Laurentian Trough in Eastern Canada revealed the presence of hypoxic waters in the bottom 50 meters of the water column. At hypoxic oxygen levels, many fish species cannot survive or reproduce, and the microbial life community undergoes significant modifications. A large sediment oxygen demand along the Lower St. Lawrence Estuary (LSLE) is proposed as the possible cause of this DO depletion. To verify this hypothesis, a laterally integrated, two-dimensional model of the DO distribution was implemented for the bottom waters of the

* Present address: *School of Earth and Ocean Sciences, University of Victoria, P.O. Box 3055 STN CSC, Victoria, BC, Canada V8W 3P6* E-Mail: pb@uvic.ca

Laurentian Trough along a transect of stations sampled in July 2003. The fluid transport was parameterized in a simple advection-diffusion finite-element grid where sedimentation of organic matter (OM) feeds the processes that lead to O₂ depletion in the deep waters. Two major types of OM are considered in this study: a fast-reacting marine component that originates from autochthonous material produced in surface waters, and a more refractory terrestrial component from continental river discharges. To counterbalance the OM oxygen sink, the deep, landward mean circulation continuously brings O₂-rich waters from the Atlantic. Both the DO and the early diagenesis model parameters were calibrated using field data collected between 1985 and 2003. Our physical parameter sensitivity study indicates that vertical diffusion from the oxygenated upper water column has the greatest impact on deep DO concentrations. The diagenetic model reproduces the oxygen penetration depths and fluxes very well along the Gulf of St. Lawrence portion of the trough but overestimates the sediment oxygen demand in the LSLE. We propose that the sediment oxygen demands calculated from DO gradients measured by micro-electrode across the sediment-water interface of cores retrieved in the Lower St. Lawrence Estuary are underestimated.

2.2 Introduction

Coastal environments that display water column dissolved oxygen (DO) deficiencies are becoming more prevalent due to anthropogenic nutrient loading and the ensuing eutrophication of the water system (Nixon, 1995; Diaz and Rosenberg, 1995; Cloern, 2001; Gray et al., 2002). As the DO levels decrease, many aquatic organisms will retreat from these waters whereas benthic community assemblages will be modified (Breitburg, 2002; Gray et al., 2002; Wu, 2002). Severe hypoxia is defined as the threshold below which significant impacts on the biota are observed and corresponds to DO levels below 62.5 $\mu\text{mol L}^{-1}$ or 2 mg/L (Rabalais and Turner, 2001). The proliferation of hypoxic and anoxic (i.e. no measurable DO) areas along inhabited coastlines is considered one of the most critical environmental problems menacing marine ecosystems in modern times (GESAMP, 2001; USCOP, 2004).

Recent measurements of DO along the Laurentian Channel (LC) of the Lower St. Lawrence Estuary (LSLE; see Fig. 2.1) in Eastern Canada revealed the presence of persistent, year-round hypoxic waters in the bottom 50 meters of the water column, with concentrations as low as $51.2 (\pm 0.2) \mu\text{mol L}^{-1}$ (16.2 % saturation) recorded in July 2003 (Fig. 2.2). A limited set of historical data (Fig. 2.3) reveals that DO levels have been decreasing for at least the last 70 years, with a trend perhaps evolving towards anoxia within the next few decades (Fig. 2.3; Gilbert et al., 2004). The area presently bathed in hypoxic waters is estimated at more than 1300 km^2 . Recent studies (Plante et al., 1998) have shown that the continuous exposure of Atlantic cod (*Gadus morhua*), a species common to the St. Lawrence ecosystem, to similar DO levels (i.e., 21% saturation) for 96 hours will result in the death of 50% of the fish. Accordingly, the presence of a hypoxic region in the LSLE may already have had profound negative impacts on this marine ecosystem and the Canadian economy since, historically, the Estuary and Gulf of St. Lawrence account for 25% of the total Canadian fish landings of the Canadian eastern sea-board (Dickie and Trites, 1983).

The St. Lawrence maritime system, including the Gulf of St. Lawrence (GSL) and the LSLE (see Fig. 2.1), forms part of a semi-enclosed sea characterized by an estuarine circulation that is generated by freshwater runoff from the Great Lakes, St. Lawrence and Northern Quebec river drainage systems (El-Sabh and Silverberg, 1990). The GSL is connected to the Atlantic Ocean by two major openings, Cabot Strait and the Strait of Belle-Isle. The former is one order of magnitude wider and deeper than the latter and is the only significant entry point for deep North Atlantic waters into the Gulf (Koutitonsky and Bugden, 1991). The dominant bathymetric feature of the St. Lawrence system is the LC (or Laurentian Trough), a deep submarine valley (250-500 m deep) that extends over 1240 km from the eastern Canadian continental margin up to the confluence of the St. Lawrence Estuary and the Saguenay Fjord. From Cabot Strait up to the mouth of the LSLE (i.e., Pointe-des-Monts), the width of the LC remains relatively constant at over 100 km. Beyond this point it narrows progressively to the head of the LSLE. Throughout most of the year, the water column in the LC is characterized by three

distinct layers (Dickie and Trites, 1983): (1) a thin surface layer (25-50 m) of low salinity (27-32) with a seaward flow, (2) an intermediate cold ($-1 - 2^{\circ}\text{C}$) and saline (31.5-33) layer which extends from about 50 to 150 m, and (3) a warmer ($4-6^{\circ}\text{C}$) and saltier (34.4-34.6) deep layer (150+ m), a nearly continuous water mass that extends to the bottom. The surface layer displays large seasonal variations in temperature and salinity due to climatic and gravitational (i.e., runoff events) forcing. The intermediate layer merges with the surface layer in winter to form one uniform layer over most of the GSL and LSLE (Gilbert et al, 1997). The deep waters are a mixture of Labrador Current and North Atlantic waters in proportions and whose properties were found to vary on a decadal or secular timescale (Bugden, 1991; Gilbert et al., 2004).

Hypoxia occurs naturally in fjords, inland seas and deep basins whose bathymetric features (e.g. high sills) restrict water circulation and the renewal of bottom waters (e.g. Nordberg, 2001). The development of hypoxic waters in shallow or seasonally stratified, open coastal and estuarine environments (e.g. the Gulf of New Mexico, Rabalais et al, 2001) as a result of eutrophication has been on the rise but such areas are not hypoxic throughout the year since they are typically ventilated through Fall and Winter mixing events. In contrast, the hypoxic region in the LSLE is a persistent feature that appears to be a geologically recent phenomenon (Gilbert et al., 2004). The oxygen deficient area is confined within the bottom waters of the LC and is isolated from the normoxic upper layers by a steep density gradient that only allows weak diffusion of oxygen through its boundary. Given the simple hydrodynamic regime of the deep layer, Gilbert et al. (2004) identified three factors that might be responsible for the emergence of hypoxic bottom waters in the LSLE: (1) a change in the properties of the oceanic water mass at the edge of the continental shelf that supplies the deep water to the LC, (2) an increase in the flux of terrigenous and/or marine organic matter (OM) to the seafloor of the LC and, (3) a decrease in the mean landward flow velocity and increase in the residence time of the deep waters in the LC. The latter was discounted because there is no evidence from field data (D. Gilbert, pers. comm.) or hydrodynamic modeling studies (Saucier et al., 2003) that the landward advection velocity of bottom waters has decreased significantly from the 1930s to the mid-1980s. The authors (Gilbert et al., 2004) demonstrated that an

increase in the temperature of oceanic waters at the continental margin boundary of the LC could account for roughly two thirds of the observed decrease in oxygen concentrations in the LSLE whereas the remainder of the decrease in DO levels was ascribed to an increase in OM export to the seafloor of the LC since European settlement.

In this paper, we present results of a preliminary modeling effort to constrain the DO budget in the deepest layer of the LSLE. Because of the inherent complexities to factor in all the possible causes of eutrophication in a given numerical model, we limited ourselves to the most obvious consequence of eutrophication which, according to Gray et al. (2002), is the development of hypoxic waters resulting from the degradation of sedimenting particulate organic carbon (POC). The proper question to ask then is: ‘Can the present sediment oxygen demand (SOD) along the seafloor of the Laurentian Channel account the recent development of hypoxic waters in the LSLE?’ To answer this question, we constructed a 2-D advection-diffusion model for the deep layer of the LC, subject to varying fluxes of organic carbon (OC) at the sediment-water interface and, through catabolic processes, concomitant sinks of DO for the water column. In the following two sections, we describe, in detail, the physical and chemical parameterizations of the model whereas the last two sections focus on the model results following a physical parameter sensitivity analysis carried out under varying OC flux regimes. We then present a discussion of the results and conclude with possible future undertakings.

2.3 Water column parameterization

The system considered is a 2-D representation of the deep waters of the LC, where the advection-diffusion of DO from the Atlantic Ocean is counterbalanced by respiration of sedimentary OM. The model requires the solution of two sets of differential equations, a mass-transfer equation of DO in the water column coupled to general diagenetic equations that describe the accumulation of OM and the resulting oxygen demand at or near the sediment-water interface. The latter is used as a boundary condition to the

former. The finite flow system under consideration reaches from $x=0$ to $x=N$ (700 km) horizontally and from $z=0$ (300 depth) to $z=M$ (100 m depth) vertically. This corresponds to a transect along the deep layer of the LC between stations 25 and 16, as displayed on Fig. 2.1. This region was chosen *a priori* because it contains all the stations sampled during the R/V Coriolis II July, 2003 cruise. Table 2.1 provides information about each station.

2.3.1 Advection-diffusion

The standard advection-diffusion equation for a chemical tracer can be concisely written as:

$$(2.1) \quad \frac{D[O_2]}{Dt} = K\nabla^2[O_2] + Q$$

where K is a diagonal matrix of eddy diffusivity coefficients, and Q is a source term. The solution of Eq. 2.1 can be considerably simplified by making a few assumptions about the flow circulation. In his seminal paper on tracer dispersion, Taylor (1953) demonstrated that fluid turbulence within a laterally-bounded channel will eliminate cross-channel concentration gradients if the tracer has been in the flow longer than its Lagrangian time scale. In other words, the ensemble mean concentration will grow linearly with time and will slowly be advected in the general flow direction.

On the basis of Taylor's results, Bugden (1991) modeled the dispersion of temperature and salinity tracers for the deep LC and found that the horizontal dispersion should be enhanced because of the interactions between vertical shear and vertical diffusion. This occurs in steady unbounded shear flows where no-flux boundary conditions cannot be applied, so that the concentration field of the tracers expands more rapidly than can be represented by a constant diffusivity (Taylor, 1953; Fischer et al., 1979). Since the deep layer of the LC is laterally bounded, the steady sheared flow can be shown to be the dominant mechanism for along-channel dispersion and can be

represented by a Fickian diffusion coefficient. Furthermore, Bugden (1991) showed that the strong cross-channel currents result in a laterally homogeneous concentration field that is slowly being advected inland at a constant velocity. This is in agreement with estimates derived from both temperature-salinity measurements (Bugden, 1991; Koutitonsky and Bugden, 1991) and numerical simulations (Han et al., 1999; Saucier et al., 2003).

Following Bugden (1991), we consider the deep water of the LC as a laterally averaged 2-D fluid influenced only by horizontal diffusion, horizontal advection and vertical diffusivities. Furthermore, the properties of the deep layer of the LC are thought to undergo changes only on decadal or secular time scales (Koutitonsky and Bugden, 1991). Finally, even though some OC remineralization likely occurs in the deep water column (Betzer et al., 1984; Martin et al., 1987; Timothy, 2004) and, hence, should be included as a sink for DO, we will assume it to be negligible relative to the oxygen demand at the sediment-water interface (Savenkoff et al., 1996). Whereas the consideration of water borne respiration would allow a better replication of the fine-scale structure of DO, it should not influence the overall deep water oxygen budget that we seek to calculate. Under these assumptions, Eq. 2.1 simplifies to:

$$(2.2) \quad u \frac{\partial [O_2]}{\partial x} = K_h \frac{\partial^2 [O_2]}{\partial x^2} + K_z \frac{\partial^2 [O_2]}{\partial z^2}$$

where u is the fluid velocity, x is the horizontal distance and z is the depth below 150 m (or the permanent pycnocline). K_h is an enhanced horizontal shear dispersion coefficient that reflects the impact of the cross-channel flow (see Bugden, 1991), whereas K_z is the vertical diffusivity coefficient. Eq. 2.2 was solved using simple boundary conditions as explained in Fig. 2.4.

2.3.2 Parameter sensitivity

To test the relative importance of the parameters u , K_h and K_z on model results, simulations were carried out by solving Eq. 2.2 at a constant sediment oxygen demand (SOD) of $40 \mu\text{mol cm}^{-2} \text{yr}^{-1}$ (i.e., imposed lower boundary condition) and a range of parameter values throughout the Channel. Table 2.2 shows the range of values reported in the literature for each parameter. Contour plots for pairs of each parameter are shown in Fig. 2.5. Evaluation of the results is made on the basis of the DO levels generated at the lower left corner of our simulation region (i.e. bottom of STN 25 shown in Fig. 2.4) since these waters will be undergoing the largest DO depletion given their long residence time and proximity to the sediment oxygen sink.

Fig. 2.5A-D show the effects of varying each physical parameter within the boundaries described in Table 2.2. Fig. 2.5A, 2.5B and 2.5D reveal the sensitivity of water column DO to the vertical diffusivity (K_z). At low K_z values, significant depletion of DO occurs in the water column. This is best seen in Fig. 2.5B where the inflexion point occurs at a K_z on the order of $3 \text{ cm}^2 \text{ s}^{-1}$. DO levels are also highly responsive to variations of the advection velocity (u). At low advection velocities and vertical diffusivities, DO levels in the water column reach minimum values but counterbalance each other when one of them is high (Fig. 2.5A). This is consistent with the balance of DO sources described by Eq. 2.2. At large K_z values, the transfer of oxygen from the upper water column is faster than the rate of oxygen consumption by respiration at depth. As K_z decreases, the influence of u on DO levels becomes increasingly important as it determines the residence time of the water in the bottom layer, i.e., a measure of the time it remains isolated from the atmosphere and subject to DO depletion by catabolic processes. Of the three physical parameters considered, K_h has the least impact, as can be clearly seen in Fig. 2.5C and 2.5D. There is a minimal change of DO over the range of horizontal diffusivities considered, thus we shall keep the standard value of $8.2 \times 10^6 \text{ cm}^2 \text{ s}^{-1}$ for all subsequent calculations performed in this publication. The DO profiles in Fig. 2.5A can be quantitatively understood by closely examining the characteristic ratio of the vertical system scale M (100 m) to the mass diffusion length. Due to the simple

geometry considered in this model, it is easy to define a dimensionless Péclet number Pe (Lumley and Panofsky, 1964) which relates the horizontal advection to the vertical diffusion term (neglecting horizontal diffusion):

$$(2.3) \quad Pe = \frac{M^2}{K_z(N/u)}$$

where N is the horizontal scale (700 km) and (N/u) can be interpreted as the aforementioned residence time of a water particle at a constant 300 m depth. Large u values result in the advection term shaping the DO concentration profiles ($Pe \gg 1$), thus physically there is minimal DO depletion because of rapid replenishment from the more oxygenated Atlantic waters that enter the LC on the continental shelf. As u decreases so does the DO level, until the water column becomes nearly stagnant ($Pe \sim 1$) and vertical diffusion becomes the dominant transport mechanism. In this case the vertical DO concentration profile will be approximately linear and depend mostly on the upper and lower model boundary conditions. The DO concentration in bottom waters will rise as u diminishes, because there will no longer be an effective, cumulative depletion of oxygen in the incoming parcels of water; the longer horizontal residence times allows a greater transfer of DO to take place between the 150 m isobath and the bottom waters. This shift in transport dominance is seen in Fig. 2.5A as an inflexion region within the $K_z - u$ lines. For example, at $K_z = 0.32 \text{ cm}^2 \text{ s}^{-1}$, $Pe = 1$ when $u = 0.224 \text{ cm s}^{-1}$ (Eq. 2.3). In the absence of horizontal diffusion, this value is smaller than the inflexion point (i.e. $u \sim 0.33$) inferred from Fig. 2.5A.

2.4 Early diagenesis model

The OM reaching the seafloor is oxidized in a specific sequence of reactions. The order is dictated by the decreasing Gibbs Free Energy yield for a specific oxidant or electron-acceptor (Froelich et al, 1979) and typically starts with oxic respiration followed by denitrification, manganese (hydr) oxide reduction, iron (hydr) oxide reduction, sulfate reduction and methanogenesis (Van Cappellen et al, 1996). This multi-step process leads

to a redox zonation of the sediment column. Numerous analytical (e.g. Berner, 1980; Gratton et al., 1990) and numerical (e.g.: Rabouille and Gaillard, 1991a, b; Meysman et al., 2003) models have been developed to quantitatively describe early diagenetic processes based on theoretical considerations (e.g., Berner, 1980; Boudreau, 1997). Following Rabouille and Gaillard (1991a), models can be subdivided in 2 major categories: mono-oxidant and multi-oxidant models. The former considers a single oxidant and its mineralization by-products (e.g. HCO_3^- , NO_3^- , HPO_4^{2-}) whereas the latter represents the behavior of two or more oxidants and the ensuing couplings between the different chemical species (e.g. oxidation of reduced species such as Mn(II), Fe(II)). Recent modeling efforts, fueled by ever increasing computer power, have yielded advanced numerical models capable of including all oxic, suboxic and anoxic reactions as well as associated processes such as bioturbation, sediment compaction, oxidation of reduced by-products (Soetaert et al., 1996; Van Cappellen and Wang, 1996; Boudreau, 1996; Meysman et al., 2003).

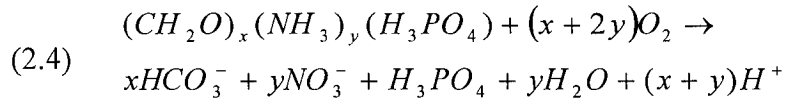
In the context of this study, we modeled the SOD and tested the sensitivity of the DO concentration in the bottom waters to OC rain rates. As a first approximation, we limited the diagenetic model to oxic layer processes, modifying an earlier model elaborated by Rabouille and Gaillard (1991a). Our justification for this approach is two-fold: (1) a more sophisticated model would require us to keep track of all electron-acceptors and account for the DO requirements of by-product oxidation. Furthermore, few measurements of diagenetic components other than oxygen and OC are readily available along the LC, which would make it difficult to constraint their fluxes at or near the sediment-water interface. (2) Suboxic and anoxic reactions in the LC sediments are assumed to have only a minor contribution on the SOD. Reactions in the suboxic and anoxic zones produce reduced dissolved substances that subsequently diffuse towards the oxic layer, where they are oxidized by oxygen and contribute to the SOD (e.g., Soetaert et al., 1996; Cai and Sayles, 1996). The importance of suboxic and anoxic processes depends largely on the rate of OC oxidation which, in turn, is a function of the amount and reactivity of the OC buried below the oxic layer. In coastal environments, suboxic and anoxic mineralization reactions often play a significant, if not dominant role, on OM

degradation as well as on the SOD. For instance, Soetaert et al. (1996) developed a water column depth-dependent model of diagenetic processes and estimated that in 200 m of water, 30% of the SOD could be ascribed to the oxidation of reduced OM degradation by-products (e.g., Mn(II), Fe(II), NH_4^+ , S(II)). Nevertheless, measurements on LC sediment cores reveal that anoxic processes do not contribute significantly to the SOD, even though sulfate is the dominant oxidant of OM in the LSLE (Silverberg et al., 1987; Edenborn et al., 1987; Colombo et al., 1996a). For example, whereas Edenborn et al. (1987) assume that 5 to 25% of OC mineralization occurs by sulfate reduction in the St. Lawrence Estuary, little or no reduced S(II) actually migrates up to the suboxic and oxic zones in these sediments because it is rapidly sequestered by the precipitation of iron sulfide minerals due to the abundance of reactive Fe (III) (Gagnon et al., 1995). Furthermore, a study conducted by Anschutz et al (2000), on sediment cores recovered from STA 23 in the LSLE, revealed that most of the Fe(II) and Mn(II) diffusing from the suboxic sediment are oxidized by nitrate whereas the latter is reduced to nitrogen gas which does not contribute to the SOD. Under these conditions, we assume that oxic OM mineralization outweighs other reactions in determining the magnitude of the oxygen flux at the sediment-water interface in the LC. Another interesting observation to make concerns the geometry of the LC itself. While water column depth has been proposed as a master variable in regards to empirically predicting rates of sediment oxygen demand and carbon burial, bioturbation and mineralization (Soetaert et al., 1996; Middelburg et al, 1997; Meile and Van Cappellen, 2003), the extremely large depth range considered in these statistical studies (e.g. from 0 to 5000+ m in Middelburg et al., 1997) cannot resolve the variability in data associated with near-constant depth regions such as found within the LC. Instead, it appears that sediment dynamics, or in other words the benthic-pelagic coupling, depend mostly on the availability of OM.

2.4.1 Biochemical reactions

The stoichiometry of the oxic mineralization reaction is dictated by the composition of the sedimentary OM (Mucci et al, 2000). The latter is poorly constrained

given the variability of organic material sources to the seafloor. In the absence of quantitative compositional data and given the relative reactivity of the OM reaching the sediment-water interface, the OM is commonly assigned a Redfield stoichiometry (Redfield et al., 1963):



where x is the moles of carbon and y the moles of nitrogen. The origin of particulate OM is often determined by its C/N ratio, a low ratio (6 to 9) is typical of autochthonous OM (i.e. algae or planktonic material, Redfield ratio = 6.6) whereas a high ratio (10+) is characteristic of material of allochthonous origin (i.e., terrestrial, vascular plants, etc.) (Colombo et al., 1996a). The OM reaching the sediment-water interface is consumed fractionally according to the reactivity of its individual molecular constituents (e.g., proteins, amino acids, polysaccharides, lipids, etc.). Accordingly, the reactivity of each substrate decreases with time as the more reactive constituents are degraded. This process has been represented by multi-G models in which the OM decays in direct proportion to its own concentration and irrespective of the oxidant concentration (Berner, 1964; Berner, 1980; Westrich & Berner, 1984; Soetaert et al, 1996; Boudreau, 1996):

$$(2.5) \quad \frac{\partial C}{\partial t} = \sum_{i=1}^N k_i C_i$$

where C is the carbon concentration, i is a specific fraction of the OM and k is the first order degradation rate constant of fraction i in units of reciprocal time. Following Colombo (1996a, b) we defined two major types of OC on the basis of their C/N ratios: a reactive autochthonous marine component with elevated nitrogen content ($C/N = x/y = 106/16 = 6.6$), and an allochthonous, terrestrial component with lower nitrogen content and reactivity ($C/N = x/y = 106/8.83 = 12$). The dependence of the carbon degradation rate on the quantity of the available oxidant is modeled using Monod kinetics (Rabouille and Gaillard, 1991a, b). The latter couples the effectiveness of a given mineralization

pathway to the decrease in the quantity of oxidant available in the system. In other words, the oxidation reaction occurs until the DO concentration becomes negligible. Under these assumptions, Eq. 2.5 becomes:

$$(2.6) \quad \frac{\partial C_i}{\partial t} = k_i C_i \frac{O_2}{(O_2 + Km)}$$

where C_i is the concentration of the i -th component of the OC per volume of solid, O_2 is the oxygen concentration per volume of interstitial water and Km is the Monod saturation constant. We selected a value of $Km = 8 \mu\text{mol } O_2$, following Boudreau (1996).

2.4.2 Transport equations

The vertical distribution of oxygen and carbon within the sediment column is influenced by molecular diffusion, sedimentation rate, compaction, and by the activity of benthic organisms (i.e., bioturbation and biologically enhanced diffusion). The diffusion rates, J , of DO and carbon bioturbation are modeled as standard Fickian relations for a chemical specie S :

$$(2.7) \quad J_i = D_i \frac{\partial^2 S_i}{\partial z^2}$$

where D is the molecular diffusion coefficient for oxygen or the biodiffusion coefficient for carbon. In addition, compaction is modeled as a variable porosity with depth, which in turn depends on advection or sedimentation rate (Rabouille & Gaillard, 1991):

$$(2.8) \quad \begin{aligned} \phi v &= \phi_f w_f \\ (1 - \phi)w &= (1 - \phi_f)w_f \end{aligned}$$

where ϕ is the porosity, v is the liquid phase advection and w the solid phase advection velocity or sedimentation rate. The subscript f refers to values at infinite sediment depth. The advection rate at the sediment-water interface is taken to be the incoming OC sedimentation rate (i.e., total sedimentation rate times the OC content). Following Rabouille and Gaillard (1991a), the differential steady state mass balance in the sediment column can be quantitatively written as:

$$(2.9) \quad -\frac{\partial}{\partial z} \left[-\phi D \frac{\partial S}{\partial z} + v\phi C \right] + \sum R = 0$$

where R represents the rate of substratum bacterial oxidation. By substituting Eqs. 2.6-2.8 into 2.9, we obtain the diagenetic equation for each carbon fraction ($i=1$ for marine carbon and $i=2$ for terrestrial carbon):

$$(2.10) \quad (1-\phi)D_B \frac{\partial^2 C_i}{\partial z^2} - \frac{\partial C_i}{\partial z} \left[(1-\phi_f)w_f + D_B \frac{\partial \phi}{\partial z} \right] = (1-\phi)k_i C_i \frac{O_2}{O_2 + Km}$$

and for oxygen:

$$(2.11) \quad \phi D_{ox} \frac{\partial^2 O_2}{\partial z^2} + \frac{\partial O_2}{\partial z} \left[\phi_f v_f - D_{ox} \frac{\partial \phi}{\partial z} \right] = (1-\phi) \gamma \frac{O_2}{O_2 + Km} \sum_{i=1}^N k_i C_i$$

The boundary value problem of Eqs. 2.10-2.11 is solved by using a set of prescribed boundary conditions. Eq. 2.10 is subject to a given flux of OC at the sediment-water interface:

$$(2.12) \quad F_{C_i} = -(1-\phi)D_B \frac{\partial C_i}{\partial z} + w(1-\phi)C_i \quad z = 0$$

whereas the oxygen concentration at the sediment-water interface is provided by the overlying water column:

$$(2.13) \quad O_2 = O_{2_{BW}} \quad z = 0$$

At the lower sediment boundary, both carbon and oxygen concentrations are assumed to reach a steady-state no-flux condition:

$$(2.14) \quad \frac{\partial C_i}{\partial z} = \frac{\partial O_2}{\partial z} = 0 \quad z = Z$$

2.4.3 Model Implementation

The set of three non-linear and coupled differential Eqs. 2.10-2.11 was solved using a finite difference code that implements the 3-stage Lobatto IIIa collocation formula (Ascher et al., 1988). This technique divides the solution interval in a mesh of points upon which a system of algebraic equations is solved by applying the boundary conditions. The returned solution must satisfy the relative error tolerance criteria of 10^{-3} , else the mesh will adapt and a new solution will be provided. Starting from the DO and OC flux boundary conditions available at the sediment water interface, a simple exponentially decreasing concentration profile is generated as an initial condition. The equations are then solved successively by continuation, i.e. the complexity of obtaining a solution is reduced by solving a sequence of simpler problems, whereas the solution of one problem is the initial condition for another. An analytical Jacobian of Eqs. 2.10-2.11 is provided within the code to accelerate the computations. The sediment column is given a thickness of 5 cm segmented into 0.01 cm layers. The flux of oxygen into the sediment was calculated from the computed profiles by estimating the linear concentration gradient across the sediment-water interface by a least-squares fitting procedure, and using this gradient in Fick's diffusion law (Eq. 2.7). The model was implemented within the MatLab® programming environment (The Mathworks) on a 1.8 GHz personal computer.

2.4.4 Parameter calibration

An extensive literature review was carried out to constrain values of the OC fluxes, sedimentation rates, oxygen penetration depths (OPD), molecular and bioturbation coefficients and kinetic reaction rates within the LC. Parameters with no available estimates were calculated either by imposing specific relationships between variables or by choosing values that produced the most realistic DO concentration profiles in the sediments.

2.4.4.1 *Carbon fluxes to the sediment and dissolved oxygen fluxes across the sediment-water interface along the Laurentian Trough*

Most of the OC flux (i.e. sediment trap, carbon burial rates) and DO concentration gradient measurements at the sediment-water interface reported to date for the LC were carried out at a limited number of stations between Tadoussac and Cabot Strait (Fig. 2.1). Table 2.3 shows a sample of important parameters measured with their locations. Undisturbed sediment core and sediment trap data were obtained in the summer of 1985 by Silverberg et al. (1987) at STN 23. DO concentration profiles across the sediment-water interface were measured using a polarographic microelectrode and oxygen fluxes were estimated at between 59 to 134 $\mu\text{mol O}_2 \text{ cm}^{-2} \text{ yr}^{-1}$. These measurements also revealed a high degree of lateral variability as OPD varied between 0.2 and 1 cm. Carbon fluxes measured at 150 m depth using free drifting sediment traps (Silverberg et al., 1985) were between 471 to 932 $\mu\text{mol C cm}^{-2} \text{ yr}^{-1}$, but no attempt was made to distinguish between the marine and terrestrial OC components. Variability in carbon flux and SOD may reflect seasonal changes. The month of May coincides with large spring blooms and, thus, peaks in carbon transport to the deep waters and sediment as well as remineralization rates. Silverberg et al. (1987) also recorded elevated burial rates of 108 to 364 $\mu\text{mol C cm}^{-2} \text{ yr}^{-1}$, estimating that a significant part of the OC reaching the sediment-water interface is buried without being degraded.

Lucotte et al. (1991) proposed an overall carbon budget as well as distinguished between the allochthonous (terrestrial) and autochthonous (marine) POC fluxes to the sediments in the LSLE. Their study revealed a strong seasonal influence on the composition of the POC. In the Spring, due to strong freshwater runoff, mostly terrigenous POC ($\delta^{13}\text{C} \approx -26.6\text{‰}$) is advected into the LC, with Fall being dominated by higher carbon-13 marine POC ($\delta^{13}\text{C} \approx -20.8\text{‰}$). Based on their results, Lucotte et al. (1991) proposed that suspended particle matter accumulating in the sediments at the head of the LC was mainly of terrigenous origin. Nevertheless, overall for the LSLE, they report a dominance of the marine OC flux ($\sim 234 \mu\text{mol C m}^{-2} \text{ yr}^{-1}$) over the terrigenous OC flux ($\sim 183 \mu\text{mol C cm}^{-2} \text{ yr}^{-1}$). These data suggest that, despite the delivery of terrigenous OC by the river, the marine OC flux dominates a short distance downstream from the head of the LC. The larger terrigenous particles appear to be quickly deposited within the boundaries of the LSLE and may not propagate into the Gulf.

Colombo et al. (1996 a, b) carried out a study of the biogeochemistry of sedimentary organic material at 2 sites in the Laurentian Trough, close to stations 24 and 22. OC fluxes and composition were obtained from material recovered from both free-drifting sediment traps set at 150 m depth and sediment box-cores. At Station 24, they observed a larger OC flux with a corresponding higher proportion of continental material, roughly 70-80% of the total OC. At the seaward Station 22, the OC flux was half as large but the marine OC component was dominant, accounting for over 60% of the total OC flux. These findings support the conclusions of Lucotte et al. (1991).

Savenkoff et al. (1996) published a series of water column CTD measurements, Winkler titrations and sediment core profiles for station 19 and for a location in Cabot Strait. Following Bugden's (1991) interpretation of a more or less homogeneous deep layer within the LC, the authors assumed a linear interpolation between their results at both stations. Consequently, they calculated that a water particle traveling from Cabot Strait to STN 19 was subject to constant carbon flux and respiration rates. Under these assumptions, they estimated that roughly 10 % of the local primary production reaches the deep waters (>150-200 m depth), where it is remineralized either in the water column

or the sediment. The POC fluxes measured from moored sediment traps at 150 m depth along the LC give an average of $\sim 137 \mu\text{mol C cm}^{-2} \text{ yr}^{-1}$ with an estimated increase of $\sim 22 \mu\text{mol C cm}^{-2} \text{ yr}^{-1}$ from Cabot Strait to STN 19. Benthic respiration was assumed to be the major sink of DO whereas averaged oxic respiration within the water column below 200-m depth was estimated at only $5.6 \mu\text{mol O}_2 \text{ L}^{-1} \text{ yr}^{-1}$. Muzuka and Hillaire-Marcel (1999) studied a series of sediment cores recovered from the same stations as Savenkoff et al. (1996) in order to determine the source of recently deposited OM and compare the burial rates of OC and N to benthic fluxes. Their OC fluxes were estimated using an empirical function relating primary productivity with sedimentary OM concentrations, water depth and sedimentation rate. This equation appears to severely underestimate (i.e. close to one order of magnitude) the OC benthic flux along the LC when results are compared to estimates obtained by other researchers (see Table 2.3). Sedimentation rates based on a few AMS ^{14}C stratigraphies varied between 0.01 and 0.015 cm yr^{-1} along the Gulf portion of the LSLE, much lower than the minimum value of 0.4 cm yr^{-1} estimated by Smith and Schafer (1999) at STN 16 using ^{210}Pb distribution profiles. The average of $\delta^{13}\text{C}$ ($-21.9 \pm 0.4\text{‰}$) signature of the OC in cores analyzed by Muzuka and Hillaire-Marcel (1999) corresponds to mostly marine OM. These observations are in agreement with the findings of Lucotte et al. (1991) that little terrestrial OM is delivered to the Gulf portion of the LC as the majority of it is trapped in the LSLE.

A more extensive study of core samples from stations 19 and Cabot Strait was carried out as part of the Canadian JGOFS program (Silverberg et al., 2000). DO profiles measured at both stations using voltammetric microelectrodes revealed an 8 to 15 mm OPD. SODs estimated from the DO gradients measured across the sediment-water interface and calculated from core incubation experiments yielded comparable values at each station. The similarity of SOD values at the two stations (Table 2.3) suggests that the Gulf portion of the LC is highly homogeneous with respect to OC flux, with perhaps a slight increase towards Cabot Strait due to the proximity of land masses (Newfoundland and Nova Scotia) and lateral transport. As mentioned in Silverberg et al. (1987), the differences in SOD and OC flux measurements is linked to seasonal variability as these were carried out both in May and June. It is worth noting that Silverberg et al. (2000)

refer to Silverberg et al. (1987) when stating that SOD values for the LSLE reach as high as $\sim 420 \mu\text{mol O}_2 \text{ cm}^{-2} \text{ yr}^{-1}$, but these values do not appear in the cited publication. In fact, OPDs and the estimated DO fluxes are similar throughout the Laurentian Trough despite clear differences in OC fluxes.

2.4.4.2 *Molecular diffusion*

Diffusive transport in the liquid phase is modeled as molecular diffusion for a porous media, which is related to porosity by:

$$(2.15) D_s = D_o \phi^2$$

where D_s is the sediment diffusion coefficient and D_o is the free solution diffusion coefficient for oxygen at 4°C ($383.5 \text{ cm}^2 \text{ yr}^{-1}$; Silverberg et al., 2000). Although diffusion coefficients vary with temperature, this property is nearly invariant in the bottom waters of the LC (Koutitonsky and Bugden, 1991).

2.4.4.3 *Bioturbation*

Bioturbation is modeled as a local transport process similar to molecular diffusion, and does not mix solids with fluids to eliminate porosity gradients (i.e. intraphase mixing as described by Boudreau, 1997). No fundamental theory for predicting bioturbation exists in the literature, thus we relied upon an empirical relation between the biodiffusion coefficient, D_B , and the sedimentation rate derived by Boudreau (1997):

$$(2.16) D_B = 15.7w^{0.69}$$

We found this relationship works remarkably well in reproducing previously estimated biodiffusion coefficients in the LSLE (e.g. Gratton et al., 1990).

2.4.4.4 Rates of bacterial organic matter degradation

The rates of OM bacterial degradation are difficult to constrain given the wide range of values that appear in the literature, as emphasized by Boudreau (1997). Much of the difficulty resides in assigning specific rate constants to different fractions of OM: typical values range from over 24 yr^{-1} decay (Westrich and Berner, 1984) for extremely labile OM to less than 10^{-10} yr^{-1} for highly refractory material (Boudreau, 1997). Estimates computed by Colombo et al. (1996b) using a one-G model for stations 22 and 24 yielded values between 0.07 to 0.16 yr^{-1} . These values are not appropriate for our purpose because they are averages for the top 35 cm of the sediment cores and, thus, greatly underestimate the reactivity of the OM in the top cm of the cores. Alternatively, we selected rate constants for each of our OC components (i.e., marine and terrestrial). The autochthonous marine carbon was assigned a reactivity of 10 yr^{-1} , a value commonly used in the literature for labile OM (Boudreau, 1997). The reactivity of the terrestrial carbon was related to the sedimentation rate according to the relationship established by Boudreau (1997):

$$(2.17) \quad k = 0.4w^{0.6}$$

In other words, Eq. 2.17 reflects the fact that the reactivity of the terrigenous OC decreases with time as it is carried from the head of the LC and the most reactive fractions are remineralized within the boundaries of the LSLE (Lucotte, 1991; Muzuka and Hillaire-Marcel, 1999).

2.4.5 Validation of the diagenetic model

In order to test the diagenetic model outputs, we conducted simulations on 2 stations of the LC for which detailed information on oxygen fluxes across the sediment-water interface is available (Fig. 2.6). Station 25 (see Fig. 2.1) is located at the head of

the LC and, thus, characterized by a high sedimentation rate and an OC flux dominated by terrestrial OM. In contrast, Station 19 is found within the Gulf of St. Lawrence and is characterized by a lower sedimentation rate and an OC flux of almost exclusively autochthonous origin. The OC upper boundary condition (Eq. 2.12) was imposed using two different approaches, first by incrementing the OC fluxes (while keeping the ratio of marine to terrigenous OC constant) until the measured OPD and SOD could be reproduced and, secondly, by using OC flux values interpolated from results by Lucotte et al. (1991). Model results for station 25 indicate that one fifth of the OC flux inferred at 150 m is required to reproduce the data (i.e., measured OPD and SOD; Fig. 2.6A&B). For station 19, the carbon fluxes needed to replicate the measured SOD were about the same as the OC flux measured by sediment traps (Fig. 2.6C). Lower OC fluxes such as those proposed by Muzuka and Hillaire-Marcel (1999) yield unreasonable SOD (Fig. 2.6D) with the oxic layer extending throughout the sediment column.

2.5 Simulation scenarios

The most striking feature from the available field data is the similarity of both SOD and OPD values measured throughout the Trough. These results contrast with OC fluxes measured at 150 m depth using drifting and moored sediment traps, which can be up to 10 times higher at the head of the LSLE than in the Gulf, as well as with the estimated sedimentation rates that decrease exponentially seaward from the head of the LC to the Gulf (Smith and Schafer, 1999). The composition or reactivity of the OC reaching the seafloor may explain this dichotomy. The review in section 4.4.1 clearly indicates that only negligible amounts of terrigenous OC are delivered to the Gulf whereas the overall flux of OC in the LSLE is also mostly of marine origin even though terrestrial OC should dominate close to the head. The DO concentration profiles measured across the sediment-water interface (Fig. 2.6C) in the Gulf are reproduced adequately by the diagenetic model using the measured carbon fluxes (i.e., drifting and moored sediment traps set at 150 m) whereas, in the lower estuary, the SOD is greatly

overestimated (Fig. 2.6A). This prompted us to elaborate two carbon flux scenarios to represent the distribution of OC rain rates along the LSLE

2.5.1 High flux scenario

In this scenario, the OC fluxes correspond to measurements obtained from sediment traps set at 150 m depth along the LC (Fig. 2.7A). The spatial distribution of total OC fluxes is consistent with the exponential decrease in sedimentation rates reported in Smith and Schafer (1999) for the LSLE and a flattening out in the Gulf. Further constraints are applied by using the proportions of marine OC reported in Colombo et al. (1996a, b). Within the first 190 km of the estuary (STN 25 to STN 21, corresponding nearly to the LSLE), the average total OC flux is $\sim 400 \mu\text{mol C cm}^{-2} \text{ yr}^{-1}$, almost identical to the estimate of Lucotte et al. (1991; $408 \mu\text{mol C cm}^{-2} \text{ yr}^{-1}$ or $50 \text{ gC m}^{-2} \text{ yr}^{-1}$). Similarly, the total OC flux of $112 \mu\text{mol C cm}^{-2} \text{ yr}^{-1}$ at STN 19 corresponds to the average of measurements reported by Silverberg et al. (2000). The dominance of terrigenous OC at the head of the LC and its near absence in the Gulf is consistent with the trapping of heavy terrigenous particles within the LSLE (Lucotte et al., 1991; Muzuka and Hillaire-Marcel, 1999). Finally, the spatial distribution of marine OC is more or less consistent with the distribution of primary productivity in the LSLE and the Gulf ($90\text{-}180 \text{ g C m}^{-2} \text{ yr}^{-1}$), of which ~ 7 to 10% is believed (Therriault et al., 1990; Savenkoff et al., 1996; Silverberg et al, 2000) to reach the sediment-water interface.

2.5.2 Low flux scenario

In this scenario, the OC flux is adjusted to reproduce the SOD calculated from oxygen gradients measured by voltammetric micro-electrodes across the sediment-water interface in cores recovered along the LC (Fig. 2.7B). Accordingly, the OC fluxes in the Gulf are similar for both scenarios but significantly smaller in the LSLE. Consequently, we must forgo the exponential relationship between the sedimentation rate and distance from the head of the LSLE (Smith and Schafer, 1999) and impose linear functions for

simplicity. The dominance of terrigenous OC at the head and subsequent disappearance in the Gulf is still represented but the spatial distribution and magnitude of the marine OC flux is modified to reproduce the sediment data. The marine OC flux at STN 25 is set at 7% (Savenkoff et al. 1996) of the minimum average primary production of the region (i.e., $90 \text{ gC m}^{-2} \text{ yr}^{-1}$; Therriault et al., 1990) and corresponds to a flux of $52 \text{ } \mu\text{mol C cm}^{-2} \text{ yr}^{-1}$. Combined with a terrigenous OC flux of $60 \text{ } \mu\text{mol C cm}^{-2} \text{ yr}^{-1}$, it yields a SOD of $84 \text{ } \mu\text{mol cm}^{-2} \text{ yr}^{-1}$, roughly the value measured in July 2003 ($\sim 85 \text{ } \mu\text{mol cm}^{-2} \text{ yr}^{-1}$ C. Magen, pers. comm.). The total OC flux remains nearly constant throughout the Estuary and correlated with the fact that almost all the SOD (i.e., fluxes) measurements carried out along the LC fall within the 75 to $100 \text{ } \mu\text{mol cm}^{-2} \text{ yr}^{-1}$ range (see Table 2.3).

2.6 Discussion

Results of the model simulations, i.e., the computed oxygen concentrations in the bottom waters of the LSLE at STN 25 (lower left corner of Fig. 2.4) are presented in Fig. 2.8 for both carbon flux scenarios. For each scenario, two physical parameters were varied over realistic ranges: the horizontal advection u and the vertical diffusivity coefficient K_z . For the sake of clarity, only four K_z values are presented: **(1)** $K_z = 11 \text{ cm}^2 \text{ s}^{-1}$, a large value more akin to turbulent rivers, but one order of magnitude smaller than the estimates of Mertz and Gratton (1995) for the head of the LC, **(2)** $K_z = 2,2 \text{ cm}^2 \text{ s}^{-1}$, derived by Bugden (1991) from fitting an equation similar to Eq. 2.2 to temperature and salinity profiles within the deep waters of the LC, **(3)** $K_z = 0.45 \text{ cm}^2 \text{ s}^{-1}$, a value obtained by inverse modeling of nutrient budgets for the St-Lawrence maritime system by Savenkoff et al. (2001) and, **(4)** $K_z = 0.1 \text{ cm}^2 \text{ s}^{-1}$, a value reminiscent of a poorly-mixed estuary, more commonly associated with deep ocean basins (Von Schwind, 1980). Fig. 2.9 shows contour plots of DO concentrations within the calculation domain, one for each carbon flux scenario (Fig. 2.9A & B) as well as the corresponding steady-state oxygen demand at the sediment-water interface (Fig. 2.9C & D).

2.6.1 Parameter variations

As expected and revealed in Fig. 2.8 A & B, the high OC flux scenario generates a much greater depletion of DO in the bottom waters of the LSLE. The absolute and relative DO depletion between the two OC flux scenarios is enhanced as the vertical diffusivity coefficient, K_z , decreases. These results underline the sensitivity of the system to the vertical diffusivity relative to the other two physical parameters (i.e., advective velocity and horizontal diffusivity) considered in the model. As illustrated in Fig. 2.5B, there is a very sharp response (i.e., gradient in DO concentrations) of the system when K_z falls below a critical value of $\sim 3 \text{ cm}^2 \text{ s}^{-1}$. In other words, the system is relatively insensitive to the advection velocity, u , when the vertical diffusivity is high, but along-channel advection of bottom waters becomes the main vector of DO to the system at low vertical diffusivities. Results obtained at various K_h are not shown because of its minimal impact on the DO budget. The DO distribution pattern shown in Fig. 2.9B reproduces satisfactorily the data illustrated in Fig. 2.2, despite the simplifying assumptions used in constructing the model, such as neglecting topography, time-dependence and assuming constant DO at the upper and eastern boundaries of the calculation domain. The spatial (i.e., along-channel) DO gradient in the bottom waters is reproduced in both scenarios and reasonable DO values are obtained at the head of the LSLE when the high OC flux scenario is coupled to realistic physical parameters.

Given the sensitivity of model results to K_z , this parameter should be better constrained. Unfortunately, very few estimates of mean diffusivity coefficients in the LC can be found in the literature, partly due to the difficulties in accounting for turbulence. Computer intensive numerical models use methods in which diffusivity coefficients are described as combinations of a background parameter and a stability function (e.g. Kantha and Clayson, 1994). Given the horizontal scale and depth of the LC, computing mean diffusion coefficients from such a model is well beyond the scope of this study. Consequently, in the discussion that follows, we restrict ourselves to the two independent estimates provided by Bugden (1991) and Savenkoff et al. (2001). The differences between oxygen profiles generated by our model using the two diffusion coefficient

estimates are staggering, even though their values differ by less than a factor of 5. For example, given a mean advection velocity of 1 cm s^{-1} (Gilbert et al., 2004), the differences in DO concentrations generated by the model using both estimates for the head of the LSLE (i.e., Station 25) are $\sim 33 \mu\text{mol L}^{-1}$ for the low OC flux scenario and up to $\sim 63 \mu\text{mol L}^{-1}$ for the high OC flux scenario. Whereas the diffusion coefficient of Savenkoff et al. (2001) will generate hypoxic waters at the head of the LSLE with the low OC flux scenario, Bugden's (1991) coefficient will do so only for the high OC flux scenario. In other words, the two OC flux scenarios and the two diffusion coefficient estimates are mutually exclusive. Understanding how the two diffusion coefficient estimates were derived may help to resolve this quandary. Bugden's (1991) vertical diffusion coefficient was obtained using the same physical framework that we used to parameterize our water column model. Furthermore, it was rigorously tested against a 40+ year old database of temperature and salinity profiles measured in the deep Laurentian Trough. In contrast, Savenkoff et al. (2001) used an inversion procedure to estimate a diffusion coefficient to would generate a mass balance in their geochemical box model and, thus, it was not based on any physical interpretation of the water column processes. We hereby consider that Bugden (1991)'s diffusion coefficient is more compatible with our model and, thus, the high OC flux scenario becomes necessary to achieve hypoxic waters in the LSLE, as is clearly seen in Fig. 2.9.

2.6.2 Sediment oxygen demand

Although our diagenetic model only considers reactions occurring within the oxic zone (namely oxic mineralization and nitrification), it successfully reproduced the oxygen gradients measured by high resolution voltammetric micro-electrodes, across the sediment-water interface in the GSL portion of the LC. Our assumptions that both respiration in the water column and non-oxic chemical reactions have an insignificant impact on the SOD is supported by the model results. On the other hand, these assumptions do not seem to hold when trying to reproduce the SOD in the LSLE, since the high OC flux scenario (based on sediment trap measurements) yields shallower OPDs

and a greater oxygen demand at the sediment-water interface (see the difference in Fig. 2.9 C, D). We propose three possible explanations for this discrepancy. (1) Respiration in the water column may not be negligible, as assumed in the model, resulting in the concomitant depletion of settling OC and DO along the LC. On the other hand, given the estimated velocity of settling particles in the LC, from $\sim 10 \text{ m day}^{-1}$ for refractive terrigenous material (Syvitski et al., 1983) up to 100 m day^{-1} and higher for biogenic autochthonous particles (Alldredge and Gotschalk, 1989; Lucotte et al., 1991) minimal mineralization of the settling OM should occur over the depth of the water column in the LC. Furthermore, whereas accounting for water column respiration in the LC may help to reproduce the fine scale structure of the DO profiles in the deep layer, it would have a minimal impact on the overall DO budget. We have also neglected possible benthic respiration originating from the side boundaries of the Laurentian Trough, which we modeled as a simple rectangular channel. The flanks of the LC, although quite steep, should nevertheless harbor an active SOD from the sediment-water interface. To determine whether or not this additional sink could influence the deep water DO budget of the LSLE will require using a more realistic geometry in future modeling implementations. (2) The OM delivered to the sediment-water interface in the LSLE may be more reactive (i.e., larger k in Eq. 2.5) than we assumed and generate a larger SOD. Yet, calculations carried out using rate constants ranging from values representative of very labile organic material, that is easily degraded in the upper layers of the water column (i.e., marine OC $k = 24 \text{ yr}^{-1}$, terrestrial OC $k = 1.2 \text{ yr}^{-1}$; Westrich and Berner, 1984), down to refractive material found in deep oligotrophic sites (i.e., marine and terrestrial OC average $k < 1 \text{ yr}^{-1}$; Sayles et al., 1994) produce less than a 1% difference in the ultimate SOD at the head of LSLE. These changes were negligible compared to the effects of other variables such as the OC flux or the bottom water oxygen concentrations. Similar findings in model sensitivity tests were reported by Soetaert et al. (1996). (3) Finally, the large discrepancies in the model results between the LSLE and the GSL may result from an underestimation of the oxygen fluxes obtained from measured OPDs or DO gradients across the sediment-water interface (SWI). As described in section 4.2, oxygen fluxes across the SWI were estimated under the assumption that the transport of DO through the clayed sediment occurs mainly by

molecular diffusion, a common assumption for non-permeable sediments (e.g. Bouldin, 1968; Di Toro et al., 1990; Rabouille and Gaillard, 1991a; Cai and Sayles, 1996; Silverberg et al., 2000; House, 2003). Whereas the application of tortuosity –corrected molecular diffusion coefficients (i.e., Fick’s first law) does reproduce sufficiently well the SOD for sediment cores sampled in the GSL, the oxygen profiles modeled using measured OC fluxes in the LSLE are far steeper than the measured micro-electrode profiles (see Fig. 2.6 for details). More realistic modeled profiles could be generated if diffusion was accelerated near the sediment-water interface. Enhanced diffusive transport, due to the mixing of pore waters by small organisms (meiofauna and microzoobenthos), has been proposed (Archer and Devol, 1992; Meile et al., 2001; Meile and Van Cappellen, 2003) to explain discrepancies between SOD estimates derived from *in-situ* benthic chamber measurements (e.g. Hall et al., 1989) and fluxes calculated from vertical high-resolution pore water concentration profiles obtained by voltammetric micro-electrodes (e.g. Luther et al., 1998) in coastal environments. Estimates of DO fluxes at the SWI derived by both methods, when available, indicate that, in areas of relatively small SOD ($\sim 100\text{-}150 \mu\text{mol cm}^{-2} \text{yr}^{-1}$, commonly found in deeper ocean basins), the difference is often negligible, whereas for regions with larger SOD ($> 200 \mu\text{mol cm}^{-2} \text{yr}^{-1}$, usually in shallower coastal settings), molecular diffusion underestimates the oxygen fluxes (Jahnke, 2001; Meile and Van Cappellen, 2003). Our modeling results largely agree with this observation, as the sediment DO profiles in a region with low SOD (i.e., the GSL) are reproduced very well by our simple diagenetic model (Fig. 2.6C). Furthermore, the modeling results imply that the LSLE is required to harbor large SOD for hypoxia to occur in the water column, yet the SOD derived from micro-electrode measurements are much smaller than the modeled values (see Fig. 2.6B). According to Meile and van Cappellen (2003), molecular diffusion may account for as little as 20% of the total SOD in coastal environments, consistent with our high OC flux model results but incompatible with field measurements that reveal invariant OPDs despite large variations in OC accumulation rates along the Laurentian Trough. At the present time, too few comparisons of oxygen fluxes estimated from ship-board DO micro-electrode profiles and whole core incubations are available for the LC to speculate on the origin of this mechanism (biological or otherwise) and hence refine the diagenetic model.

2.7 Conclusions

In this paper, we elaborated a simple 2-D coupled advection-diffusion-diagenetic model to test the sensitivity of DO level in the deep waters of the LC to varying OC fluxes at the sediment-water interface and to physical parameters of the circulation regime. An extensive literature review of the regional water column and sediment properties was conducted in order to better constrain all the model parameters. Although many assumptions were used in the conception of the model (i.e. steady-state, prescribed hydrodynamic flow, diagenesis restricted to oxic mineralization, use of empirical extrapolations, etc.), it is able to generate appreciable DO depletion along the LC when realistic water column parameters are used. This meets the objectives set forth by this model as a tool to investigate the benthic-pelagic coupling in the LC. As to the question put forth in the introduction: ‘Can the present SOD along the seafloor of the Laurentian Channel account for the recent development hypoxic waters in the LSLE?’, our model results indicate that oxic mineralization of OC plays an important role in generating hypoxic bottom waters in the LSLE. These results are also likely to support other lines of evidence about claims of eutrophication in the LSLE. For example, Gilbert et al. (2004) showed that while the properties of the waters entering the LC since the 1980’s underwent only minimal changes, the DO gradient between Cabot Strait and the LSLE has continually increased during that period of time, possibly due to growing OC fluxes along the seafloor and a concomitant increase in SOD. Other evidence of increasing OC deposition comes from recent proxy studies on sediment cores taken in the LSLE. A compilation of the preserved OM in a sediment core taken near STN 25 by St-Onge et al. (2003) showed a gradual increase in $\delta^{13}\text{C}$ since the 1970’s, which the authors interpret as a higher contribution of marine OM to the sediment. This shift in isotopic composition was related to greater abundances of dinoflagellates and organic linings of benthic foraminifera by Thibodeau et al (2004). According to Cloern (2001), both these sedimentary OM tracers are commonly associated with eutrophied marine ecosystems. Thus, the integrating of our study results with geochemical and micro-paleontological

proxies, serve to show that a gradual increase in the accumulation rates of POC in the LSLE, possibly due to the eutrophication of the system, would produce a concomitant depletion in DO levels as revealed by the different carbon flux scenario model calculations.

According to a sensitivity analysis of the model, the most important parameters in controlling DO levels in the LSLE were the vertical diffusivities in the water column and the OC rain rate. The diagenetic model successfully reproduces the sediment oxygen profiles measured in the Gulf portion of the LC but fails to do so in the LSLE. Nevertheless, a greater SOD than calculated from measured DO gradients (i.e. micro-electrode profiles) is required to reproduce the observed DO depletion in the water column of the LSLE. The diagenetic model results hence support the hypothesis that oxygen fluxes calculated using molecular diffusion and oxygen gradients obtained from micro-electrode profiles greatly underestimate the actual SOD at large OC accumulation rates. In order to resolve this conundrum, SOD measurements obtained using different methods (i.e., micro-electrode profiles, core incubations, benthic chambers ...) should be carried out in order to refine the diagenetic model. Future modeling efforts should be directed towards adding time dependency to the benthic-pelagic coupling, in order to verify claims that eutrophication may be at least partly responsible for the development of hypoxic bottom waters in the LSLE. Additional improvements would be achieved by a more realistic system setting (variable width and depth) for the LC, and use of depth-dependant vertical diffusivities based on the strong (20 cm s^{-1}) tidal velocities found in the LSLE.

2.8 Tables

Stations	Latitude	Longitude	Depth (m)	Distance from channel head (km)
25	48°13.98'	69°27.00'	310	0
24	48°25.99'	68°06.01'	314	34.9
23	48°42.04'	68°39.05'	350	79.8
22	48°56.04'	68°05.44'	322	128.4
21	49°06.97'	67°16.93'	330	191.5
20	49°25.37'	66°19.39'	332	268.9
19	49°29.00'	65°11.89'	375	350.6
18	49°16.06'	64°15.86'	390	422.3
17	48°57.98'	63°07.02'	409	512.3
16	48°23.96'	60°44.05'	434	698.2

Table 2. 1 Characteristics of the sampled stations in the Laurentian Channel.

DESCRIPTION	UNITS	STANDARDVALUE	UPPERLIMIT	LOWERLIMIT
Advection velocity (u)	$\text{cm} \cdot \text{s}^{-1}$	1.0 (<i>Gilbert et al., 2004</i>)	22 (<i>Han et al., 1999</i>)	0.0011 (<i>Savenkoff et al., 2001</i>)
Horizontal diffusion (K_y)	$\text{cm}^2 \cdot \text{s}^{-1}$	8.2E6 (<i>Bugden, 1991</i>)	8.2E6 (<i>Bugden, 1991</i>)	2.8E4 (<i>Savenkoff et al., 2001</i>)
Vertical diffusion (K_z)	$\text{cm}^2 \cdot \text{s}^{-1}$	22 (<i>Bugden, 1991</i>)	220 *	0.1 (<i>Von Schwind, 1980</i>)

Table 2. 2 Physical parameters used in the hydrodynamic model. * A value ~ 5 times less than estimates for the turbulent head region of the Laurentian Trough ($100 \text{ cm}^2 \text{ s}^{-1}$; Mertz and Gratton, 1995).

Stations	Source	SR cm/yr	OC flux $\mu\text{mol cm}^{-2}\text{ yr}^{-1}$	OC buried $\mu\text{mol cm}^{-2}\text{ yr}^{-1}$	MOC %	OPD cm	SOD $\mu\text{mol cm}^{-2}\text{ yr}^{-1}$
STN 25	<i>Lucotte et al. (1991)</i>	-	-	-	~30	-	-
	<i>Smith & Schafer (1999)</i>	0.545	-	-	-	-	-
STN 24	<i>Colombo et al. (1996a,b)</i>	-	1050	509	~30	-	-
	<i>Smith & Schafer (1999)</i>	0.7	-	-	-	-	-
STN 23	<i>Edenborn et al. (1987)</i>	-	350	-	~57	-	-
	<i>Silverberg et al. (1987)</i>	0.61	471 to 932	108 to 364	-	0.2 to 1	59 to 134
	<i>Lucotte et al. (1991)</i>	-	~ 417 *	-	~55	-	-
	<i>Smith & Schafer (1999)</i>	0.539	-	-	-	-	-
STN 22	<i>Colombo et al. (1996a,b)</i>	-	573	158	~60	-	-
	<i>Smith & Schafer (1999)</i>	0.45	-	-	-	-	-
STN 21	<i>Lucotte et al. (1991)</i>	-	-	-	~64	-	-
	<i>Smith & Schafer (1999)</i>	0.223	-	-	-	-	-
STN 20	<i>Smith & Schafer (1999)</i>	0.139	-	-	-	-	-
	<i>Muzuka & Hillaire-Marcel (1999)</i>	0.015	~ 22	~ 13	~95	-	-
STN 19	<i>Savenkoff et al. (1996)</i>	-	~ 137	-	~90	-	~ 100
	<i>Smith & Schafer (1999)</i>	0.237	-	-	-	-	-
	<i>Silverberg et al. (2000)</i>	0.08	66 to 160	~ 46	-	0.8 to 1.5	37 to 100
STN 18	<i>Smith & Schafer (1999)</i>	0.115	-	-	-	-	-
	<i>Muzuka & Hillaire-Marcel (1999)</i>	0.01	~ 19	~ 10	~100	-	-
STN 17	<i>Smith & Schafer (1999)</i>	0.15	-	-	-	-	-
STN 16	<i>Smith & Schafer (1999)</i>	0.042	-	-	-	-	-
	<i>Muzuka & Hillaire-Marcel (1999)</i>	0.011	~ 22	~ 13	~100	-	-
Cabot Strait	<i>Muzuka & Hillaire-Marcel (1999)</i>	0.011	~ 20	~ 11	~100	-	-
	<i>Silverberg et al. (2000)</i>	-	-	-	-	0.8 to 1.5	44 to 151

Table 2.3 Compilation of sediment data along the Laurentian Trough. The term definitions are: sedimentation rate (SR), organic carbon flux (OC flux), organic carbon buried (OC buried), marine organic carbon (MOC), oxygen penetration depth (OPD) and sediment oxygen demand (SOD).

* Average estimated between STA 25 and 21.

2.9 Figures

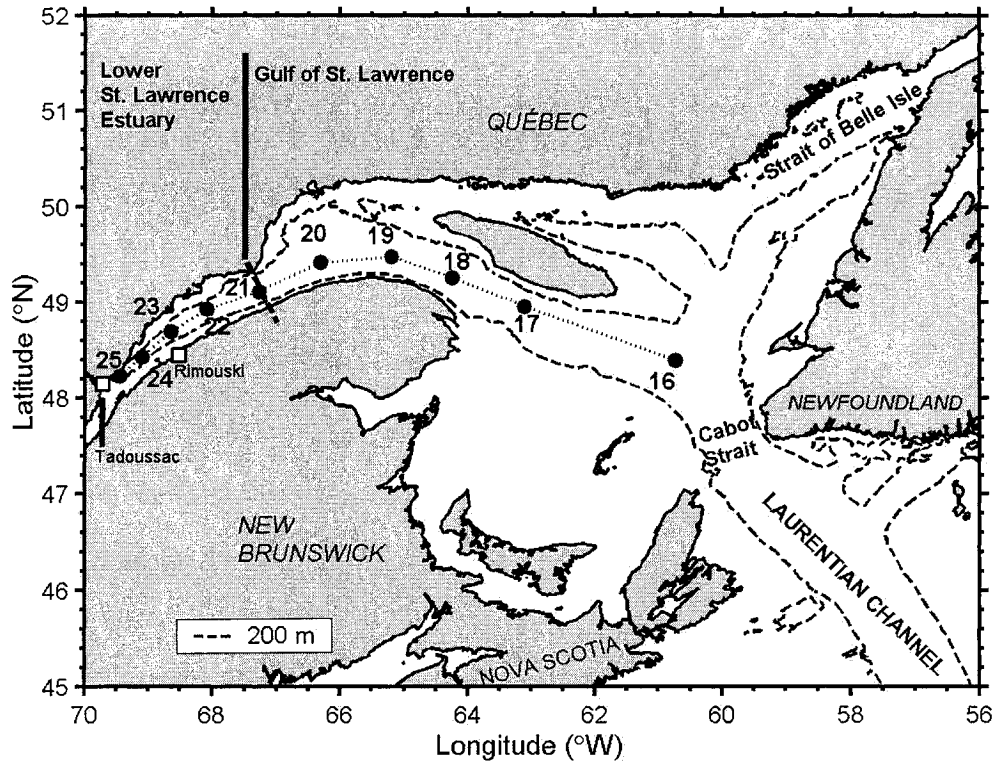


Fig. 2. 1 The Estuary and Gulf of St. Lawrence system in Eastern Canada, showing some of the stations sampled during the R/V Coriolis II, July 2003 cruise.

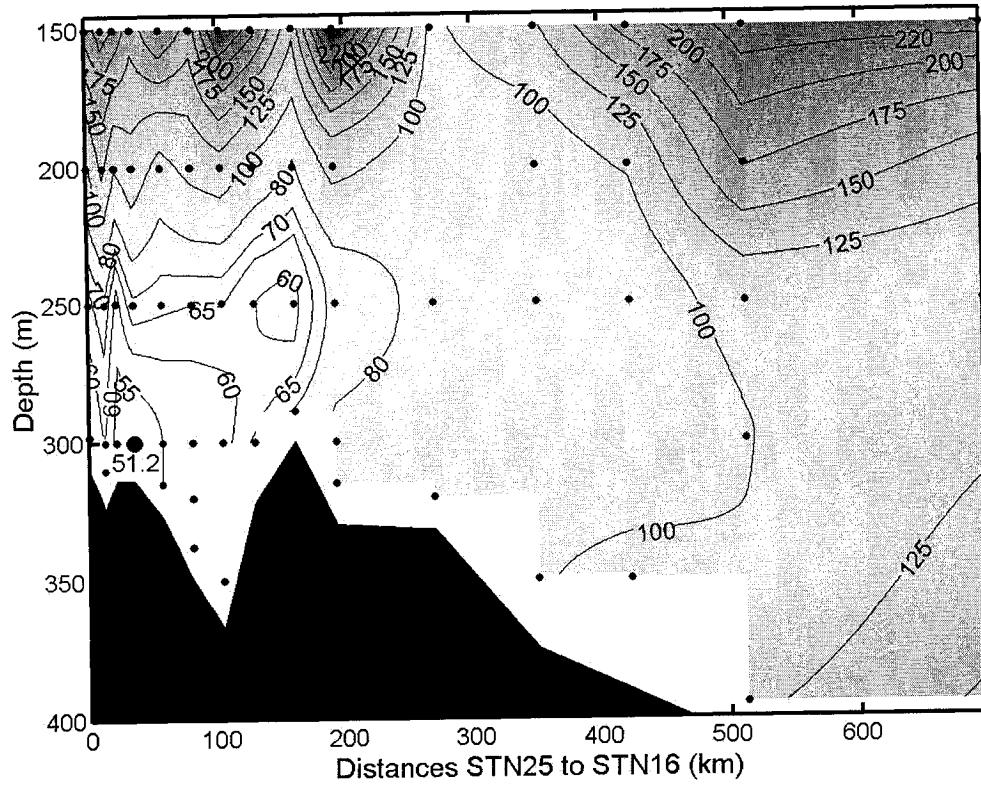


Fig. 2. 2 Dissolved oxygen concentrations (in $\mu\text{mol L}^{-1}$) in the lower 150 m of the Laurentian Channel measured in July 2003.

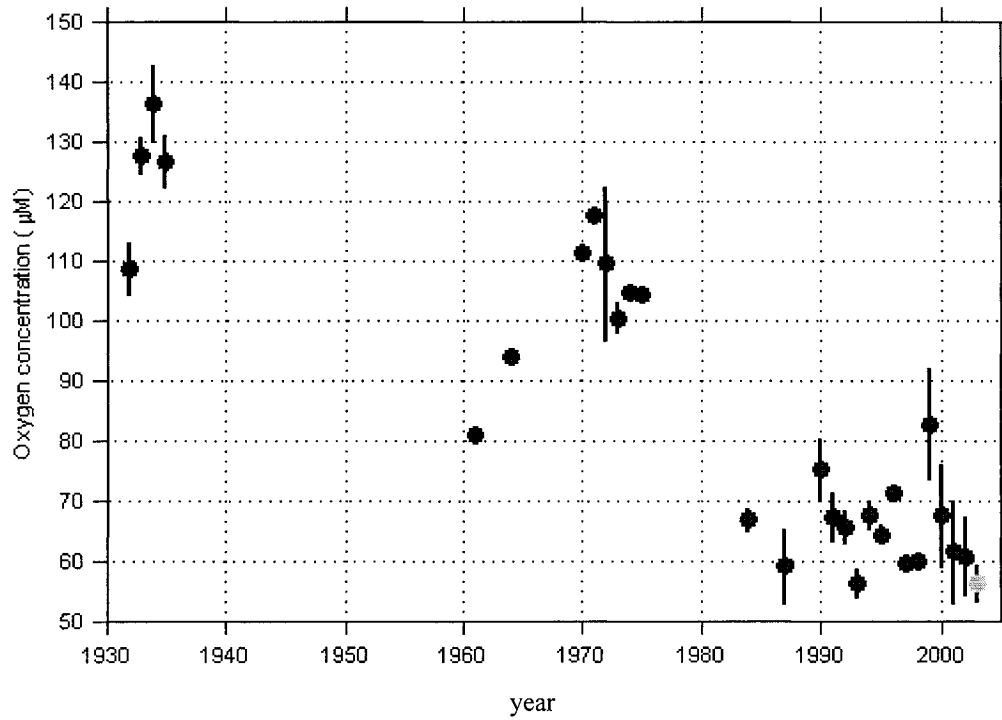


Fig. 2.3 Historical record of dissolved oxygen concentrations measured between 300 m and 355 m depth in the LSLE. The error bars show the 95% confidence intervals for the means when three or more measurements were made in a given year. The pale grey dot is the average of measurements carried out in 2003. Modified from Gilbert et al. (2004).

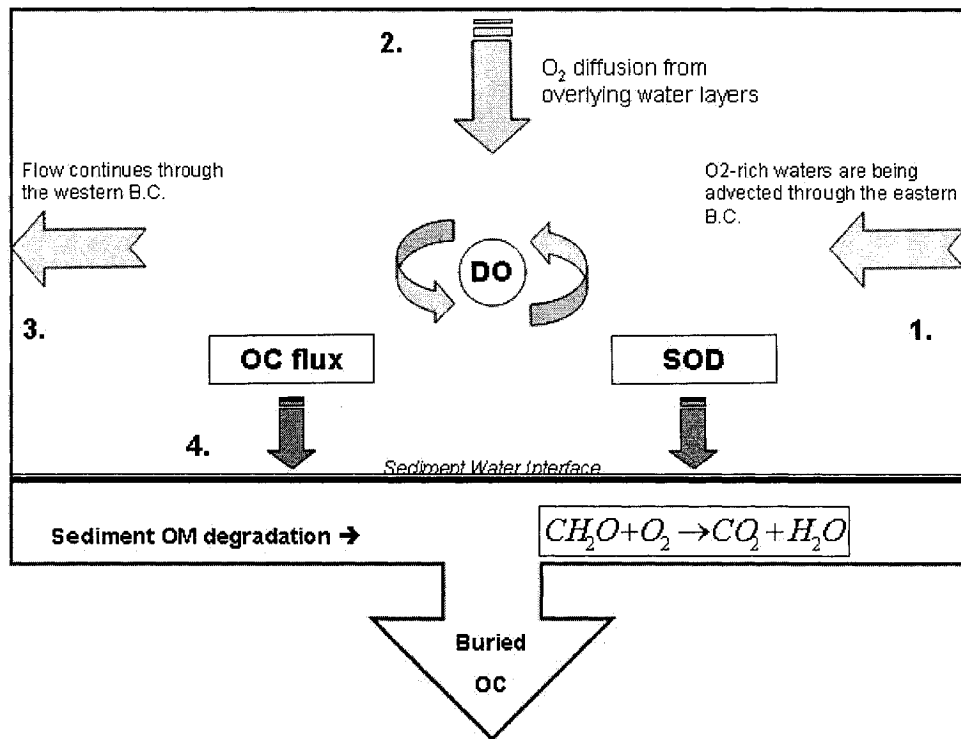


Fig. 2. 4 Schematic diagram of the advection-diffusion system conceptualized in this study.

The boundary conditions (B.C. in figure) are the following:

1. At STA 16 (200 km from Cabot Strait), an imposed Dirichlet condition :

$$[O_2]_{x=N} = C_N$$

2. At the 200 m isobath an imposed Dirichlet condition:

$$[O_2]_{z=M} = C_M$$

3. At the head of the estuary, the boundary is open as the numerical grid ends but the fluid motion remains unrestricted (Chapman, 1985). We impose a no-gradient Neumann condition:

$$\frac{\partial [O_2]_{x=0}}{\partial x} = 0$$

4. The lower boundary of the water column is defined as a Neumann condition and the magnitude of the oxygen flux (or demand) is given by results of the early diagenetic model.

Except for a few small-scale oscillations, conditions 1 and 2 do not vary much spatially, as can be seen in Fig. 2.2. Furthermore, both average DO values are quite similar, being $110.6 \mu\text{mol L}^{-1}$ for the 200 m isobath and $122.8 \mu\text{mol L}^{-1}$ for a vertical integration of station 16. Consequently, both values of C_N and C_M have been set at $120 \mu\text{mol L}^{-1}$ for this paper, which greatly facilitates the interpretation of model results.

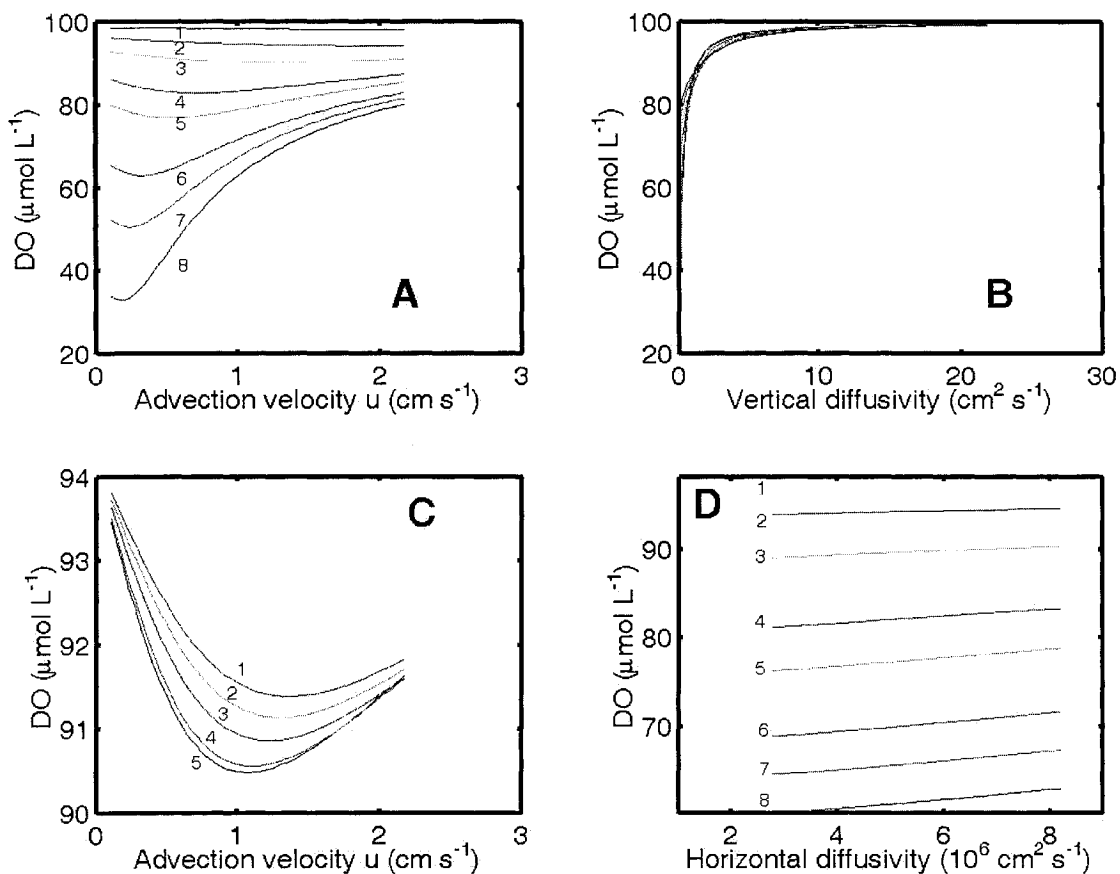


Fig. 2. 5 Sensitivity of modeled DO concentrations at STN 25 to horizontal advection and horizontal + vertical diffusivity (A) DO vs. u for lines of constant K_z ($\text{cm}^2 \text{s}^{-1}$) = 1: 9.80 2: 3.47 3: 1.91 4: 0.96 5: 0.64 6: 0.32 7: 0.20 8: 0.10, (B) DO vs. K_z for lines of constant u (cm s^{-1}), the results are too cluttered for proper discernment of specific curves, (C) DO vs. u for lines of constant K_h ($10^6 \text{cm}^2 \text{s}^{-1}$) = 1: 7.94 2: 6.35 3: 4.77 4: 3.18 5: 2.80, (D) DO vs. K_h for lines of constant K_z ($\text{cm}^2 \text{s}^{-1}$) = 1: 9.80 2: 3.47 3: 1.91 4: 0.96 5: 0.64 6: 0.32 7: 0.20 8: 0.10. (Note the different vertical DO scales.)

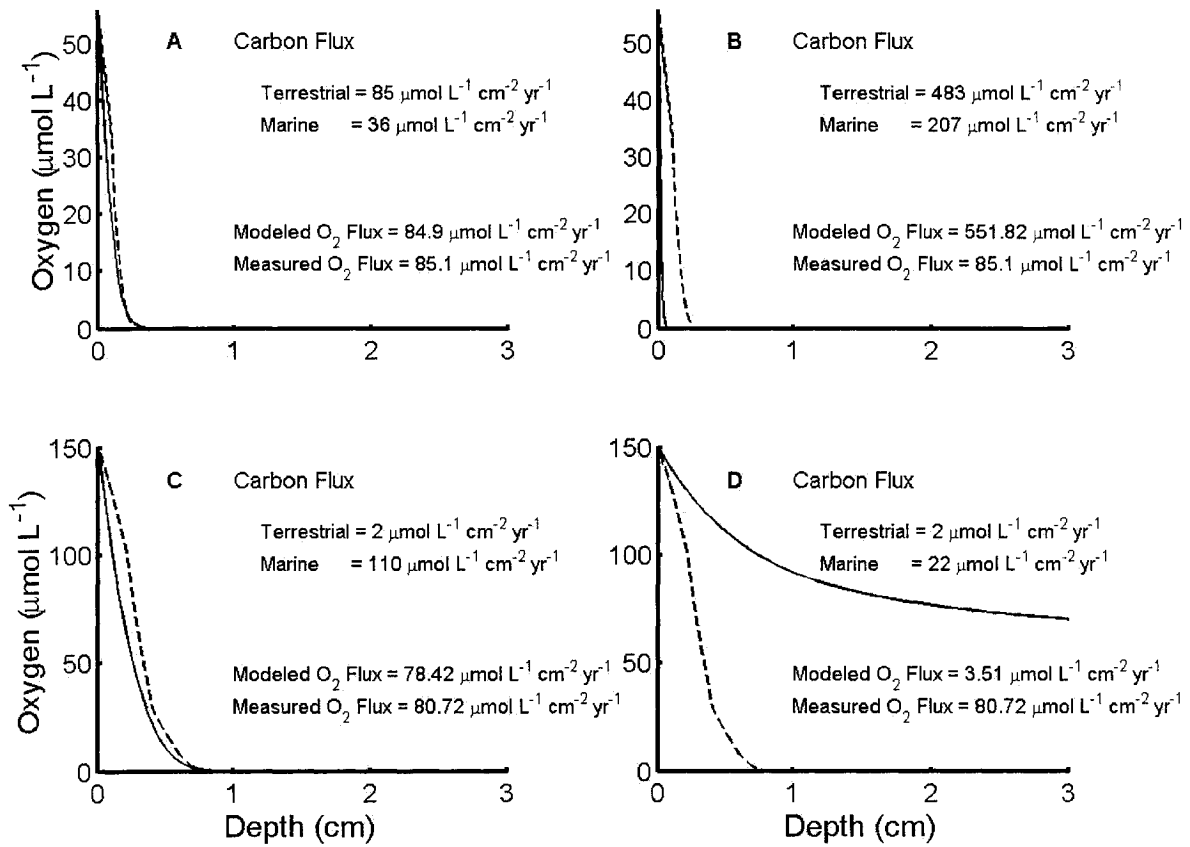


Fig. 2. 6 Comparison between modeled (full lines) and measured (dashed lines) O_2 sediment fluxes for stations 25 (A-B) and 19 (C-D). The input carbon fluxes and output oxygen fluxes are noted on each subplot, the parameter values are: (A-B) sedimentation rate $w = 0.8 \text{ cm/yr}$, biodiffusion coefficient $D_B = 13.4 \text{ cm}^2/\text{yr}$, terrigenous organic matter degradation rate constant $k_T = 0.35 \text{ yr}^{-1}$ (C-D) sedimentation rate $w = 0.08 \text{ cm/yr}$, biodiffusion coefficient $D_B = 2.68 \text{ cm}^2/\text{yr}$, terrigenous organic matter degradation rate constant $k_T = 0.088 \text{ yr}^{-1}$.

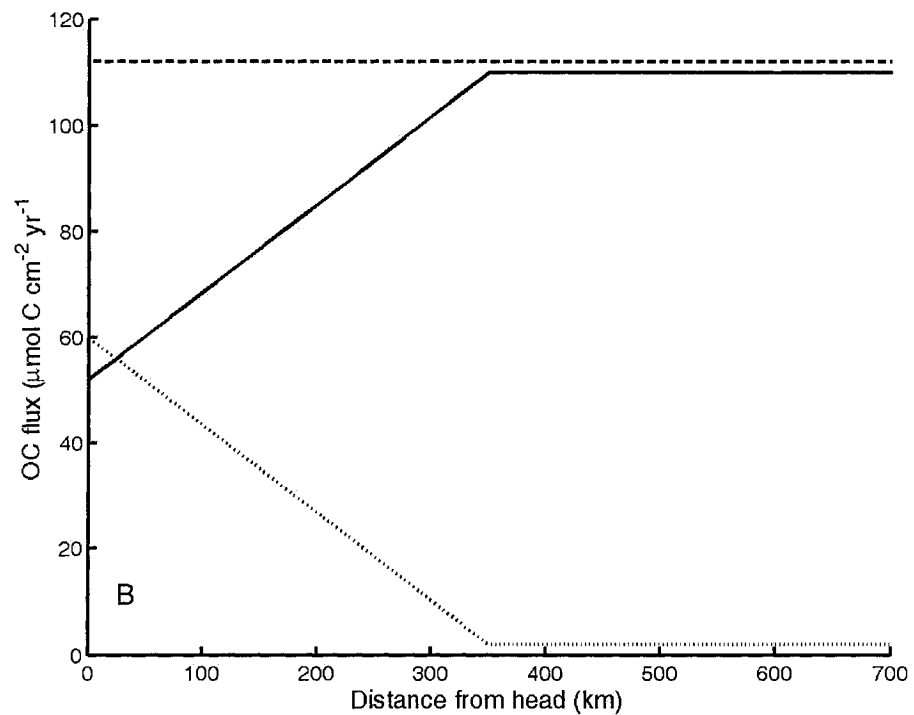
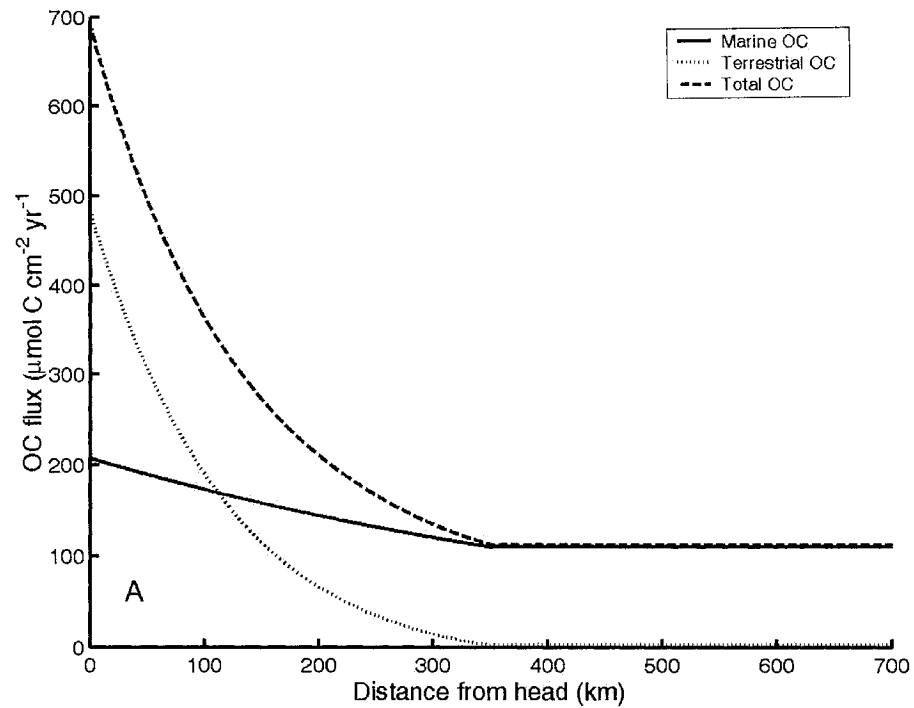


Fig. 2. 7 Organic carbon flux scenarios along the Laurentian Channel. (A) High flux scenario based on data acquired from 150 m depth sediment traps. (B) Low flux scenario that reproduces the oxygen fluxes calculated from oxygen gradients measured with voltammetric micro-electrodes across the sediment-water interface on cores recovered along the Laurentian Channel.

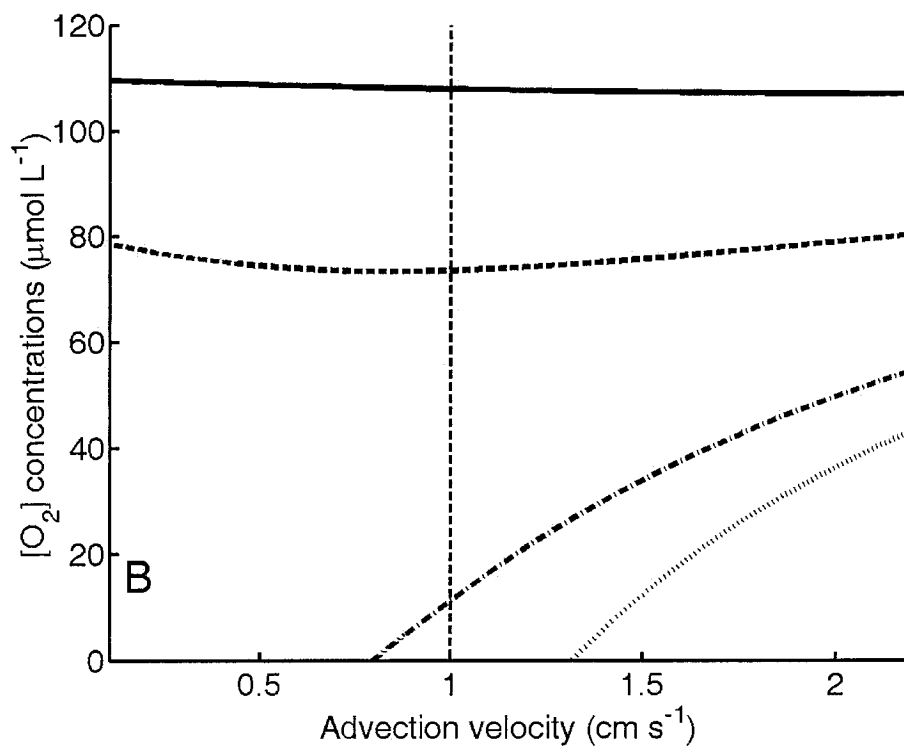
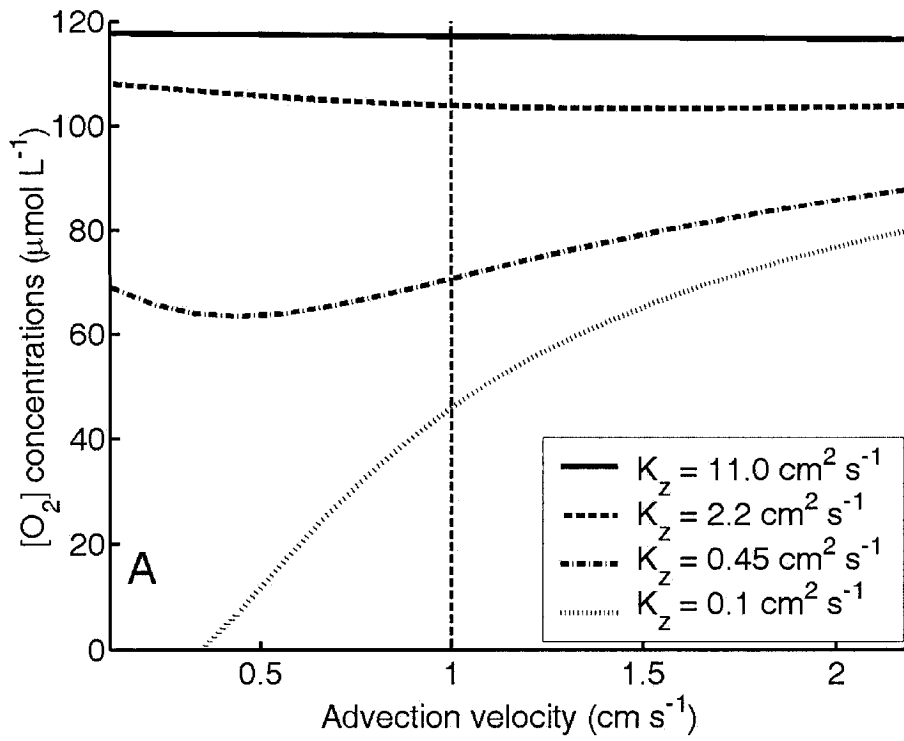


Fig. 2. 8 Modeled DO values at the bottom of STN 25. (A) Low carbon flux scenario. (B) High carbon flux scenario. The dashed, vertical line represents an average flow velocity of 1 cm s^{-1} .

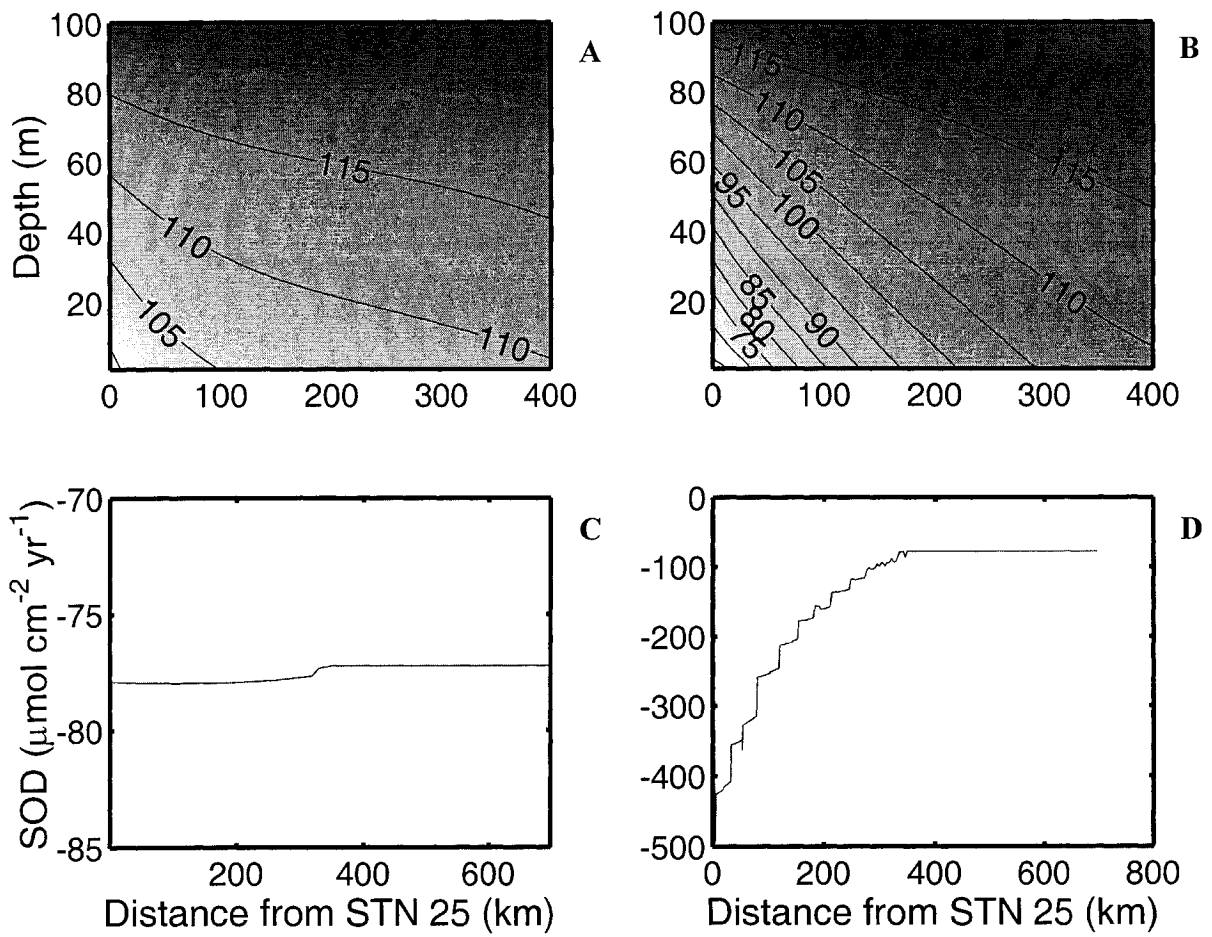


Fig. 2. 9 Water column DO (in $\mu\text{mol L}^{-1}$) concentration isolines and sediment oxygen demand along the Laurentian Channel for (A, C) the low carbon flux scenario and (B,D) the high carbon flux scenario.

2.10 Acknowledgements

This research was funded by National Sciences and Engineering Research Council (NSERC) of Canada Discovery grants to A.M. and Y.G. as well as by a graduate scholarship from NSERC and a McGill Tomlinson fellowship to P. Benoit. Discussions and comments by B. Sundby were very helpful. Special thanks go to D. Gilbert for a thoughtful review of this manuscript and for providing the data for Fig. 3 and the code to generate Fig. 1, and to C. Magen for providing sediment profiles. The authors also wish to thank the captain and crew of the R/V Coriolis II.

2.11 References

- Allredge, A.L. and Gotschalk, C.C., 1989. Direct observations of the mass flocculation of diatoms blooms: characteristics, settling velocities and formation of diatom aggregates. *Deep-Sea Res. I*, 36: 159-171.
- Anschutz, P., Sundby, B., LeFrançois, L., Luther, G.W., III and Mucci, A., 2000. High resolution profiles and fluxes of redox species in continental margin sediments: implications for the cycles of nitrogen, iodide, manganese, and iron. *Geochim. Cosmochim. Acta*, 64: 2751-2763.
- Apel, J.R., 1987. Principles of ocean physics. Academic Press, New York.
- Archer, D. and Devol, A.H., 1992. Benthic oxygen fluxes on the Washington shelf and slope: A comparison of in situ microelectrode and chamber flux measurements. *Limnol. Oceanogr.*, 37: 614-629.
- Ascher, U.M., Mattheij, R.M.M. and Russell, R.D., 1988. Numerical solution of boundary value problems for ordinary differential equations. Prentice-Hall, Inc, New Jersey.
- Berner, R.A., 1964. An idealized model of dissolved sulfate distribution in recent sediments. *Geochim. Cosmochim. Acta*, 28: 1497-1503.
- Berner, R.A., 1980. Early diagenesis: A theoretical approach. Princeton University Press, Princeton, NJ.
- Betzer, P.R., Showers, W.J., Laws, E.A., Winn, C.D., DiTullio, G.R. and Kroopnick, P.M., 1984. Primary productivity and particle fluxes on a transect of the equator at 153°W in the Pacific Ocean. *Deep-Sea Res.*, 31: 1-11.
- Boudreau, B.P., 1996. A method-of-line code for carbon and nutrient diagenesis in aquatic sediments. *Computers & Geosciences*, 22: 249-284.
- Boudreau, B.P., 1997. Diagenetic models and their implementation. Springer-Verlag, New York.
- Boudreau, B.P. and Ruddick, B.R., 1991. On a reactive continuum representation of organic matter diagenesis. *Amer. J. Sci.*, 291: 507-538.
- Bouldin, D.R., 1968. Models for describing the diffusion of oxygen and other mobile constituents across the mud-water interface. *J. Ecol.*, 56: 77-87.

- Breitburg, D., 2002. Effects of hypoxia, and the balance between hypoxia and enrichment, on coastal fishes and fisheries. *Estuaries*, 25: 767-781.
- Bugden, G.L., 1991. Changes in the temperature-salinity characteristics of the deeper waters of the Gulf of St. Lawrence over the past several decades. In: J.-C. Therriault (Editor), *The Gulf of St. Lawrence: small ocean or big estuary?* *Can. Spec. Publ. Fish. Aquat. Sci.*, 113 : 139-147.
- Cai, W.-J. and Sayles, F.L., 1996. Oxygen penetration depths and fluxes in marine sediments. *Mar. Chem.*, 52: 123-131.
- Chapman, D.C., 1985. Numerical treatment of cross-shelf open boundaries in a barotropic coastal ocean model. *J. Phys. Oceanogr.*, 15: 1060-1075.
- Cloern, J.E., 2001. Our evolving conceptual model of the coastal eutrophication problem. *Mar. Ecol. Prog. Ser.*, 210: 223-253.
- Colombo, J.C., Silverberg, N. and Gearing, J.N., 1996a. Biogeochemistry of organic matter in the Laurentian Trough, I. Composition and vertical fluxes of rapidly settling particles. *Mar. Chem.*, 51: 277-293.
- Colombo, J.C., Silverberg, N. and Gearing, J.N., 1996b. Biogeochemistry of organic matter in the Laurentian Trough, II. Bulk composition of the sediments and relative reactivity of major components during early diagenesis. *Mar. Chem.*, 51: 295-314.
- Di Toro, B.M., Paquin, P.R., Subburamu, K. and Gruber, D.A., 1990. Sediment oxygen demand model: methane and ammonia oxidation. *J. Env. Eng.*, 116: 945-985.
- Diaz, J.R. and Rosenberg, R., 1995. Marine benthic hypoxia: a review, its ecological effects and the behavioural responses of benthic macrofauna. *Oceanogr. Mar. Bio. Ann. Rev.*, 33: 245-303.
- Dickie, L. and Trites, R.W., 1983. The Gulf of St. Lawrence. In: (Editors), *Estuaries and semi-enclosed seas*. Elsevier Scientific Publication, Amsterdam, pp. 403-425.
- Edenborn, H.M., Silverberg, N., Mucci, A. and Sundby, B., 1987. Sulfate reduction in the sediments of a deep coastal environment. *Mar. Chem.*, 21: 329-345.
- Fisher, H.B., List, E.J., Koh, R.C.Y., Imberger, J. and Brooks, N.H., 1979. *Mixing in inland and coastal waters*. Academic Press, New York, NY.
- Froelich, P.N., Klinkhammer, G.P., Bender, M.L., Luedtke, N.A., Heath, G.R., Cullen, D., Dauphin, P., Hammond, D., Hartman, B. and Maynard, V., 1979. Early oxidation of organic matter in pelagic sediments of the eastern equatorial Atlantic: suboxic diagenesis. *Geochim. Cosmochim. Acta*, 43: 1075-1090.

- Gagnon, C., Mucci, A. and Pelletier, E., 1995. Anomalous accumulation of acid-volatile sulphides in a coastal marine sediment (Saguenay Fjord, Canada). *Geochim. Cosmochim. Acta*, 59: 2663-2675.
- George, P.L., 1991. Automatic mesh generation: Applications to finite element methods. Wiley, New York, NY.
- GESAMP, 2001. A sea of troubles. GESAMP Rep Stud 70 : 1-35.
- Gilbert, D. and Pettigrew, B., 1997. Interannual variability (1948-1994) of the CIL core temperature in the Gulf of St. Lawrence. *Can. J. Fish. Aquat. Sci.*, 54: 57-67.
- Gilbert, D., Sundby, B., Gobeil, C., Mucci, A. and Tremblay, G.H., 2004. A seventy-year record of diminishing deep-water oxygen levels in the St. Lawrence estuary - the northwest Atlantic connection. *Limnol. Oceanogr.*, (*in press, accepted with minor revisions Nov, 2004*).
- Gratton, Y., Edenborn, H.M., Silverberg, N. and Sundby, B., 1990. A mathematical model for manganese diagenesis in bioturbated sediments. *Amer. J. Sci.*, 290: 246-262.
- Gray, J.S., Wu, R.S.-S. and Or, Y.Y., 2002. Effects of hypoxia and organic enrichment on the coastal marine environment. *Mar. Ecol. Prog. Ser.*, 238: 249-279.
- Hall, P., Anderson, L.G., Rutgers van der Loeff, M.M., Sundby, B. and Westerlund, S.F.G., 1989. Oxygen uptake kinetics in the benthic boundary layer. *Limnol. Oceanogr.*, 34: 734-746.
- Han, G., Loder, J.W. and Smith, P.C., 1999. Seasonal-mean hydrography and circulation in the Gulf of St. Lawrence and on the eastern Scotian and southern Newfoundland shelves. *J. Phys. Oceanogr.*, 29: 1279-1301.
- House, W.A., 2003. Factors influencing the extent and development of the oxic zone in sediments. *Biogeochem.*, 63: 317-333.
- Jahnke, R.A., 2001. Constraining organic matter cycling with benthic fluxes. In: B.P. Boudreau and B.B. Jørgensen (Editors), *The benthic boundary layer*. Oxford University Press, pp. 144-179.
- Kantha, L.H. and Clayson, C.A., 1994. An improved mixed layer model for geophysical applications. *J. Geophys. Res.*, 99: 25,235-25,266.
- Koutitonsky, V.G. and Bugden, G.L., 1991. The physical oceanography of the Gulf of St. Lawrence: a review with emphasis on the synoptic variability of the motion. In:

- J.-C. Therriault (Editor), *The Gulf of St. Lawrence: small ocean or big estuary?* Can. Spec. Publ. Fish. Aquat. Sci., 113 : 57-90.
- Kwon, Y.W. and Bang, H., 1997. *The finite element method using MATLAB*. CRC Press, Boca Raton, FL.
- Louchouart, P., Lucotte, M., Canuel, R., Gagné, J.-P. and Richard, L.-F., 1997. Sources and early diagenesis of lignin and bulk organic matter in the sediments of the Lower St. Lawrence Estuary and the Saguenay Fjord. *Mar. Chem.*, 58: 3-26.
- Lucotte, M., Hillaire-Marcel, C. and Louchouart, P., 1991. First-order organic carbon budget in the St. Lawrence Lower Estuary from ^{13}C data. *Estuarine Coastal Shelf Sci.*, 32: 297-312.
- Lumley, J. and Panofsky, H.A., 1964. *The structure of atmospheric turbulence*. John Wiley & Sons, New York, NY.
- Luther, G.W., III, Brendel, P.J., Lewis, B.L., Sundby, B., LeFrançois, L., Silverberg, N. and Nuzzio, D.B., 1998. Simultaneous measurement of O_2 , Mn, Fe, I- and S (-II) in marine porewaters with a solid-state voltammetric microelectrode. *Limnol. Oceanogr.*, 43: 325-333.
- Martin, J.H., Knauer, G.A., Karl, D.M. and Broenkow, W.W., 1987. VERTEX: carbon cycling in the northeast Pacific. *Deep-Sea Res.*, 34: 267-285.
- Meile, C., Koretsky, C. and Van Cappellen, P., 2001. Quantifying bioirrigation in aquatic sediments: An inverse modelling approach. *Limnol. Oceanogr.*, 46: 164-177.
- Meile, C. and Van Cappellen, P., 2003. Global estimates of enhanced solute transport in marine sediments. *Limnol. Oceanogr.*, 48: 777-786.
- Mertz, G. and Gratton, Y., 1995. The generation of transverse flows by internal friction in the St. Lawrence Estuary. *Cont. Shelf Res.*, 15: 789-801.
- Meysman, F.J.R., Middelburg, J.J., Herman, P.M.J. and Heip, C.H.R., 2003. Reactive transport in surface sediments. II. Media: an object-oriented problem-solving environment for early diagenesis. *Computers & Geosciences*, 29: 301-318.
- Middelburg, J.J., Soetaert, K. and Herman, P.M.J., 1997. Empirical relationships for use in global diagenetic models. *Deep-Sea Res. I*, 44: 327-344.
- Mucci, A., Sundby, B., Gehlen, M., Arakaki, T., Zhong, S. and Silverberg, N., 2000. The fate of carbon in continental shelf sediments of eastern Canada; a case study. *Deep-Sea Res. II*, 47: 733-760.

- Muzuka, A.N.N. and Hillaire-Marcel, C., 1999. Burial rates of organic matter along the eastern Canadian margin and stable isotope constraints on its origin and diagenetic evolution. *Mar. Geo.*, 160: 251-270.
- Nixon, S.W., 1995. Coastal marine eutrophication: a definition, social causes, and future concerns. *Ophelia*, 41: 199-220.
- Nordberg, K., Filipsson, H.L., Gustafsson, M., Harland, R. and Roos, P., 2001. Climate, hydrographic variations and marine benthic hypoxia in Koljoe Fjord, Sweden. *J. Sea Res.*, 46: 187-200.
- Plante, S., Chabot, D. and Dutil, J.-D., 1998. Hypoxia tolerance in Atlantic cod. *J. Fish Bio.*, 53: 1342-1356.
- Rabalais, N.N. and Turner, R.E., 2001. Hypoxia in the Northern Gulf of Mexico: Description, Causes and Change. In: N.N. Rabalais and R.E. Turner (Editors), *Coastal Hypoxia: consequences for living resources and ecosystems*. American Geophysical Union, Washington, D.C., pp. 1-37.
- Rabouille, C. and Gaillard, J.-F., 1991a. A coupled model representing the deep-sea organic carbon mineralization and oxygen consumption in surficial sediments. *J. Geophys. Res.*, 96: 2761-2776.
- Rabouille, C. and Gaillard, J.-F., 1991b. Towards the Edge: Early diagenetic global explanation. A model depicting the early diagenesis of organic matter, O₂, NO₃, Mn and PO₄. *Geochim. Cosmochim. Acta*, 55: 2511-2525.
- Ramsing, N. and Gundersen, J., 1994. Seawater and gases. Tabulated physical parameters of interest to people working with microsensors in marine systems. Version 1.0. Revised tables compiled at Max Planck Institute for Marine Microbiology, Bremen, Germany.
- Redfield, A.C., Ketchum, B.J. and Richards, F.A., 1963. The influence of organisms on the composition of seawater. In: M.R. Hill (Editors), *The Sea*. J. Wiley & Sons, pp. 26-77.
- Saucier, F.J., Roy, F., Gilbert, D., Pellerin, P. and Ritchie, H., 2003. Modeling the formation and circulation processes of water masses and sea ice in the Gulf of St. Lawrence, Canada. *J. Geophys. Res.*, 108: 3269-3289.
- Savenkoff, C., Vézina, A.F., Packard, T.T., Silverberg, N., Therriault, J.-C., Chen, W., Bérubé, C., Mucci, A., Klein, B., Mesplé, F., Tremblay, J.-E., Legendre, L., Wesson, J. and Ingram, R.G., 1996. Distributions of oxygen, carbon, and respiratory activity in the deep layer of the Gulf of St. Lawrence and their implications for the carbon cycle. *Can. J. Fish. Aquat. Sci.*, 53: 2451-2465.

- Savenkoff, C., Vézina, A.F., Smith, P.C. and Han, G., 2001. Summer transports of nutrients in the Gulf of St. Lawrence estimated by inverse modelling. *Estuarine Coastal Shelf Sci.*, 52: 565-587.
- Sayles, F.L., Martin, W.R. and Deuser, W.G., 1994. Response of benthic oxygen demand to particulate organic carbon supply in the deep sea. *Nature*, 371: 686-689.
- Silverberg, N., Bakker, J., Edenborn, H.M. and Sundby, B., 1987. Oxygen profiles and organic carbon fluxes in Laurentian Trough sediments. *Neth. J. Sea Res.*, 21: 95-105.
- Silverberg, N., Edenborn, H.M. and Belzile, N., 1985. Sediment response to seasonal variations in organic matter input. In: A.C. Sigleo and A. Hattori (Editors), *Marine and estuarine geochemistry*. Lewis Publishing inc., Chelsea, MI, pp. 69-80.
- Silverberg, N., Sundby, B., Mucci, A., Zhong, S., Arakaki, T., Hall, P., Landén, A. and Tengberg, A., 2000. Remineralization of organic carbon in eastern Canadian continental margin sediments. *Deep-Sea Res. II*, 47: 699-731.
- Smith, J.N. and Schafer, C.T., 1999. Sedimentation, bioturbation, and Hg uptake in the sediments of the estuary and Gulf of St. Lawrence. *Limnol. Oceanogr.*, 44: 207-219.
- Soetaert, K., Herman, P.M.J. and Middelburg, J.J., 1996. A model of early diagenetic processes from the shelf to abyssal depths. *Geochim. Cosmochim. Acta*, 60: 1019-1040.
- St-Onge, G., Stoner, J.S. and Hillaire-Marcel, C., 2003. Holocene paleomagnetic records from the St. Lawrence Estuary, eastern Canada: centennial to millennial-scale geomagnetic modulation of cosmogenic isotopes. *Earth and Planetary Sciences Letters*, 209: 113-130.
- Syvitski, J.P.M., 1989. Quaternary sedimentation in the St. Lawrence Estuary and adjoining areas, eastern Canada: an overview based on high resolution seismography. *Geogr. Phys. Quat.*, 43: 291-310.
- Taylor, G.I., 1953. Dispersion of soluble matter in solvent flowing slowly through a tube. *Proc. Royal Soc. London. Series A.*, 219: 186-203.
- Therriault, J.-C., Legendre, L. and Demers, S., 1990. Oceanography and Ecology of phytoplankton in the St. Lawrence Estuary. In: M.I. El-Sabh and N. Silverberg (Editors), *Oceanography of a large-scale estuarine system*. Springer-Verlag, New York, pp. 269-281.

- Thibodeau, B., de Vernal, A. and Mucci, A., 2004. Development of micropaleontological and geochemical indicators of eutrophication in the St. Lawrence Estuary. Abstract, Spring AGU meeting, May 17-21, Montreal, QC, Canada.
- Timothy, D.A., 2004. Organic matter remineralisation and biogenic silica dissolution in a deep fjord in British Columbia, Canada: a regression analysis of upper ocean sediment-trap fluxes. *Deep-Sea Res. I*, 51: 439-456.
- Ullman, W.J. and Aller, R.C., 1982. Diffusion coefficients in nearshore marine sediments. *Limnol. Oceanogr.*, 27: 552-556.
- Van Cappellen, P. and Wang, Y., 1996. Cycling of iron and manganese in surface sediments: A general theory for the coupled transport and reaction of carbon, oxygen, nitrogen, sulfur, iron, and manganese. *Amer. J. Sci.*, 296: 197-243.
- Von Schwind, J.J., 1980. *Geophysical fluid dynamics for oceanographers*. Prentice-Hall, Englewood cliffs.
- Westrich, J.T. and Berner, R.A., 1984. The role of sedimentary organic matter in bacterial sulfate reduction: The G model tested. *Limnol. Oceanogr.*, 29: 236-249.
- Wu, R.S.-S., 2002. Hypoxia: from molecular responses to ecosystem responses. *Mar. Poll. Bull.*, 45: 35-45.

CHAPTER 3

3 General Conclusions

3.1 *Summary and review of objectives*

The present thesis is a preliminary attempt to tackle one of the key environmental issues affecting the Lower St. Lawrence Estuary (LSLE): the progressive development of hypoxic bottom waters as described by Gilbert et al., 2004. The authors of this latter publication showed that over the past several decades, a severe depletion of dissolved oxygen (DO) (in excess of $60 \mu\text{mol L}^{-1}$ since the early 1930s) has occurred in the bottom waters of the LSLE, of which up two thirds can be related to a change in the oceanic regime on the continental shelf edge of the northwest Atlantic (i.e., composition and properties of the waters that enter the Estuary at the mouth of the Laurentian Channel (LC)). The other third was tentatively related to an increase in sediment oxygen demand (SOD) in response to a progressive increase in the delivery of metabolizable organic matter (OM) to the sediment over the last century (St-Onge et al., 2003) and more recent eutrophication (Thibodeau et al., 2004). In order to verify the latter hypothesis, we implemented a simple model to determine if the actual SOD along the LC can generate sufficiently low oxygen levels in the LSLE. The landward increase in particulate OM delivery and concomitant decrease in DO levels in the bottom waters of the Laurentian Trough has often been reported (e.g., Savenkoff et al., 1996), yet no specific study has ever focused on this phenomenon. A simple, coupled benthic-pelagic model of the deep layer in the LC within which the fluid transport in the water column was parameterized as a 2-D advective-diffusive process was elaborated. The DO sink was provided by the oxic mineralization of organic carbon accumulating at the sediment-water interface. Details of the model implementation and its results were thoroughly discussed in the previous

chapter. In the text that follows I review in detail how each of the major objectives described in the General Introduction were met in the course of this study.

- *Testing the sensitivity of the water column with respect to DO levels to the following physical parameters: advection (horizontal) and diffusion (horizontal and vertical).*

As described in section 2.2 (Chapter 2), the parameter sensitivity test results for the water column clearly show that the bottom water DO concentrations are highly responsive to variations in the coefficient of vertical diffusivity. For sufficiently high coefficient values ($> 3 \text{ cm}^2 \text{ s}^{-1}$), there is relatively little depletion of oxygen in the bottom waters as it is rapidly replenished by mixing with the overlying normoxic waters. In contrast, under a specific threshold value ($\sim < 3 \text{ cm}^2 \text{ s}^{-1}$), DO levels become extremely sensitive to the vertical diffusivity. In other words, diffusivity is weak enough that the replenishment of bottom water DO is dominated by horizontal advection of waters from the eastern boundary (see Fig. 2.5B). Most of the variability associated with the advection velocity occurs within a factor of two of the best average estimate (i.e. 1 cm s^{-1} ; Han et al., 1999; Saucier et al., 2003). For large velocities ($> 2 \text{ cm s}^{-1}$) the flow is sufficiently strong to quickly replenish bottom water oxygen in the LSLE, such that DO levels remain relatively high. A subsequent decrease in velocity, down to $< 0.5 \text{ cm s}^{-1}$, results in a depletion of DO until a threshold is reached where the advection velocity is so low that diffusion again will overcome the incoming flow, and DO levels will subsequently rise (see Fig. 2.5A). As can be seen in Fig. 2.5D (Chapter 2), the system was not very sensitive to changes in the horizontal diffusivity coefficient. Given the sensitivity of the system to vertical diffusivity, realistic estimates were sought in the literature but very few spatially-averaged estimates could be found. Only two independent estimates were considered, $K_z = 2.2 \text{ cm}^2 \text{ s}^{-1}$ evaluated by Bugden (1991) based on advection-diffusion modeling of Temperature-Salinity in the deep waters and, $K_z = 0.45 \text{ cm}^2 \text{ s}^{-1}$ estimated by Savenkoff et al. (2001) based on inverse modeling of the nutrient field. Although these estimates differ only by a factor of ~ 5 , modeled DO levels at the head of the LSLE head varied by 30 to 80%, depending on the carbon flux scenario. The estimate by Bugden (1991) was deemed more relevant to this study since it

was based on a physical framework similar to the one used to parameterize the advection-diffusion model developed in this thesis.

- *Determining the organic carbon flux required to reproduce, to a first approximation, the DO profiles measured across the sediment-water interface on sediment cores recovered along the Laurentian Trough.*

In Chapter 2 we described in detail the physical and chemical justifications behind the conception of the early diagenesis model. The latter's main shortfall is its restriction to purely oxic mineralization pathways, which are assumed to dominate the SOD for the LC seafloor. The organic carbon (OC) input was separated in two distinct components: a highly reactive marine autochthonous fraction primarily composed of algal and planktonic detritus, and a more refractory allochthonous fraction originating from land-based plant material. Model results (i.e., SOD and/or DO profiles/gradients across the sediment-water interface) were then compared against field measurements at two test sites, one in the LSLE and one in the Gulf portion of the LC. Modeled and measured oxygen profiles for both sites and their resulting SOD are presented in Fig. 2.6. These indicate that the OC flux needed to reproduce the SOD in the Gulf is nearly equal to the flux measured by sediment traps set at 150 m depth, justifying the assumptions (i.e., oxic mineralization) of the simplified diagenesis model. On the other hand, the OC flux required to reproduce the SOD in the LSLE was far less than the sediment trap measurements, suggesting that the simple model cannot handle very large OC fluxes or that processes (e.g., enhanced biodiffusion) operating in the LSLE remove a fraction of the incoming OC without being recorded in the sediment record..

- *Developing realistic scenarios of organic carbon fluxes to the sediment along the Laurentian Channel based on other proxies (i.e., OC burial rates, sediment trap measurements, primary production in the overlying waters) and distinguishing between terrestrial and marine components.*

A comprehensive literature review of OC accumulation rates and SOD along the LC was presented in section 2.4.4.1 of Chapter 2, with an emphasis on extracting parameters important to the elaboration of the diagenetic model. Although little data are available over the length of the LC floor, the information compiled in Table 2.3 was combined with insight gained by testing the early diagenetic model to formulate two possible OC sediment flux scenarios (Fig. 2.7). A high flux scenario was devised on the basis of sediment trap measurements from 150 m depth. Under this scenario, the total flux of OC is large in the LSLE but diminishes exponentially to a constant value outside the estuary. This spatial function is set to mimic the pattern of sediment accumulation rates along the LC as measured by Smith and Schafer (1999) using ^{210}Pb . In the LSLE, the terrestrial component dominates the carbon load but its contribution decreases quickly seaward until it becomes a negligible component in the Gulf. The flux of marine OC does not vary as much throughout the LC, decreasing linearly seaward to almost half its value between the LSLE and the Gulf where it is the dominant OC component. This scenario is compatible with the fact that the LSLE receives most of the terrestrial OC river discharges and most the terrestrial particulate matter settles within the LSLE (Lucotte et al., 1991).

Alternatively, a low flux scenario was generated to reproduce the micro-electrode DO profiles (and, therefore SOD) measured on sediment cores collected along the LSLE and the Gulf. Since all of the measured sediment oxygen profiles reveal similar oxygen penetration depths (i.e., 3-5 mm), the total OC flux to the sediment-water interface was fixed at a constant rate. Under this scenario, the marine carbon component of the TOC flux at the head of the LSLE was set to a fraction of the minimum estimated surface water primary productivity and was increased linearly until it reached its maximum value in the Gulf. Conversely, the terrestrial OC source function was a mirror image of the marine OC distribution. The scenarios can thus be considered as end-members in the range of possible particulate OM fluxes to the bottom waters of the LC.

- *Ascertaining whether or not the sediment oxygen demand resulting from the above-mentioned OC flux scenarios can reproduce the recently observed hypoxic DO levels in the LSLE.*

The water column and the sediment model were coupled using the two aforementioned carbon flux scenarios as input functions and the DO concentrations in the bottom waters at the head of the LSLE were computed. The results (displayed in Fig. 2.8 and 2.9) emphasize the model sensitivity to the vertical diffusivity and the interpretation of the resulting oxygen depletion. Using Bugden's (1991) estimate of the vertical diffusion coefficient as the most realistic value for the deep Laurentian Trough requires large oxygen fluxes, prescribed by the high flux scenario in the LSLE, to achieve hypoxic DO levels. Whereas this latter scenario ultimately appears more realistic for the St. Lawrence system, there remains the discrepancy between the large SOD modeled using that scenario and the smaller SOD extracted from sediment micro-electrode profiles in the LSLE. Three possible explanations were suggested: either the excess OM is removed by respiration in the water column below the 150 m isobath, the OC reactivities are much higher than anticipated in the LSLE or that the early diagenesis model does not account for mechanisms (e.g. enhanced biodiffusion; Meile and Van Cappellen, 2003) that will remove oxygen from the water column without being recorded in the sediment. The former is not likely due to fast particle sinking rates in the LSLE (Lucotte et al., 1991, Savenkoff et al., 1996), and the fact that over 75% of the material would have to be removed, which seems unreasonable compared to maximum estimates of 40% removal in deep fjords (Timothy, 2004). An increased reactivity of the settling OC to explain the flux discrepancy was dismissed due to its small impact on the DO modeled profiles across the sediment-water interface (SWI) in the LSLE. Thus, we concluded that refinements (e.g., enhanced diffusion near the SWI) to the diagenesis model would be required to solve this problem.

3.2 Conclusions

The benthic-pelagic model developed and used in this study was successful in meeting all the major objectives established for this M.Sc. Despite all the simplifying assumptions in the conception of the model, both the water column and sediment components used realistic parameters in order to reproduce, to a first approximation, the DO levels observed in the LSLE. Both the benthic and pelagic components of this model are heavily influenced by specific parameters. For the water column, DO levels at the head of the LSLE are highly dependant on the coefficient of vertical diffusivity and, to a lesser extent, on the advection velocity of the flow. For the sediment model, the major factors influencing the computed oxygen profiles are the combined marine and terrestrial OC flux rates, the concentrations of DO in the water column, and the molecular diffusion and bioturbation coefficients. Whereas the sediment DO profiles and fluxes were successfully reproduced in the GSL, there were not in the LSLE. Because a large SOD in the LSLE seafloor is required to generate hypoxia in the water column, our model results implicitly confirmed observations reported by other researchers (e.g., Miele and Van Capellen, 2003) that SOD estimates from measured micro-electrode profiles underestimate the true oxygen flux across the sediment-water interface in high OC flux settings such as the LSLE.

In order to offer a tentative answer to the question raised in Chapter 1 'Have the bottom waters of the LSLE become hypoxic as a result of eutrophication?', the major lines of evidence for eutrophication in the LSLE will be reviewed and placed within the context of the current model results.

The most concrete evidence of eutrophication lies with the sediment record. As explained in Chapter 1, a composite profile of a sediment core taken near STN 23 (see Fig. 1.8) in the LSLE revealed an increase in total OC content starting from the 17th century, corresponding nearly with the emergence of European colonies (St-Onge et al., 2003). This is accompanied by an increase of the C:N molar ratio and a decrease of the ¹³C signature of the OC. An increase of the ¹³C signature since the 1970's, is interpreted

as an increase of the proportion of marine OC delivered to the seafloor. Complementing these results is a new proxy study of a sediment core from STN 23 showing a significant increase in the abundance of dinoflagellates and benthic foraminiferal organic linings over the same period (Thibodeau et al., 2004). These changes in the abundance of fossil pelagic and benthic faunal assemblages reflect an increase in production, which is possibly linked to a greater availability of nutrients in the surface waters (i.e., eutrophication; Cloern, 2001).

Further lines of evidence for eutrophication reside in multi-decadal DO water column profiles for the LC, which were analyzed by Gilbert et al. (2004). The latter authors showed that a gradual increase in the temperature of waters entering the LC since the 1930's up to the end of the 1970's can account for 30 to 50 $\mu\text{mol L}^{-1}$ of the 60 $\mu\text{mol L}^{-1}$ loss of DO levels in the LSLE. For the past two decades however, only negligible changes in temperatures were recorded at 250 m depth at Cabot Strait and in the bottom waters of the LSLE. In contrast to the DO gradient between these two locations has increased by $20.5 \pm 11.9 \mu\text{mol L}^{-1}$ during the same time period. Gilbert et al. (2004) suggest this recent decline in O_2 levels is not due to climate variability but to other factors, the most likely among them being an increase in the SOD along the LC.

The model developed in this study lends support the importance of the sediment as the primary sink of oxygen within the LC and its role in the generation of hypoxic waters at the LSLE head. Furthermore, our simulations for the low and high OC flux regimes to the LC seafloor imply that an increase in the amount of OM delivered to the sediment will generate a further decrease of DO levels in the bottom waters of the LSLE. If a similar change in OC flux occurred within the last three decades, as suggested by the sediment core data (St-Onge et al., 2003; Thibodeau et al., 2004), then the increase of the DO gradient along the LC reported by Gilbert et al. (2004) could directly be related to an increase in SOD. The integration of all these factors suggest that the LSLE has indeed become eutrophic within the past few decades, i.e. that the amount of OM produced within its boundaries is beyond what can be effectively removed by grazing organisms and exported by physical processes.

This study becomes an important first step in identifying the role of OM degradation on the development and maintenance of hypoxic deep waters in the LSLE. Continuous monitoring of this problem is crucial for the future health of the large St. Lawrence marine ecosystem. As stated in the introduction, hypoxic or anoxic regions affect thousands of km² of coastal waters along each of the five major continents (Nixon, 1995; Diaz and Rosenberg, 1995; Wu, 2002; USCOP, 2004). More often than not, the reduction in DO is due to excessive anthropogenic inputs of nutrients and OM in systems with limited circulation (Cloern, 2001). It is important to ascertain whether or not such a phenomenon is occurring in the St. Lawrence and how serious it is in order to build public awareness of this generally unknown environmental problem as well as establish stringent policies for remediation. As further incentive, Diaz and Rosenberg's (1995) argued that the recovery of a marine ecosystem severely affected by hypoxia is generally a lengthy process (i.e., years to decades), with no evidence of large systems ever recovering after the development of persistent oxygen depleted regions. Such an event in the St. Lawrence could be disastrous both socially and economically for the Canadian east coast in years to come.

3.3 Recommendations for future work

In order to provide a more realistic estimate of DO levels in the LSLE, substantial modifications would have to be made to the model. A first modification to be applied in a future extension of this thesis is the addition of time as a parameter. This would allow testing of the bottom water response to temporally varying boundary conditions (e.g., properties of the waters that enter the Estuary at the mouth of the LC). This would require additional assumptions when considering past levels of O₂ supply, OC flux, OPD, DO, etc. as no extensive multi-decadal dataset for the LC is available with respect to these variables. Nevertheless, annually variable OC flux scenarios along the LC could be applied for different time intervals to verify the impact on DO levels. The scenarios could also incorporate intra-annual variability to account for seasonal inputs of nutrients and resulting phytoplankton and algal blooms. The integration of all these temporal factors would provide a new tool to investigate possible eutrophication in the LSLE.

On the hydrodynamic aspect of the model, too many constraints are in place within the simple parameterization of the water column (i.e. steady-state, constant diffusivity and flow) to allow anything but a first-order approximation of the tracer distribution. The addition of bathymetric features, more accurate boundary conditions and a more realistic geometry for the LC (i.e., cone as opposed to a cylinder) would likely provide a clearer distribution pattern for DO. In addition, the use of spatially and temporally varying coefficients within the water column parameterization in Eq. 2.2 would supersede the need to assign constant values to the diffusion coefficients and advection velocity. This is particularly important with regards to the vertical diffusivity, as it represents a measure of the stratification in the water column and is the most sensitive model parameter. A spatially and temporally variable vertical diffusivity, as used by Saucier et al. (2003), may allow a reconciliation of the modeled and measured DO concentrations. Another term that has been neglected in Eq. 2.2 is the Q source term, which is associated with respiration in the water column. Although respiration was assumed to have little impact on the overall budget of DO in the LC, it would help in reproducing the fine-scale patterns of oxygen in the water column.

As previously mentioned, further modeling efforts would be greatly improved with the availability of a larger quantity of sediment core analyses from the LC. The latter are few and far between, as documented in Table 2.3. Additional measurements would allow the elaboration of more realistic carbon flux scenarios and the comparison of various methods for the evaluation of the SOD, notably micro-electrode profiling, benthic chamber measurements and ship-board incubations. Silverberg et al. (2000) compared oxygen fluxes estimated from ship-board DO micro-electrode profiles to whole core incubations and reported that the latter gave slightly larger oxygen fluxes. The authors attributed this to possible bacterial degradation at the sediment-water interface, but still found good agreement between both methods of measurements, since the resulting values were generally contained within the uncertainty of the methods. A similar comparison on sediment cores recovered at the head of the LSLE would help to resolve the quandary and

verify the validity of the large fluxes generated by the current diagenetic model (see Fig. 2.6).

Further refinements could be applied to the early diagenesis model, particularly in making the transition from a mono-oxidant to a multi-oxidant model (e.g. see Meysman et al., 2003), where the oxidation of migrating reduced species from deeper within the sediment could contribute to the SOD. Although this contribution to the SOD was assumed to be negligible in this thesis, further investigation would be well-advised. However, in order to fully represent all the important species (e.g. Fe, Mn, C, S, etc...) in a diagenetic model, a more complete database of sediment concentration profiles is required for the LC seafloor. The large discrepancy between measured and modeled O_2 fluxes at the sediment-water interface in the LSLE in the case of the high carbon flux scenario need to be addressed further. The discrepancy may reflect limitations imposed by the sediment diagenetic model and the contribution of enhanced bio-diffusion to the exchange of DO between the sediment water interface and the overlying waters (e.g. see Meile and Van Cappellen, 2003). Other processes could accelerate the exchange of DO, including pressure gradients resulting from topographic features and strong bottom water currents, as documented for permeable sediments (i.e., sands; Ziebis et al., 1996; Roy et al., 2002; Lorke et al., 2003). Such considerations are beyond the scope of this study but should be investigated in future field and modeling efforts. In this respect, the LSLE remains an interesting region for the study of diagenetic processes, as it is a very deep coastal estuary receiving massive amounts of OC, a setting that cannot be resolved via standard empirical relationships for sediment models (e.g. Middelburg et al., 1997).

3.4 References

- Bugden, G.L., 1991. Changes in the temperature-salinity characteristics of the deeper waters of the Gulf of St. Lawrence over the past several decades. In: J.-C. Therriault (Editor), *The Gulf of St. Lawrence: small ocean or big estuary?* Can. Spec. Publ. Fish. Aquat. Sci., 113 : 139-147.
- Cloern, J.E., 2001. Our evolving conceptual model of the coastal eutrophication problem. *Marine Ecology Progress Series*, 210: 223-253.
- Diaz, J.R. and Rosenberg, R., 1995. Marine benthic hypoxia: a review, its ecological effects and the behavioural responses of benthic macrofauna. *Oceanography and Marine Biology Annual Review*, 33: 245-303.
- Gilbert, D., Sundby, B., Gobeil, C., Mucci, A. and Tremblay, G.H., 2004. A seventy-year record of diminishing deep-water oxygen levels in the St. Lawrence estuary - the northwest Atlantic connection. *Limnology and Oceanography*, (*in press, accepted with minor revisions Nov, 2004*).
- Han, G., Loder, J.W. and Smith, P.C., 1999. Seasonal-mean hydrography and circulation in the Gulf of St. Lawrence and on the eastern Scotian and southern Newfoundland shelves. *Journal of physical oceanography*, 29: 1279-1301.
- Lorke, A., Müller, B., Maerki, M. and Wüest, A., 2003. Breathing sediments: The control of diffusive transport across the sediment-water interface by periodic boundary-layer turbulence. *Limnology and Oceanography*, 48: 2077-2085.
- Lucotte, M., Hillaire-Marcel, C. and Louchouart, P., 1991. First-order organic carbon budget in the St. Lawrence Lower Estuary from ^{13}C data. *Estuarine, Coastal and Shelf Science*, 32: 297-312.
- Meile, C. and Van Cappellen, P., 2003. Global estimates of enhanced solute transport in marine sediments. *Limnology and Oceanography*, 48: 777-786.
- Meysman, F.J.R., Middelburg, J.J., Herman, P.M.J. and Heip, C.H.R., 2003. Reactive transport in surface sediments. II. Media: an object-oriented problem-solving environment for early diagenesis. *Computers & Geosciences*, 29: 301-318.
- Middelburg, J.J., Soetaert, K. and Herman, P.M.J., 1997. Empirical relationships for use in global diagenetic models. *Deep-Sea Research I*, 44: 327-344.
- Nixon, S.W., 1995. Coastal marine eutrophication: a definition, social causes, and future concerns. *Ophelia*, 41: 199-220.

- Roy, H., Hüttel, M. and Jørgensen, B.B., 2002. The role of small-scale sediment topography for oxygen flux across the diffusive boundary layer. *Limnology and Oceanography*, 47: 837-847.
- Saucier, F.J., Roy, F., Gilbert, D., Pellerin, P. and Ritchie, H., 2003. Modeling the formation and circulation processes of water masses and sea ice in the Gulf of St. Lawrence, Canada. *Journal of Geophysical Research*, 108: 3269-3289.
- Savenkoff, C., Vézina, A.F., Packard, T.T., Silverberg, N., Therriault, J.-C., Chen, W., Bérubé, C., Mucci, A., Klein, B., Mesplé, F., Tremblay, J.-E., Legendre, L., Wesson, J. and Ingram, R.G., 1996. Distributions of oxygen, carbon, and respiratory activity in the deep layer of the Gulf of St. Lawrence and their implications for the carbon cycle. *Canadian Journal of Fisheries and Aquatic Science*, 53: 2451-2465.
- Savenkoff, C., Vézina, A.F., Smith, P.C. and Han, G., 2001. Summer transports of nutrients in the Gulf of St. Lawrence estimated by inverse modelling. *Estuarine, Coastal and Shelf Science*, 52: 565-587.
- Silverberg, N., Sundby, B., Mucci, A., Zhong, S., Arakaki, T., Hall, P., Landén, A. and Tengberg, A., 2000. Remineralization of organic carbon in eastern Canadian continental margin sediments. *Deep-Sea Research II*, 47: 699-731.
- Smith, J.N. and Schafer, C.T., 1999. Sedimentation, bioturbation, and Hg uptake in the sediments of the estuary and Gulf of St. Lawrence. *Limnology and Oceanography*, 44: 207-219.
- St-Onge, G., Stoner, J.S. and Hillaire-Marcel, C., 2003. Holocene paleomagnetic records from the St. Lawrence Estuary, eastern Canada: centennial to millennial-scale geomagnetic modulation of cosmogenic isotopes. *Earth and Planetary Sciences Letters*, 209: 113-130.
- Thibodeau, B., de Vernal, A. and Mucci, A., 2004. Development of micropaleontological and geochemical indicators of eutrophication in the St. Lawrence Estuary. Abstract, Spring AGU meeting, May 17-21, Montreal, QC, Canada.
- Timothy, D.A., 2004. Organic matter remineralisation and biogenic silica dissolution in a deep fjord in British Columbia, Canada: a regression analysis of upper ocean sediment-trap fluxes. *Deep-Sea Research I*, 51: 439-456.
- USCOP, 2004. Preliminary report of the US commission on ocean policy - Governor's draft. U.S. commission on ocean policy, Washington, D.C.
- Wu, R.S.-S., 2002. Hypoxia: from molecular responses to ecosystem responses. *Marine Pollution Bulletin*, 45: 35-45.

Ziebis, W.S., Huettel, M. and Forster, S., 1996. Impact of biogenic sediment topography on oxygen fluxes in permeable beds. *Marine Ecology Progress Series*, 140: 227-237.